6-1-2015

Serum messenger RNA, protein biomarkers and metabolomic profiling in diabetes mellitus

Ana Rakovac Tisdall
Royal College of Surgeons in Ireland, araktis@gmail.com

Serum messenger RNA, protein biomarkers and metabolomic profiling in diabetes mellitus

Volume 1 of 1

Ana Rakovac Tisdall

School of Postgraduate Studies

Royal College of Surgeons in Ireland

St. Stephen's Green, Dublin 2, Ireland

A thesis submitted for the degree of Doctor of Medicine
to School of Postgraduate Studies of the Royal College of Surgeons in Ireland on
9th of April 2015

The research work described in this thesis was performed under the supervision of Professor Seamus Sreenan; Department of Endocrinology, Connolly Hospital, Blanchardstown.

CANDIDATE THESIS DECLARATION

I declare that this thesis, which I submit to RCSI for examination in consideration of the award of a higher degree of Doctor of Medicine, is my own personal effort. Where any of the content presented is the result of input or data from a related collaborative research programme, this is duly acknowledged in the text such that it is possible to ascertain how much of the work is my own. I have not already obtained a degree in RCSI or elsewhere on the basis of this work. Furthermore, I took reasonable care to ensure that the work is original, and, to the best of my knowledge, does not breach copyright law, and has not been taken from other sources except where such work has been cited and acknowledged within the text.

Signed _____

RCSI Student Number _____08506558_____

Date ___9th April 2015_____

Acknowledgements

Firstly, my heartfelt thanks to my supervisor, Professor Seamus Sreenan—your support and understanding was crucial in getting through the difficult times. And, yes, that bet is still on.

Thanks to the magnificent research nurses in the Connolly Hospital Diabetes Centre, Sandi McAteer and Ger McGovern—if it was not for you and your help with organisation and phlebotomy, this study might have taken a lot longer than it already did!

Thanks to all the patients and volunteers who gave of their time and blood to help with this research—nothing would have happened without you.

Thanks to our collaborators in the Dublin City University, National Institute for Cellular Biotechnology: Dr Sweta Rani, who first introduced me to the magic of qRT-PCR; Dr Erica Hennessy, who taught me more about PCR, pipetting and laboratory techniques, ran ELISA confirmation experiments and was a great friend altogether; Dr Paul Dowling, who oversaw the proteomics experiment and helped with his wealth of knowledge in proteomics; Dr Lorraine O'Driscoll, whose cell experiment we aimed to investigate in human subjects and who was a great help in setting the project, Dr Martin Clynes, who helped supervise and steer the project with Professor Sreenan.

Heartfelt thanks to Dr Ronan Conroy, who painstakingly went through the data analysis with me and marvelled at the possibility of doing so much work and finding so few significant p values—laughing with you made it easier to bear.

To Dr Tom King, my room-mate in Diabetes Research Centre in Connolly Hospital, thanks for coffee, chats and preservation of sanity.

And, finally, thanks to my family: my darling sister and mother, who helped any way they could, and my sons, who, while actively not helping, brought joy, as always.

Table of contents

List of abbreviations

1,5-AG, 1,5-anhydroglucitol

2-DIGE, 2-dimensional gel electrophoresis

ACCORD, Action to Control Cardiovascular Risk in Diabetes

ACEI, angiotensin-converting enzyme inhibitors

Actb, actin β

ADVANCE, Action In Diabetes And Vascular Disease: Preterax And Diamicron MR Controlled Evaluation

AGE, advanced glycation products

ALT, alanine aminotransferase

ANOVA, analysis of variance

ARB, angiotensin receptor blockers

AST, aspartat aminotransferase

BP, blood pressure

BCAA, branched chain amino acid

BMI, body mass index

C4bBP, C4b binding protein

cAMP, cyclic adenosine monophosphate,

Chgb, chromogranin B

ChREBP, carbohydrate response element-binding protein

Co-A, acetyl-coenzyme A

CMPF, 3-carboxy-4-methyl-5-propyl-2-furanpropanoate

CPS-1, carbamoyl phosphate synthetase

CRP, C-reactive protein

Ct, cycle threshold

CTLA4, cytotoxic T lymphocyte-associated protein 4

DAG, diacylglycerol

DCU, Dublin City University

DCCT, Diabetes Control and Complications Trial

EDIC, Epidemiology of Diabetes Interventions and Complications

Egr1, early growth response 1

ELISA, Enzyme-linked immunosorbent assay

Erk/MAPK, extracellular signal-regulated kinase/ mitogen-activated protein kinase

ESR, erithrocyte sedimentation rate

FBC, full blood count

FFA, free fatty acids

FH, family history

FPA, fibrinopeptide A

FVa, activated factor V

FVIIIa, activated factor VIII

GAD, antibody to glutamic acid decarboxylase

GC-MS, gas chromatography-mass spectrometry

GGPPS, geranylgeranyl diphosphate synthase

GGT, gama-glutamyl transferase

GPCR, G protein-coupled receptor

HbA1c, haemoglobin A1c,

HDL, high density lipoprotein

HLA, human leukocyte antigen

HMDB ID, Human Metabolome Database ID

HOMA-IR, homeostatic model assessment of insulin resistance

IAA, insulin autoantibody

ICA, islet cell antibody

IGT, impaired glucose tolerance

IL2Ra, interleukin-2 receptor alpha

IL-6, interleukin-6

IMCL, intramyocellular lipid

Ins1, insulin 1

Ins2, insulin 2

KEGG ID, Kyoto Encyclopaedia of Genes and Genomes

LC, liquid chromatography

LC—MS, liquid chromatography-mass spectrometry

LCFA-CoA, long chain fatty acyl-CoA

LDL, low density lipoprotein

LPL, lipoprotein lipase

MIN-6, mouse insulinoma cell line

miRNA, micro ribonucleic acid

mRNA, messenger ribonucleic acidNADPH, nicotinamide adenine dinucleotide phosphate

MS, mass spectrometry

m/z, mass to charge ratio

NAFLD, non-alcoholic fatty liver disease

NGT, normal glucose tolerance

NH_3, amino group

Npy, neuropeptide Y

PAI-I, plasminogen activator inhibitor

PC, phosphatidylcholine

PCA, principal component analysis

PDX-1, pancreas duodenum homeobox 1

PI3K/Akt, phosphatidylinositide 3-kinases/ protein kinase B

PKC, proteine kinase C

Pld1, phospholipase D1

PPI, preproinsulin

PTEN, phosphatase and tensin homologue

PTPN22, protein tyrosine phosphatase, non-receptor type 11

qRT-PCR, quantitative real time reverse transcription-polymerase chain reaction

RNA, ribonucleic acid

ROS, reactive oxygen species

RQ, relative quantification

RSD, relative standard deviation

RT, reverse transcription

SD, standard deviation

SGLT4 (sodium-glucose co-transporter 4)

T1DM, type 1 diabetes mellitus

T2DM, type 2 diabetes mellitus

TBP-2, thioredoxin-binding protein 2

TCA, tricarboxylic acid cycle

TGF-β, transforming growth factor β

TNF-α, tumour necrosis factor alpha

TRX, thioredoxin

TXN, thioredoxin

Txnip, thioredoxin-interacting protein

UHPLC/MS/MS, ultra-high performance liquid chromatography / tandem mass spectrometry

UKPDS, United Kingdom Prospective Diabetes Study

VADT, Veterans Affairs Diabetes Trial

VCAM 1, vascular cell adhesion molecule 1

VDUP, vitamin D up-regulated protein, VEGF, vascular endothelial growth factor

Vero-PPI, monkey kidney fibroblast cells engineered to produce human preproinsulin

Summary

While there is consensus on what biological parameters are consistent with diagnosis of diabetes, there is a scarcity of biomarkers which might identify different biochemical phenotypes of disease, underlying β cell mass or propensity to complications in diabetes. The studies presented in this thesis were undertaken based on observations from our research group's previous study, which identifed differentially expressed mRNAs in extracellular medium of glucose-responsive vs. glucose-non-responsive cell lines. As level of expression of mRNAs was dependent on glucose responsiveness and cell mass, we aimed to investigate whether similar mRNA expression pattern changes would be observed in human serum in patients with known diabetes.

We collected samples from patients with impaired fasting glucose, impaired glucose tolerance, newly diagnosed type 2 diabetes, newly diagnosed type 1 diabetes, poorly controlled type 2 diabetes and long-standing type 1 diabetes as well as healthy controls. In this work, I present findings from studies on patients newly diagnosed with type 2 diabetes, newly diagnosed type 1 diabetes and long-standing diabetes, compared to their healthy controls.

We have not found differential expression of mRNA identified in the cell lines study in our newly diagnosed type 2 diabetes patients and the research group's decision was not to extend mRNA studies to other groups of subjects, which may be attempted with resolution of current financial constraints.

We also examined sera of patients with type 1 diabetes with proteomic and novel metabolomic methods. Proteomic analysis identified down-regulation of anticoagulant protein S in patients with newly diagnosed type 1 diabetes, but no reported thrombotic events. While proteomics also identified reduced levels of vitronectin in patients with established type 1 diabetes, this is of unknown signficance.

In metabolomic analysis, the most consistently altered metabolic pathway was the caffeine metabolism, with five caffeine metabolites being significantly down-regulated in patients with newly diagnosed type 1 diabetes, possibly indicating increased caffeine consumption by controls. Other pathways significantly altered were those of carbohydrate and lipid metabolism. 1,5-anhydroglucitol, a known marker of glycemic control, was unsurprisingly significantly down-regulated in patients with newly diagnosed type 1 diabetes, in conjunction with significantly raised glucose levels in these patients. Lipid metabolites were were lower in patients with type 1 diabetes than in controls; this was coupled with higher total and LDL cholesterol in controls than in patients with type 1 diabetes. Therefore it is unknown if changes in lipid metabolites are reflective of type 1 diabetes, or due to the high cholesterol in control samples

1 Introduction

1.1 Diabetes

Diabetes is a disease affecting a growing proportion of the world's population. According to the World Health Organisation, 346 million people in the world have diabetes (1). At least 90% of these are affected by type 2 diabetes (1). It is expected that the number of people with diabetes will rise to 552 million by 2030, according to the International Diabetes Federation (2) . Albeit there are many causes and types of diabetes, this research focused on the two predominant types: type 1 and type 2 diabetes mellitus.

1.1.1 Type 1 Diabetes

Type 1 diabetes (T1DM) is an autoimmune disease precipitated in genetically susceptible individuals by environmental factors resulting in destruction of pancreatic β cells (3). In 2010, 479 000 children younger than 14 in the world suffered from type 1 diabetes. Its incidence is growing by 3% yearly and the reasons behind this increase are not known (2).

Type 1 diabetes can occur at any age, but the peak incidence is just before school and in puberty (2).

Type 1 diabetes is associated with the appearance of humoral and cellular islet autoimmunity and defective immunoregulation (4). The original trigger for the autoimmune destruction cascade is elusive. According to current genetic research, the following genes are the likeliest susceptibility genes for diabetes: human leukocyte antigen (HLA), insulin, protein tyrosine phosphatase, non-receptor type 22 (lymphoid)(PTPN22), interleukin-2 receptor alpha (IL2Ra), and cytotoxic T lymphocyte-associated protein 4 (CTLA4) (5).

The products of HLA class II genes on chromosome 6p21 are associated with presentations of antigen to the cellular immune system (6). Several HLA class II genes are implicated: from those making the individual highly prone to development of T1DM (DR3/4-DQ8 heterozygous haplotype to those conferring protection (DRB1*1501-DQA1*0102-DQB1*0602 haplotype, found in ~20% of the population but only 1% of patients) (7). HLA-B*39 allele, a class I gene, was found to be a significant risk factor for development of T1DM, associated with a lower age at diagnosis (8). Insulin gene variability, caused by polymorphisms of the IDDM2 locus on chromosome 11, accounts for lesser genetic predisposition. One form of polymorphism (variable number of tandem repeats, VNTR, type I) results in lower transcription rates of insulin and its precursors in the thymus, leading to reduced tolerance and T1DM development. A protective polymorphism also exists, VNTR type III. Individuals with this polymorphism have higher thymic clearance of insulin-reactive T-cells and hence less chance of developing autoimmunity to the β cells (5).

The PTPN22 gene encodes the lymphoid protein tyrosine phosphatase (LYP). LYP is an important negative regulator of T-cell receptor signalling (5).

An allelic variation of the interleukin (IL)-2 receptor-a gene (IL2RA) region has been described as a risk factor for T1DM. This receptor is an essential molecule expressed on T cells upon activation. The mechanism by which it confers autoimmunity is unclear at present (5).

The CLTA-4 gene, another gene implicated in development of T1DM, encodes cytotoxic T lymphocyte-associated protein 4 (CTLA-4. It is necessary for negative regulation of immune responses, as evidenced by the severe lymphoproliferative disorders seen in knock-out mice. It is also associated with other autoimmune conditions (multiple sclerosis, rheumatoid arthritis, systemic lupus erythematosus) (5).

At least 40 new loci, possibly implicated in T1DM pathogenesis, were found in recent genome-wide studies, some of them encoding interleukin-10 (9). Almost all of the identified loci appear to alter risk of diabetes by effects on the immune system (6).

Most patients with type 1 diabetes at diagnosis have circulating antibodies although the presence of autoantibodies is not a diagnostic criterion: islet cell antibody (ICA), insulin autoantibody (IAA); antibody to glutamic acid decarboxylase (GAD) 65; antibody to tyrosine phosphatases (IA-2 and IA2-β); zinc transporter 8 antibodies (ZnT8) (10). The prevalence of diabetes-associated autoantibodies in the general population is unknown. In the Finnish Type 1 Diabetes Prediction and Prevention study, 7410 children positive at birth for presence of type 1-associated HLA-haplotypes were followed up and tested for the presence of diabetes-associated autoantibodies. Over 10 years, 15.8% (1173) of them became ICA-positive and, of those, 155 developed type 1 diabetes. The combination of persistent ICA and IAA positivity resulted in the highest positive predictive value (91.7%), positive likelihood ratio (441.8), cumulative disease risk (100%), and specificity (100%) (11).

Once islet autoantibodies have developed, the progression to diabetes in antibody-positive individuals is determined by the age of antibody appearance and by the magnitude of the autoimmunity, in turn related to the age of the subject (4). In a study by Verge, individuals with two or more positive autoantibodies had a 68% 5-year risk for developing type 1 diabetes, and those with all three (ICA, IAA and GAD) antibodies had an estimated 100% 5-year risk (12). Approximately 4% of normal individuals will be positive for one diabetes-related autoantibody (13). Family members of patients with T1DM may be antibody positive even without progression to diabetes (14).

Various environmental factors have been implicated as triggers of autoimmune β cell destruction. Enteroviruses, in particular Coxsackie viruses, have been extensively investigated as a possible precipitant, but definitive confirmation of their role as triggers is lacking. In a Finnish prospective study, enteroviral infections were detected in 57% of the children in a 6-month period preceding the first appearance of autoantibodies compared with 31% of the matched control children in the same age-group (odds ratio 3.7, 95% CI 1.2-11.4) (15). Other viruses (rotaviruses, rubella) have been found to be connected to the onset of T1DM in small studies, but these results were not consistently replicated (5). An argument against rubella being a significant cause of T1DM is in the fact that widespread immunisation programmes in wealthier countries since 1969 have effectively eradicated the infection. Concerns that, on the contrary, immunisation against rubella and mumps, might be contributing to the rise in T1DM incidence, although postulated, have not been confirmed (5). Other environmental factors have been investigated: Mycobacterium avium in cow's milk, cow's milk protein per se and vitamin D deficiency. Vitamin D levels were found to be low in young adults at the onset of

T1DM in Sweden (16). Further support for the vitamin D hypothesis was provided by a recent Indian study which found an interaction between the vitamin D receptor and HLA alleles, postulating that vitamin D deficiency in early childhood might prompt autoimmunity via poor expression of HLA DRB1 0301 in thymus (17).

Interesting data came from a recent prospective study of Finnish children which showed that changes in metabolic profiling preceded the onset of autoimmunity in children who had been followed from birth and proceeded to develop T1DM. Children who developed diabetes had reduced serum levels of succinic acid and phosphatidylcholine (PC) at birth, reduced levels of triglycerides and antioxidant ether-phospholipids throughout the follow up, and increased levels of proinflammatory lysophosphatidylcholines (lysoPCs) months before seroconversion to autoantibody positivity. Diminished levels of ketoleucine and elevated glutamic acid also preceded appearance of insulin and glutamic acid decarboxylase autoantibodies (18). Lysophosphatidylcholine appears to be a proinflammatory mediator and may be intricately involved in disrupting endothelial barrier function resulting in inflammatory responses in the vessel wall (19). It is, therefore, for the first time possible to speculate that changes in the metabolic milieu might trigger the autoimmune reaction.

1.1.2 Type 2 Diabetes

Type 2 diabetes mellitus (T2DM) is increasing in prevalence at an even more alarming rate than T1DM, and this is often referred to as an epidemic. It is a disease of relative insulin deficiency, gradually

progressing to absolute insulin deficiency in some, caused primarily by reduced insulin sensitivity (insulin resistance).

In the healthy human, insulin decreases lipolysis in the adipose tissue and promotes lipogenesis. In the skeletal muscle, insulin promotes glucose entry and glycogen synthesis. In the liver, insulin promotes glycogen synthesis and de novo lipogenesis, while also inhibiting gluconeogenesis (20). Insulin resistance is the inability of peripheral target tissues (muscle, adipose tissue and liver, primarily) to respond appropriately to normal circulating concentrations of insulin produced in the pancreas. To maintain euglycaemia, the pancreas compensates by secreting greater amounts of insulin, which is effective in overcoming insulin resistance in some patients but in others this compensatory mechanism fails and type 2 diabetes ensues. In patients with type 2 diabetes, insulin resistance precedes the onset of the disease by several years and gradually increases over time due to a combination of environmental and genetic factors (21).

There is a strong relationship between insulin sensitivity and body weight. Worldwide obesity is the driving force behind globally increased insulin resistance and thus type 2 diabetes, but it is not the only factor; there is a strong genetic predisposition such that family members of subjects with T2DM can be shown to be insulin resistant even when they have normal body weight (22). Aging and decreased physical activity further increase insulin resistance which, combined with an impaired insulin secretory response of pancreatic β cells to glucose, results in type 2 diabetes mellitus. To date, 44 different loci increasing the susceptibility to diabetes have been identified as part of genome-wide studies and large scale meta-analyses; these, however, account for only 10% of observed familial clustering in patients of European descent (23). The mechanism by which the

genetic susceptibility leads to insulin resistance is still poorly understood.

Insulin resistance in obesity is associated with overabundance of free fatty acids (FFAs), released from the adipose tissue by lipase and from other tissues by lipoprotein lipase (LPL). FFAs reduce insulin sensitivity in muscle partly by inhibiting insulin-mediated glucose uptake (24).

Another mechanism for muscle insulin resistance is intramyocellular lipid (IMCL) accumulation, i.e. increased fat content within the muscle. It causes an imbalance in skeletal muscle lipid influx, lipid metabolism, and oxidative capacity. (25). A number of compounds are accumulated: diacylglycerols (DAGs), long chain fatty acyl-CoAs (LCFA-CoAs), acylcarnitines, and ceramides (25). The mechanisms by which accumulation of IMCL causes insulin resistance are not completely elucidated. It is clear, however, that total levels of DAG, ceramides and LC-FA-CoA are not adequate predictors of obesity-induced insulin resistance. It appears that specific characteristics of these molecules (degree of saturation, chain length, stereo specificity and intracellular localisation) might be factors influencing the level of insulin resistance in the muscle (25).

As insulin-mediated glucose uptake in the muscle is impaired, glucose is diverted to the liver. In the liver, increased liver lipid also impairs the ability of insulin to regulate gluconeogenesis and activate glycogen synthesis. In contrast, lipogenesis remains unaffected and, together with the increased delivery of dietary glucose, leads to worsening non-alcoholic fatty liver disease (NAFLD) (20). Impaired insulin action in the adipose tissue allows for increased lipolysis, which will promote re-esterification of lipids in other tissues (such as liver) and further exacerbates insulin resistance. In addition, in obesity, adipose tissue macrophages are activated and secrete inflammatory cytokines,

interleukin-6 (IL-6) and tumour necrosis factor-alpha (TNF-a). In adipocytes, these cytokines promote lipolysis. In muscle cells, cytokines can promote increase lipid oxidation and, in extreme situations, may promote muscle atrophy via increased proteolysis. In the liver, cytokine signalling may serve to increase lipogenesis and impair lipid oxidation (20).

In the preclinical period, pancreatic β-cells respond to insulin resistance by increasing their cell mass and insulin secretion. When this fails to compensate for insulin resistance, overt type 2 diabetes ensues.

1.2 Clinical features of diabetes

The onset of autoimmune type 1diabetes is usually fast, with a history ranging in days to weeks, whereas progress from insulin resistance to frank diabetes is a lot slower in type 2 diabetes. It is estimated that type 2 diabetes may be present for 9-12 years before diagnosis (26). Regardless of whether diabetes onset is fast, as in T1DM, or slower, as in T2DM, the resulting hyperglycaemia will, once it regularly exceeds the renal threshold, cause osmotic symptoms. These are polyuria and nocturia, due to osmotic effects of glucose excreted in the urine; polydipsia, due to haemoconcentration and activation of thirst mechanisms. Fatigue, chronic skin and genitourinary tract infections are common.

In patients with type 1 diabetes, the clinical presentation is usually dramatic with an abrupt onset of symptoms when the level of insulin reaches a point at which euglycaemia can no longer be maintained.

When the lack of insulin is severe enough, the inability to stimulate glucose uptake, coupled with increased fat breakdown, causes diversion to energy production from lipolysis, yielding ketones as a by-product, and may result in diabetic ketoacidosis and coma.

In patients with T2DM, the presentation is usually more insidious and diagnosis may be accidental. Because of the association with obesity, particularly abdominal obesity, there may be other metabolic abnormalities associated and this has led to the use of the term metabolic syndrome which also incorporates dyslipidaemia and hypertension with some level of dysglycaemia (27, 28).

1.3 Complications of diabetes

Four molecular mechanisms have been proposed as pathways through which hyperglycaemia causes micro- and macrovascular complications: increased polyol pathway flux; increased intracellular advanced glycation end product (AGE) formation; activation of protein kinase C; increased hexosamine pathway flux (10).

Increased flux through the polyol pathway consumes the reduced form of nicotinamide adenine dinucleotide phosphate (NADPH). NADPH depletion is thought to exacerbate intracellular oxidative stress and cause cellular injury (10). Intracellular auto-oxidation of glucose results in production of intracellular dicarbonyls (glyoxal, 3-deoxyglucosone, methylglyoxal), also known as AGE precursors(10). They damage intracellular and extracellular proteins and matrix components. Intracellular protein modifications may alter cellular functions. Modifications of extracellular matrix proteins result in abnormal interactions with other matrix proteins and integrins (receptors mediating attachment of the cell to the surrounding tissue) (29) . The modified proteins bind to receptors on endothelial cells, mesangial cells, and macrophages causing expression of cytokines and growth factors including interleukin 1, IGF-1, TNF-a, transforming growth factor-β (TGF-β), macrophage colony stimulating factor, granulocyte-macrophage stimulating factor, platelet-derived growth factor, thrombomodulin, tissue factor, vascular cell adhesion molecule 1 (VCAM 1) and vascular endothelial growth factor (VEGF). Induction of VEGF has been implicated in the vascular hyperpermeability associated with diabetes (30).

Increased intracellular glucose causes rise in diacylglycerol; this in turn activates protein kinase C (PKC) isoforms β and delta (10). The activation of PKC initiates a complex network of intracellular signalling that alters transcription factor binding to the promoter regions of responsive genes, which in turn alters gene expression. Activation of these isoforms also leads to a change in expression of endothelial nitric oxide synthase, endothelin 1, VEGF, TGF-β, plasminogen activator inhibitor (PAI-1), which modulates vascular endothelial permeability and neovascularisation and activation of nuclear factor κB and nicotinamide adenine dinucleotide phosphate (NADPH) oxidases, which in turn increases superoxide production (31)(Figure 1.3.1).

Superoxide presence causes impairment of endothelium-dependent relaxations, increase in smooth muscle contractions, and release of constrictor prostanoids, leading to impairment of endothelial cell function (31, 32).

Increases in vascular permeability, angiogenesis, cell growth and apoptosis, vessel dilation, cytokine activation, basement membrane thickening and extracellular matrix expansion have all been observed with increased PKC activity (31, 33). Support for the hypothesis that PKC is involved in complication development comes from the observation that inhibitors of protein kinase b isoform improve retinopathy and nephropathy in experimental models (30).

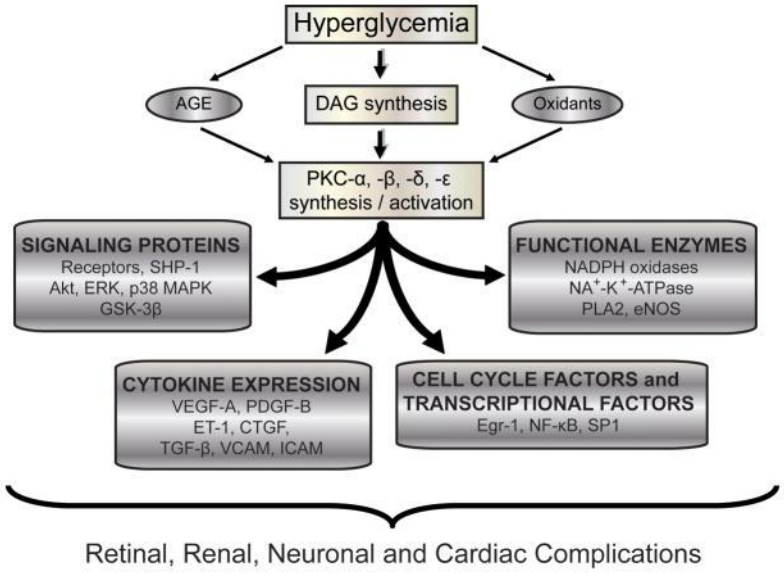

Figure 1.3.1 Mechanisms of protein kinase C activation of transcriptional factors involved in development of diabetes complications; SHP-1 protein tyrosine phosphatase, Akt, serine-threonine kinase, ERK extracellular signal-regulated kinase; p38 MAPK mitogen-activated protein kinase; GSK-3β glycogen synthase kinase β; VEGF-A vascular endothelial factor A; PDGF-B, platelet-derived growth factor β; ET-1 endothelin 1; CTGF, connective tissue growth factor; TGF-β, transforming growth factor β; VCAM, vascular cell adhesion molecule, ICAM, intercellular adhesion molecule; Egr-1, early growth response 1, NF-κB, nuclear factor of kappa light polypeptide gene enhancer in B-cells 1, SP1, specificity protein 1; NADPH oxidase, nicotinamide adenine dinucleotide phosphate oxidase; PLA2, phospholipase 2; eNOS, endothelial nitric oxid synthase; Na-K-ATPase, sodium-potassium-adenosine-triphosphatase; DAG, diacylglycerol; PKC, protein kinase C, AGE, advanced glycation products. *Adapted from Geraldes (31).*

Hyperglycaemia increases hexosamine pathway flux by providing more fructose-6-phosphate for the rate-limiting enzyme of the pathway glutamine: fructose-6-phosphate amidotransferase. Activity of this pathway leads to increased donation of N-acetylglucosamine moieties to serine and threonine moieties of complication-promoting factors such as PAI-1 or TGF-β. It has been proposed that all four of these pathways are associated with overproduction of superoxide by mitochondria. (30).

Regardless of the mechanism leading to hyperglycaemia, its long-term effect is micro- and macrovascular damage. Damage to the capillaries and precapillary arterioles causes thickening of the capillary basement membrane. This in turn causes damage to the retina (causing retinopathy), kidneys (causing nephropathy) and autonomic and peripheral nerves (causing neuropathy). Atherosclerosis is significantly accelerated in diabetes, particularly in type 2 diabetes, resulting in higher incidence of macrovascular complications (ischaemic heart disease, stroke) with higher haemoglobin A1C (HbA1C) (34).

1.4 Laboratory findings and treatment targets in diabetes

1.4.1 Criteria for diagnosing diabetes

According to the American Diabetes Association and World Health Organisation, diabetes is diagnosed either in a symptomatic individual with a random glucose of ≥11.1 mmol/L or, in an asymptomatic subject, with two separate measurements of fasting plasma glucose ≥ 7.0 mmol/L or 2h-post glucose load reading of ≥11.1 mmol/L or, alternatively, a HbA1C of ≥6.5% (1, 35).

Fasting plasma glucose is defined as a morning blood sample taken after a fast lasting at least 8 hours. Two-hour plasma glucose is understood to be a sample taken two hours after a standard load of 75g of glucose has been taken orally.

Haemoglobin A1c (HbA1c) is the product of glycation of haemoglobin. When blood glucose enters the erythrocytes, it glycates the amino group of lysyl residues as well as the amino terminals of haemoglobin. The fraction of glycated haemoglobin, normally about 5%, is proportionate to blood glucose concentration. Since the half-life of an erythrocyte is typically 60 days, the level of glycated haemoglobin (HbA1c) reflects the mean blood glucose concentration over the preceding 6–8 weeks (36).

The definition of normal fasting plasma glucose varies depending on whether one takes ADA or WHO criteria into consideration: by ADA standards, fasting glucose of 5.6-6.9 mmol/L is in the impaired fasting glucose range, while for European Association for Study of Diabetes and WHO, the cut-off begins at 6 mmol/L (1, 37). Postprandial glucose values at 2-hours after ingestion of glucose above 7.8 mmol/L and below 11.1 mmol/L are considered as impaired glucose tolerance by ADA, EASD and WHO (1, 38).

1.4.2 Treatment targets for prevention of complications of diabetes

In order to prevent complications of diabetes, laboratory and clinical targets are set for all cardiovascular and other risk factors. HbA1C is to be kept at < 53 mmol/mol (<7%) or even <48 mmol/mol (<6.5%) if possible, taking individual characteristics of the patient in the account and allowing for more lenient target in older patients with comorbidities (39). Blood pressure is to be controlled at <130/80 mmHg (38). Dyslipidaemia needs to be treated particularly vigorously in patients with existing cardiovascular disease or in patients over 40 years of age with at least one cardiovascular risk factor. Low density lipoprotein (LDL) target in patients without overt cardiovascular disease should be < 2.6 mmol/L, while in those with known cardiovascular disease, a target of <1.8 mmol/L should be considered. High density lipoprotein level of > 1.0 mmol/L and triglyceride level <1.7 mmol/L are desirable (38).

Spot urine testing for microalbuminuria, reported as ratio between urinary albumin and urinary creatinine, is currently the preferred method for monitoring for development of nephropathy, as it compares adequately with 24-hour proteinuria measurements (40). Prevention of microalbuminuria and subsequent nephropathy is best achieved with treatment of hyperglycaemia as well as hypertension control, using angiotensin-converting enzyme inhibitors (ACEI) or angiotensin receptor blockers (ARB) (38).

While we have a reasonable understanding of the pathophysiology of diabetes, the processes that lead to its complications and good evidence for the benefit of interventions in preventing complications, we still have a poor understanding of why some individuals with diabetes are relatively more or less prone to developing complications. While glycaemic parameters are good biomarkers of complication risk, some patients appear not to develop severe complications despite poor control. A greater understanding of why this is the case and which might allow a more personalised approach to diabetes management could be provided by novel biomarkers if they could be shown to reflect the severity of β cell mass loss at diagnosis or be predictive of future complication development.

1.5 Biomarkers of interest in this study

1.5.1 Definition

The term "biomarker" was defined by the National Institutes of Health (U.S. Department of Health and Human Services) as a "characteristic that is objectively measured and evaluated as an indicator of normal biological processes, pathogenic processes, or pharmacologic responses to a therapeutic intervention" (41). There are currently no known biomarkers for β cell mass. As type 1 diabetes has been suggested to occur when 90-95% of β cells have been destroyed, and at diagnosis of type 2 in obese people there is about 60% of β cell mass remaining, finding either cell components or cell products associated with β cell mass would be helpful in quantifying the severity of the pancreatic lesion at diagnosis and might inform treatment (42, 43)

The biomarkers currently used (fasting and postprandial glucose, HbA1c) reflect the degree of serum and tissue hyperglycaemia, the final consequence of β cell exhaustion and destruction, rather than the β cell mass or pathophysiological processes that led to the occurrence of the disease.

1.5.2 Whole genome microarray studies of insulin-producing cell lines previously undertaken by our group

In order to investigate the mechanism behind the loss of glucose-stimulated insulin secretion, which may be part of the answer to the oetiology of β-cell insensitivity to high glucose in diabetes, our collaborators performed whole genome microarray studies on insulin-producing cell lines (44).

The cell cultures used in these experiments were MIN6(L) (glucose-responsive), MIN6(H) (glucose non-responsive) and MIN6 B1 cells as well as monkey kidney fibroblast cells engineered to produce human preproinsulin (PPI) (Vero-PPI) (44, 45).

MIN6 cells come from a transformed mouse β-cell line and exhibit glucose-stimulated insulin secretion comparable with cultured normal mouse islet cells (46). Glucose-stimulated insulin secretion (GSIS) is lost in long-term cultured MIN 6 heterogeneous cells. MIN6(L) cells (passage 18) and MIN6(H) (passage 40) cells were established from MIN6 to be glucose responsive (L) and nonresponsive (H), respectively (44).

Whole genome microarray and conditioned medium mRNA studies were performed on these cell lines (44).

MIN6 B1 cell line, a subclone of MIN6 cell line, is a highly glucose-responsive cell line that responds to glucose in a concentration-dependent manner (47). MIN6 B1 cell line maintains glucose responsiveness in short-term cultures. However, when passaged repeatedly, Dr Rani observed that MIN6 B1 cells start losing the glucose responsiveness and determined the passage at which the

GSIS was lost by performing GSIS assays as the cells were grown from lower to higher passage (44). Whole genome microarray analysis on biological triplicate samples of glucose-responsive low passage (p19) (MIN6 B1(GSIS)) and glucose-non-responsive higher passage (p23) (MIN6 B1(Non-GSIS)) was performed (44).

Vero cells are derived from epithelial cells of kidney from African green monkey (Cercopithecus aethiops) and engineered by one of our collabolators, Dr. Lorraine O'Driscoll, to produce and process human preproinsulin by transfection of the human preproinsulin cDNA (48). Vero-PPI cells secreted mature human insulin but did not show glucose-stimulated insulin secretion.

Whole genome microarray studies were performed on both MIN 6 and MIN6 B1 cell lines.

Whole genome microarray analysis on biological triplicate samples of glucose-responsive low passage (p19) (MIN6 B1(GSIS)) and glucose-non-responsive high passage (p23) (MIN6 B1(Non-GSIS)) has identified 111 differentially-regulated genes (44). Of these, 16 gene transcripts were selected based on p-value <0.05, fold change ≥1.2, for validation using qRT-PCR, including thyoredoxin interacting protein *(Txnip),* endothelial growth factor 1 *(Egr1),* glucagon *(Gcg)* and proprotein convertase subtilisin/kexin type 9 (*Pcsk)*(44). qRT-PCR was performed in triplicate for each gene transcript, and the fold change was determined after normalisation to the expression of a housekeeping gene, β-actin. Comparison of qRT-PCR data with microarray data demonstrated matching trends in expression changes for both methods.

Txnip and Egr1 were up-regulated, whereas Gcg and Pcsk9 were down-regulated in MIN6 B1(Non-GSIS) compared to MIN6 B1(GSIS).

When MIN 6 and MIN 6 B1 microarray studies were compared, a set of 33 common differentially regulated gene transcripts were found. There were 7 common upregulated (among them, *Txnip*) and 18 down-regulated genes in MIN6 and MIN6 B1 cells (among them, *Gcg*). Eight gene transcripts which were down-regulated in MIN6 were up-regulated in MIN6 B1 cells (among them, *Egr1*) and 1 gene transcript that was down-regulated in MIN6 B1 was up-regulated in MIN6 cells (44).

To investigate the relevance of Txnip in glucose- stimulated insulin secretion, silencing of Txnip was performed using small interfering RNA (siRNA) transfection in high passage (glucose non-responsive) MIN6 cells (44). Silencing of Txnip increased glucose-stimulated insulin secretion (44).

1.5.3 Extracellular ribonucleic acids (RNAs) analysis performed by our grup

Further experiments were performed by members of our group to evaluate the ocurrence of mRNAs in the extracellular medium of the above named cell cultures (45).

Over the last 25 years, contrary to previous beliefs that RNA is to be found only within cells, significant amounts of RNA have been found extracellularly, particularly in cancer patients. In patients with cancer, extracellular mRNAs were found to correlate to the tumour mass and/or activity in various cancers, including melanoma and cancers of the lung, thyroid, breast, bladder and prostate (49-51). Extracellular RNAs have been detected in majority of body fluids (serum, plasma, saliva, milk, urine, bronchial lavage), as well as cell culture

supernatants (52-57). In particular, messenger RNAs (mRNAs) were proven to be extractable from fresh and frozen serum samples (58).

It is unclear how the RNAs are released from cells: whether by active secretion, as a result of apoptosis and necrosis or some combination of the above (59). In serum of cancer patients, increased levels of serum ribonucleases are found; mRNA may be protected from these by apoptotic bodies (50, 60). Mammalian cells might be communicating between each other by secreting mRNA and short mRNAs (micro RNAs) into exosomes, small membrane vesicles of endocytic origin released into the extracellular environment on fusion of multivesicular bodies with the plasma membrane (61). Exosomes secreted into urine by all kidney cells have been found to contain mRNA, micro-RNA and proteins and their utility as biomarkers for kidney disease is currently being investigated. (62). Exosome-transferred mRNA was described as capable of coding for exosome-specific proteins in the recipient cells (61).

Over the last decade, a number of circulating mRNAs were detected to be significantly differently expressed in sera of patients with diabetes. Differential expression of serum mRNAs has been found in diabetic retinopathy and neuropathy, in particular serum neuron-specific enolase mRNA, which is higher in patients with diabetes compared to healthy controls, but decreases in patients with diabetic neuropathy (63). In patients with diabetic retinopathy, serum rhodopsin (biological pigment in retinal photoreceptor cells) mRNA level is higher than in normal controls, while retinal amine oxidase (a candidate for the role of retinal signal transmission modulator) levels are lower (64, 65). Nephrin (a cell adhesion molecule from the kidney glomerular filtration barrier) mRNA levels were found to be higher in

normoalbuminuric patients with diabetes when compared to healthy subjects (66).

While enolase, rhodopsin and nephrin show promise in identifiying patients with complications, it would be very exciting if a serum biomarker could be identified able to foretell the loss of β cells before the disease or indeed the complications had time to develop.

Our group further investigated whether any of the mRNAs identified in whole genome microarray studies would be found in the extracellular matrix of the cell lines. Several mRNAs were isolated from the conditioned medium of the three types of cell lines mentioned above: MIN 6 low and high passage (L, 18 and H, 40, respectively), MIN6 B1 and Vero-PPI. The isolated mRNAs were encoded by *Pdx1* (murine pancreatic and duodenal homeobox gene 1), *Pld1* (murine phospholipase D gene), *Npy* (murine neuropeptide y gene), *Egr1* (murine early growth response gene 1), *Chgb* (murine chromogranin B), *Ins1* (murine insulin 1 gene), *Ins2* (murine insulin 2 gene), *Pax4* (murine paired box transcription factor 4 gene) and *Actb* (murine β-actin gene). Degrees of gene expression of *Pdx1*, *Egr1* and *Chgb* reflected the numbers of MIN6 B1 cells conditioning the medium (45). This made us wonder whether mRNAs released from β-cells of the human pancreas into the serum of patients with diabetes might reflect the amount of remaining β-cells.

1.5.3.1 Thyoredoxin interacting protein (Txnip)

Txnip, thioredoxin-interacting protein is part of a ubiquitous mammal antioxidative cell mechanism for regulating cellular redox balance (67, 68). It was also called or thioredoxin-binding protein-2 (TBP-2) and vitamin D up-regulated protein 1 (VDUP), because of its relationship to 1,25$(OH)_2$-cholecalciferol (69) . It was first discovered in 1994 in leukaemia HL60 cells treated with vitamin D (70).

Intracellular redox balance is maintained by reactive oxygen species (ROS) scavenging systems. Two major intracellular thiol-reducing mechanisms are the interacting glutathione and thioredoxin systems. Thioredoxin reduces ROS through reversible oxidation of thioredoxin at two cysteine residues (Cys-32 and Cys-35); thioredoxin is then reduced by thioredoxin reductase and NAPDH (71) . Thioredoxin-interacting protein (Txnip), the endogenous inhibitor of thioredoxin inhibits thioredoxin antioxidative function by binding to its redox-active cysteine residues (67) (Figure 1.5.1.)

Txnip was recently found to be part of the family of arrestin signalling proteins (72). Arrestins were originally identified as intracellular proteins that bind to phosphorylated G protein-coupled receptors (GPCRs) and cause their desensitization, thus 'arresting' their activation (72). In diabetic mouse models, deficiency of another arrestin, β-arrestin-2, was recently described to affect insulin receptor signalling and contribute to insulin resistance (73) and yet another, α-arrestin, arrestin domain-containing protein 4, is an equally potent inhibitor of glucose uptake in vitro despite its inability to bind thioredoxin (74).

It is known from cell culture studies that hyperglycaemia inhibits thioredoxin ROS-scavenging function through induction of Txnip (75). However, Txnip does not act on glucose metabolism through inhibition of thioredoxin; glucose-uptake function is intrinsic to the arrestin domains of Txnip (72). The molecular mechanisms for how arrestin domains regulate glucose uptake remain unknown (72).

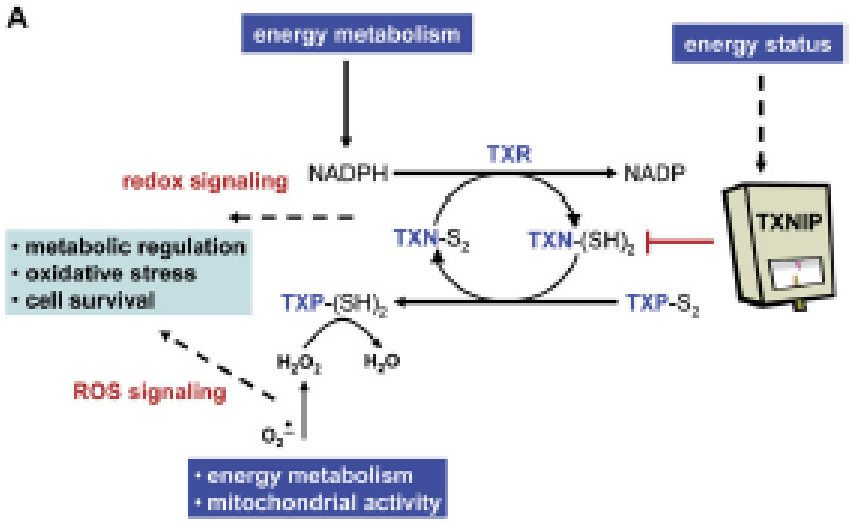

Figure 1.5.1 Role of TXNIP in the thioredoxin system. Thioredoxin (TXN) reduces oxidised cysteine residues (protein-S2) on cellular proteins. Reduced TXN (TXN-(SH)2) is regenerated via the action of thioredoxin reductase (TXR) at the expenditure of NADPH. When TXN reduces the oxidised form of thioredoxin peroxidise (TXP), the reduced enzyme (TXP-$(SH)_2$) is available to scavenge reactive oxygen species (ROS) such as hydrogen peroxide (H_2O_2) and the superoxide anion ($O_2^{\bullet-}$). TXNIP binds and inhibits the reduced form of TXN, thereby functioning as a rheostat that modulates both redox status and ROS-mediated signalling to regulate metabolism and other cellular processes. (Dashed lines indicate unknown processes) ***From Muoio, Cell Metabolism, 2007 (68)***

The metabolic functions of Txnip were revealed when a nonsense mutation in the Txnip gene was identified as being responsible for the phenotype of the 'hyplip' mouse, which has high triglyceride levels along with elevated ketone and lactate levels, consistent with decreased fatty acid flux through the tricarboxylic acid cycle in the

mitochondria (76). Hui described a similar phenotype in his Txnip-knockout mice: insulin levels were three times higher than normal, with animals suffering from hypoglycaemia, hypertriglyceridaemia and hepatic steatosis with a block in gluconeogenesis (77).

Txnip acts on the liver, most likely by inducing gluconeogenesis (74). Txnip-null mice in Chutkow's experiment were hypoglycaemic, hypoinsulinaemic, and had blunted glucose production following a glucagon challenge, consistent with a central liver glucose-handling defect (74). Glucose release from isolated Txnip-null hepatocytes was 2-fold lower than wild-type hepatocytes, whereas β-hydroxybutyrate release was increased 2-fold, supporting an intrinsic defect in hepatocyte glucose metabolism(74). While hepatocyte-specific gene deletion of Txnip did not alter glucose clearance compared with littermate controls, Txnip expression in the liver was required for maintaining normal fasting glycaemia and glucose production. In addition, hepatic over-expression of a Txnip transgene in wild type mice resulted in elevated serum glucose levels and decreased ketone levels (78).

In a clinical human study which combined euglycaemic-hyperinsulinaemic clamps with genome-wide expression profiling, in healthy subjects insulin suppressed expression of Txnip in the muscle, while glucose stimulated its expression (79). In healthy people and those with pre-diabetes, as glucose uptake rates increased, Txnip expression decreased but this inverse correlation was missing in people with diabetes (79). Forced expression of Txnip in cultured adipocytes significantly reduced glucose uptake, while silencing with RNA interference in adipocytes and in skeletal muscle enhanced glucose uptake (79). Txnip is consistently elevated in muscle of people with diabetes and pre-diabetes (79). Txnip thus seems to act as a

negative feedback regulator for glucose uptake: when glucose is plentiful, Txnip is induced and then inhibits further glucose uptake, most likely through enhanced flux through the mitochondrial citric acid cycle (72, 74, 79) (Figure 1.5.2.).

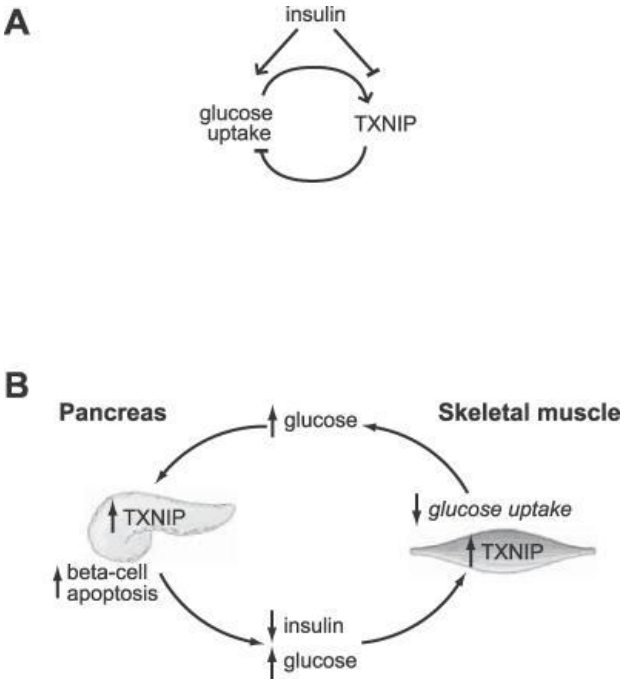

Figure 1.5.2 Model of *TXNIP* regulation and action and its potential role in the pathogenesis of type 2 diabetes . A. Glucose induces the expression of TXNIP in a variety of cells and tissues. Insulin suppresses the expression of TXNIP. Forced expression of *TXNIP* results in reduced glucose uptake, while inhibition of *TXNIP* enhances glucose uptake. This suggests that TXNIP serves as a glucose- and insulin-sensitive homeostatic switch that regulates glucose uptake in the periphery. (B) Role of *TXNIP* in glucose toxicity in the β-cell and in impaired glucose uptake in the periphery. Insulin deficiency or hyperglycaemia can increase *TXNIP* levels in muscle, resulting in impaired peripheral glucose uptake. The pancreatic β-cell is initially able to compensate by secreting more insulin, but eventually the β-cell compensation fails. The resulting hyperglycaemia may then elevate pancreatic β-cell *TXNIP* expression, which can induce apoptosis (80). The loss of β-cells, in turn, results in decreased insulin production that further exacerbates peripheral IGT. The vicious cycle would eventually spiral to T2DM. *Adapted from Parikh et al (79).*

In human muscle from healthy subjects, microarray genome profiling before and after euglycaemic-hyperinsulinaemic clamp, glucose stimulated and insulin suppressed Txnip expression (79). As glucose uptake rates increased, Txnip expression decreased in healthy subjects, but also those with pre-diabetes; however, this was not observed in subjects with diabetes (79).

It has long been known that hyperglycaemia exacerbates β-cell failure and impaired skeletal muscle glucose uptake, the process referred to as 'glucose toxicity' (81-83) Currently it is thought that this happens through ROS, but Parikh et al. propose that Txnip might be the missing link through its role in control of peripheral glucose uptake and β-cell toxicity (79-81, 84).This seems like a plausible hypothesis, considering that Txnip is essential for maintenance of fasting normoglycaemia through its effects on the hepatocytes and that hepatic over-expression of Txnip results in hyperglycaemia (74).

In Parikh's study, in biopsies of vastus lateralis muscles after the 2-h euglycemic hyperinsulinemic clamp, Txnip was more expressed in the muscles patients with diabetes than in subjects with normal glucose tolerance (Figure 1.5.3) (79, 85). The same held when vastus lateralis muscle biopsies of fasting subjects who subsequently underwent 2h-hyperinsulinemic euglycemic clamp to assess glucose disposal were analysed: Txnip was more expressed in patients with type 2 diabetes than in normoglycaemic subjects (79, 86) .

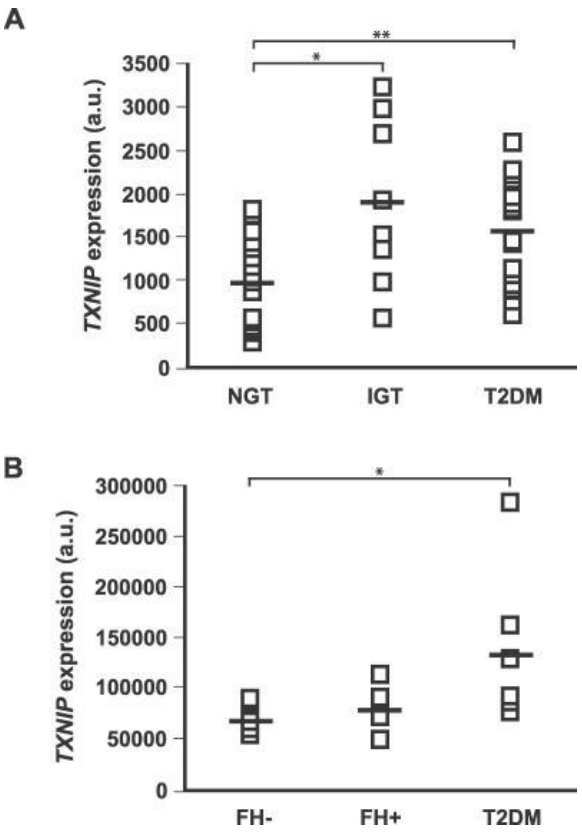

Figure 1.5.3. TXNIP expression in individuals with diabetes or at risk of developing diabetes. A) TXNIP expression levels from males from Northern Europe with NGT, IGT, or T2DM. * p < 0.02; ** p < 0.01, Mann-Whitney U-test. B) TXNIP expression levels from NGT individuals of Mexican-American descent with (FH+) or without (FH−) family history of T2DM, as well as individuals with T2DM; * p < 0.03, Mann-Whitney U-test. ***(Adapted from Parikh et al (79)***

In Parikh's clamp studies, Txnip expression was inversely correlated with the total body rate of insulin-stimulated glucose metabolism in males with normal glucose tolerance and impaired glucose tolerance but not in type 2 diabetes(Figure 1.5.4).

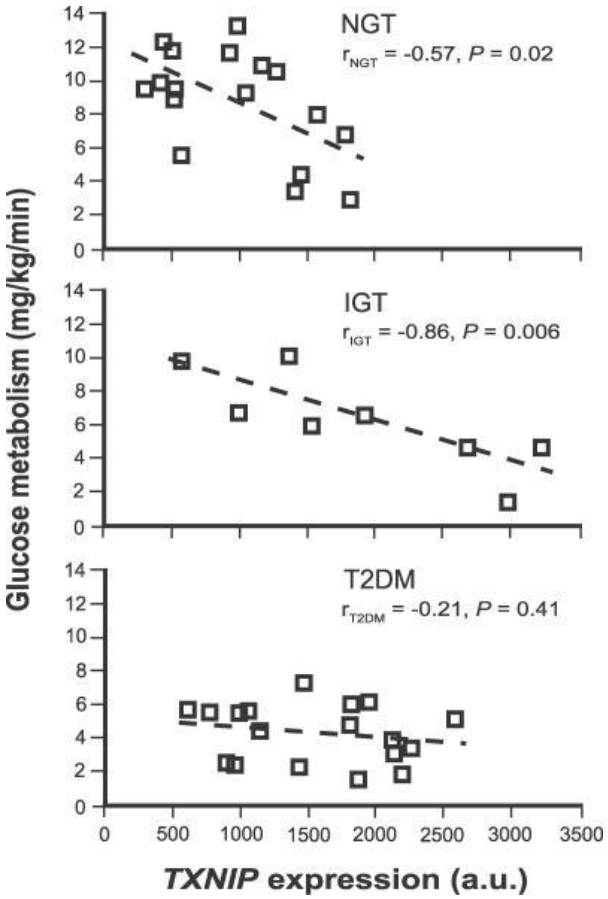

Figure 1.5.4. Insulin-mediated glucose uptake vs Txnip expression in a microarray in 43 males from Northern Europe with normal glucose tolerance (NGT, n=17), impaired glucose tolerance (IGT, n=8) and type 2 diabetes (T2DM, n=18) who underwent euglycaemic-hyperinsulinaemic pump studies; a.u.-arbitrary units, i.e. relative numbers of Txnip expression normalised to cyclophilin A reference. *Adapted from Parikh et al (79)*

Apart from mediating insulin sensitivity, Txnip causes pancreatic β cell apoptosis and death, as described by Minn in 2005 and by Chen in 2008 (80, 87). Recently it was shown that Txnip mediates endoplasmatic reticulum stress-mediated β cell death by increasing interleukin-1β mRNA transcription and activating interleukin-1β production (88). It is proposed that Txnip might be the 'switch' that integrates glucose sensing and insulin signalling in controlling the cell energy status (68)(Figure 1.5.1). Txnip gene transcription is supressed by

metformin, raising a possibility that Txnip regulation might be part of metformin's elusive mode of action (89).

Txnip also has a role in human cancer in growth suppression, inhibition of metastasis and proapoptosis through inhibition of thioredoxin (TRX) (90).

As Txnip was differentially more expressed in the conditioned media of the glucose-unresponsive (MIN-6) vs glucose-responsive cells in our group's recent cell study (91) and similar trend has been observed in studies of human biopsies, we set out to investigate if human serum, would replicate the differential expressions seen in the extracellular medium.

1.5.3.2 Early growth response 1 (Egr1)

Egr 1 is a zinc-finger protein, functioning as a transcriptional regulator. In cell cultures, Egr1 is inducible by insulin (92) and glucose induces Egr1 mRNA transcription in various β-cell models. In diabetic Zucker rats, Egr1 was up-regulated, but this did not have any effect on glucose-stimulated insulin secretion; however, in the same study, Egr1 gene silencing inhibited proliferation of INS-1 cells (an insulinoma β-cell line), in a glucose-independent manner, suggesting reduced Egr1 expression may contribute to decreased β-cell proliferation and consequent β cell failure (82).

Egr1 belongs to the EGR family of C2H2-type zinc-finger proteins. It is a nuclear protein and functions as a transcriptional regulator. The products of target genes it activates are required for differentiation

and mitogenesis (93). The gene coding for it is based on the short arm of 5th chromosome (93).

Upon stimulation by a variety of extracellular signalling molecules, including insulin, the biosynthesis of Egr1 is increased and its transcription is regulated by Ca^{2+} (92, 94). Many biological roles have been attributed to Egr1, ranging from controlling synaptic plasticity, wound repair, female reproductive capacity, inflammation, coagulation and vascular hyperpermeability of the lung, growth control, and apoptosis (94). In unstimulated cells, only low levels of Egr1 are detectable, while upon stimulation by a variety of extracellular signalling molecules, the biosynthesis of Egr-1 is increased (92, 94). Alterations of Egr1 by mitogenic stimuli have been reported in vivo, especially in normal and pathophysiological states associated with rapid cellular proliferation (92). It has been reported that infusion of growth factors (vascular endothelial growth factor, VEGF, and epidermal growth factor, EGF) induced Egr1 in the heart, brain, liver spleen, lung, brain and skeletal muscle of investigated animals.

Glucose increases Egr1 mRNA transcription in various cell models of β cells, and this induction is particularly associated with insulin secretion (95). As a transcription factor, Egr1 can regulate expression of tumour necrosis factor alpha, a known promoter of insulin resistance (96). Egr1 was also found to be implicated in development of adipocyte insulin resistance (97). In pancreatic β cells, Egr1 regulates expression of pancreas duodenum homeobox-1 (PDX-1), a key regulator of pancreatic β cell development, function and survival (98). Deficit in PDX-1 expression result in insulin deficiency and hyperglycaemia and Egr1 up-regulates this expression by activation of the pdx-1 promoter (98). These data suggest that Egr1 may be a potential marker of β-cell mass and/or function.

1.5.4 Serum proteomics

While measuring mRNA levels in serum and tissues will partly determine the transcriptome, made of messenger RNA and micro RNA (miRNA), it is impossible to predict the amount of protein produced by any given mRNA (99). Proteomics simultaneously measures large numbers of proteins in a complex tissue, making it a snapshot of cell's, tissue's or organism's protein production. The difficulty with assessing serum proteins is in the abundance of albumin and globulins. Various techniques have been used to extract and map low abundance proteins by depleting high-abundance proteins (100). The most common technologies in proteomics are based on two-dimensional gel electrophoresis and chromatographic separation methods combined with mass spectroscopy (101). Protein concentrations in biological fluids are determined by genetic variation, but environmental factors play a dominant role (102).

Considering that diabetes type 2 is a disease of many organs, serum is a potentially interesting sample for proteomics studies as blood is in contact with all tissues in the body. So far, a number of studies have looked at proteome in serum of patients with type 1 and type 2 diabetes (103, 104).

Within the last 10 years, several studies have reported differentially expressed proteins in skeletal muscle from patients with diabetes (105, 106). In Giebelstein's muscle study of patients with type 2 diabetes, there was a switch towards increased abundance of proteins from the glycolytic pathway and decreased abundance of mitochondrial

proteins; this was inversely correlated to glucose disposal during euglycaemic-hyperinsulinaemic clamp (107).

A number of differentially expressed proteins was described in animal and human pancreata, involved in protein biosynthesis, endoplasmic reticulum stress, microvascular endothelial dysfunction, impaired glucose sensitivity, mitochondrial dysfunction and impaired hormone secretion (108).

Serum proteomics studies have been done previously in patients with type 1 diabetes. Metz reported 2-fold up-regulation of alpha-2-glycoprotein 1 (zinc), corticosteroid-binding globulin, and lumican in type 1 diabetic samples relative to control samples, whereas clusterin and serotransferrin were 2-fold down-regulated in patients with type 1 diabetes These proteins have been linked to mobilisation of lipids, cytoprotection and kidney adaptation to hyperglycaemia (103). Another study identified 50 differentially expressed proteins between patients with type 1 diabetes and their controls; this protein list is prepared for publication (109).

A serum proteome study found extracellular glutathione peroxidase and apolipoprotein E to be progressively reduced in diabetic patients with microalbuminuria and chronic renal failure (110). Transthyretin, apolipoprotein A1, apolipoprotein C1 and cystatin C were also identified as markers for diabetic nephropathy in patients with type 1 diabetes (111).

Anti-aldolase antibody was identified in serum proteomic analysis as a marker for diabetic retinopathy and clusterin levels were found to be reduced in the vitreous fluid of patients with proliferative diabetic retinopathy (112, 113) .

Area of urinary proteomic markers in diabetes is thriving: a recent study four urinary proteins were found to be predictive for development of microalbuminuria in the cohort of 465 patients with type 1 diabetes who were prospectively followed and monitored for occurrence of microalbuminuria for 6 years (114). Four urinary proteins were found to be predictive of development of microalbuminuria: Tamm-Horsfall glycoprotein, a-1 acid glycoprotein, clusterin, and progranulin (114).

Further studies of protein expression in diabetes patients with better techniques for extraction of low-abundance proteins and label-free approach are necessary in order to create a map of proteomic biomarkers which might be used in early assessment of the disease and its complications.

1.5.5 Serum metabolomics

Metabolomic profiling is a relatively new method of identifying huge volumes of metabolites present at any given time in a substrate—a serum sample, a cell culture or an organism. It has been made possible by the development of methods capable of rapid, high throughput characterization of the small molecule metabolites. It provides an insight into genotype-phenotype-environment interactions as it will be dependent as much on the genetic make-up of an organism and its expression in phenotype as it will be on what an organism eats or breaths.

The metabolome makes up the smallest set of biomarkers (102). The Human Metabolome Project began in January 2005 with a grant from Genome Canada, a non-profit organisation engaged in genome research. Human Metabolome Project established freely-availably Human Metabolome Database, maintained by the University of Alberta, Canada (www.hmdb.ca), in which there are currently 41,519 metabolite entries, including lipids, sugars, nucleotides, amino acids, organic acids and other low-molecular-weight compounds. Additionally, there are about 7200 protein and DNA sequences linked to these metabolite entries (115, 116). Considering the diversity of metabolites and the span of their concentration levels, a combination of techniques is used for their identification. The most commonly used techniques are nuclear magnetic resonance and various types of mass spectrometry (MS), most often combined with a chromatographic separation process, such as gas or liquid chromatography (102).

Several metabolomic profiles have been described in diabetes. Orešič described increased levels of succinic acid and phosphatidylcholine at birth in patients who would later develop type 1 diabetes(18). He also shows reduced levels of triglycerides and antioxidant ether phospholipids through childhood and increased levels of proinflammatory lysophosphatidilcolines before seroconversion and occurrence of anti-GAD antibodies (18). Li & Xu found increased levels of 2-hydroxyisobutyric acid, linoleic acid, palmitic acid and phosphate in patients with diabetes when compared to healthy controls, reflecting induction of insulin resistance (117). A German study analysing the metabolome on multiple platforms unsurprisingly found increased levels of sugar metabolites and a reduced level of 1,5-anhidroglucitol, increased level of branched chain amino acids (used in gluconeogenesis), lower phosphatidylcholine and higher

phosphatidylethanolamine (subtler markers of dyslipidaemia), β-hydroxibutyrate (reflecting a shift to fatty acid metabolism as source of energy), but also higher levels of 3-indoxyl sulphate, a known nephrotoxin and stimulant of progression of renal failure. Further metabolomic studies are required, particularly in type 1 diabetes and they may enhance our understanding of the pathophysiology of the condition.

1.6 Aims of this thesis

The aims of this work were:

To establish whether extracellular mRNAs previously found to be significantly differentially expressed in glucose-non-responsive cells from insulin-producing cell lines were found in human serum,

To establish whether the extracellular mRNAs identified in the cell line work were differentially expressed in humans with newly diagnosed type 2 diabetes when compared to healthy controls,

To investigate the proteomic profile of the patients with newly diagnosed type 1 diabetes, as well as changes occurring later in the course of type 1 diabetes, and

To determine the metabolomics profile of patients with new onset type 1 diabetes when compared to healthy controls.

2 Materials & methods

2.1 Subjects

The local ethics committee approved the study and all subjects gave written informed consent before entering it.

We recruited patients with newly diagnosed type 2 diabetes, patients with newly diagnosed type 1 diabetes, patients with long-term type 1 diabetes and healthy controls.

Samples from patients with newly diagnosed type 2 diabetes were labelled T2Nx. Samples from patients with newly diagnosed type 1 diabetes were labelled T1Nx, while samples from patients with established diabetes were labelled T1Ox. Samples from controls were labelled Ux, when their BMI was <30 kg/m^2, and Mx, where their BMI was over 30 kg/$m^{2..}$

2.1.1 Patients with newly diagnosed type 2 diabetes

We recruited 19 patients (10 male, 9 female) in whom type 2 diabetes (T2DM) has been diagnosed up to 6 months previously and 19 age/sex/BMI-matched controls. The patients with new type 2 diabetes were all referred by their general practitioners (GPs) to the Department of Endocrinology and Diabetes in Connolly Hospital, Blanchardstown between January 2008 and January 2009. Their diabetes was either diet-controlled (N=8) or they were treated with

metformin only (N=11). Characteristics of these patients and their controls are presented in table 3.2.1.

We analysed samples from these patients and their controls for extracellular mRNAs, previously found to be differentially expressed in conditioned medium of glucose-unresponsive vs. glucose-responsive cell lines (45, 91).

2.1.2 Patients with newly diagnosed type 1 diabetes

Eight patients with type 1 diabetes diagnosed within six months prior to entering the study were invited to take part (labelled as 'T1DM new' or T1Nx). They presented to the Department of Endocrinology in Connolly Hospital Blanchardstown following referral by their GPs between April 2008 and April 2010.

The patients were instructed to come in fasting (defined as no food from midnight). They were instructed not to take any insulin on the morning of testing. The last 'allowed' insulin dose was long-acting insulin the night before.

The samples of patients with newly diagnosed type 1 diabetes were analysed by proteomic and metabolomic methods. These patients and their controls are presented in table 4.2.1.

2.1.3 Patients with established type 1 diabetes

From the cohort of patients with established diabetes type 1, we recruited 8 patients with long-term type 1 diabetes, defined as 18 months and more, with average duration of disease of 14±9 years (range 5-26 years).

The patients were instructed to come in fasting (defined as no food from midnight). They were instructed not to take any insulin on the morning of testing. The last 'allowed' insulin dose was long-acting insulin the night before.

Proteomic and metabolomic analyses were performed on these samples, labelled 'T1DM old' or T1Ox.

These patients and their controls are presented in table 4.2.2.

The results of proteomic analysis were validated by extending ELISA validation on the sample of 30 patients with established type 1 diabetes, recruited with same inclusion/exclusion criteria. Characteristics of the cohort of 30 patients with established type 1 diabetes are presented in table 4.2.3.

2.1.4 Healthy controls

The healthy controls were recruited from the employees of the Connolly Hospital through written advertisements on department boards, as approved by the Ethics Committee. They were age-, BMI- and sex-matched to patients. Their samples were labelled at recruitment as Ux, if their BMI was ≤30kg/$m^{2.}$ and Mx, if their BMI was >30kg/$m^{2.}$

All healthy controls had oral glucose tolerance tests done to exclude diabetes, using a standard oral glucose load of 75g. The accepted normal values used were: for fasting glucose, 5.6 mmol/L and for 2-hour postprandial glucose, 7.8 mmol/L, as per American Diabetes Association guidelines (38).

Samples from healthy controls were used for mRNA extraction, proteomic and metabolomic profiling. The characteristics of healthy controls are presented in tables 3.2.1, 4.2.1, 4.2.2 and 4.2.3.

2.2 Study protocol and laboratory methods

In this section, laboratory methods common to all analyses are described.

At screening, a full history was taken, including diabetes history, symptoms of diabetes complications, past medical history, family history, history of gestational diabetes (in females), smoking history, steroid use in the six months preceding the diagnosis, and current prescribed and over-the-counter medications. on exercise was collected by patients' self-reporting; no grading of intensity of physical activity was attempted. Full physical examination was performed, including retinal exam in patients with diabetes. Biometric data (height, weight, waist circumference, hip circumference, blood pressure, heart rate) were collected. Blood pressure was measured once, sitting, after completion of the questionnaire. Heart rate was measured at the same time, sitting, counting the beats in 30 s and

multiplying by 2; this was confirmed by ECG . Waist circumference was measured on bare skin, half-way between lower ribs and iliac crest. Hip circumference was measured at the maximum buttock circumference level.

Blood was drawn for measurement of fasting plasma glucose, insulin, HbA1c, total cholesterol, HDL, LDL (calculated), triglycerides, bilirubin, aspartate aminotransferase (AST), alanine transaminase (ALT), gama-glutamyl transferase (GGT), urea, creatinine, sodium (Na), potassium (K), C-reactive proteine (CRP), calcium (Ca), phosphate (PO4), erythrocyte sedimentation rate (ESR) and full blood count (FBC). All samples were coded at collection (T2N for patients with newly diagnosed type 2 diabetes, T1N for patients with newly diagnosed type 1 diabetes, T1O for patients with established, 'old', type 1 diabetes, U for controls with BMI<30, M for controls with BMI > 30).

Homeostatic model assessment (HOMA) of insulin resistance (IR) was calculated in type 2 diabetes patients and their controls, from fasting glucose and fasting insulin values using the online calculator supplied by the Diabetes Trials Unit at The Oxford Centre for Diabetes, Endocrinology and Metabolism (118, 119)

Most routine blood tests were performed in the local laboratory. Biochemistry tests were analysed using Vitros 5600 and the Vitros 5.1 Fusion analysers from Ortho-Diagnostics (Johnson & Johnson, UK): glucose by glucose oxidation colorimetry, cholesterol and triglyceride by enzymatic reactions colorimetry, HDL by colorimetric selective hydrolisation, bilirubin by end-point dual wavelentgth absorbance colorimetry, AST by multi-point enzymatic spectrophotometry, ALT by multi-point enzymatic reflectance spectrophotometry, GGT by multi-point rate enzymatic spectrophotometry, urea by urease enzymatic colorimetry, creatinine by enzymatic two-point rate colorimetry,

sodium and potassium by direct potentiometry, calcium by Arsenazo III dye colorimetry, phosphate by ammonium molibdate colorimetry. Haemoglobin A1C was analysed using reversed phase cation exchange chromatography on Adams™ HA-8160 (Arkray Inc, Kyoto, Japan/ Menarini, UK). Spot urine was collected and checked for microalbuminuria using Olympus microalbumin kit on Olympus 5400 analyser (Olympus, UK). Full blood count was analysed on Coulter LH780 (Beckman Coulter Inc, Brea, CA, USA) and ESR on Alifax Test 1 (HAEM-008) (Alifax S.p.A, Padova, Italy). Insulin was analysed in St. James's Hospital, Dublin, using the ST AIA-PACK IRI two-site immunoenzymometric assay (TOSOH Bioscience, Inc, San Francisco, USA).

Samples, identified by code only, were transported to Dublin City University, National Centre for Cellular Biotechnology for RNA and proteomics analyses. Metabolomic analyses were performed by Metabolon Inc. USA

The blood for RNA, proteomic and metabolomic analyses was sent to Dublin City University (DCU) within 1-2 hours of venepuncture. Two blood specimens of approximately 10mL were taken and the red blood cells were allowed to clot naturally. These specimens were processed in DCU within 3-4 hours of blood draw. Serum specimens from control volunteers (no history or symptoms of diabetes) were also collected and processed the same way. Upon arrival to Dublin City University, samples were re-coded (DS-1, DS-2…).

Blood specimens were processed by removing the serum from the clotted blood and placing into a 10mL centrifuge tube. The tubes were then centrifuged at room temperature for 15 minutes at 400 rcf (relative centrifugal force). After centrifugation the cleared serum was carefully removed and passed through a 0.45µm filter to further ensure

no particles / platelets were retained. The serum was then aliquoted into 1mL aliquots and stored at -80°C until analysed.

For metabolomic studies, blood specimens were re-coded by Metabolon Inc, as described in section 5.1.

Details of mRNA extraction, proteomics and metabolomic methods are presented in sections 3.1, 4.1 and 5.1.

Data were analysed using Microsoft Office Excel 2007 (Microsoft, , Redmond, WA 98052-6399, USA) and IBM SPSS 20 (IBM Corporation, New York, NY10504-1722, USA). Differences between groups were assessed using T-tests and Chi-squares, as appropriate. Relationships were assessed by correlation calculation, using Spearman's coefficients because of small group size.

3 Serum mRNA analysis in newly-diagnosed type 2 diabetes patients

3.1 Materials and methods

3.1.1 Identification of mRNA targets

Several differentially expressed mRNAs were recently investigated in glucose-responsive vs. glucose-unresponsive mouse insulinoma (MIN-6) cell lines. Our colleagues in Dublin City University recently reported a direct association between thioredoxin-interacting protein (Txnip) and glucose-stimulated insulin secretion in MIN-6 cell lines; specifically, increasing Txnip levels correlated with increased intracellular reactive oxygen species levels and with significant glucose-sensitive insulin secretion loss (91). Conversely, both transient and stable knock-down of Txnip expression was associated with glucose-stimulated insulin secretion recovery (91). In addition, mRNA encoded by following genes was detected in extracellular conditioned medium of MIN-6 and monkey kidney fibroblast cells engineered to produce human preproinsulin (PPI) (Vero-PPI): pancreatic and duodenal homeobox 1 (Pdx1), neuropeptide Y (Npy), early growth response 1 (Egr1), phospholipase D1 (Pld1), chromogranin B (Chgb), insulin 1 (Ins1), insulin 2 (Ins2), and actin β (Actb). (45). Serum from patients with type 2 diabetes and healthy controls was analysed for all of these.

3.1.2 RNA isolation from serum using TriReagent

Frozen serum samples were allowed to thaw on ice. Upon thawing, serum samples were aliquoted into 250μL in labelled Eppendorf tubes.

To each 250μL serum aliquot 750μL TriReagent was added. TriReagent/serum samples were allowed to sit for 5 minutes to ensure complete dissociation of nucleoprotein complexes. 0.2mL of chloroform was added to each tube and shaken vigorously for 15 seconds, then allowed to stand for 15 minutes at room temperature. The resulting mixture was then centrifuged at 13,000 rpm in a microcentrifuge for 15 minutes at 4°C. The colourless upper aqueous phase (containing RNA) was removed into a fresh RNase-free Eppendorf tube. Glycogen (Sigma, G1767) 1.25 µl (final concentration 120 µg/ml) and 0.5 ml of ice-cold isopropanol (Sigma, I9516) were added. The samples were mixed by inverting, incubated at room temperature for 10 minutes and stored at -20˚C overnight, to ensure maximum RNA precipitation.

Tubes were then centrifuged at 12,000 rpm for 30 minutes at 4˚C to pellet the precipitated RNA. Taking care not to disturb RNA pellet, the supernatant was removed and the pellet was subsequently washed by the addition of 750µL of 75% of ethanol and vortexed. Centrifugation was followed at 7,500 rpm for 5 minutes at 4°C. The supernatant was removed and the wash step was repeated. Each RNA pellet was allowed to air-dry for 10 minutes and subsequently re-suspended in 5µL of RNase free water. To facilitate dissolution, repeated pipetting was done (Figure 3.1.1).

3.1.3 RNA quantification using NanoDrop

RNA was quantified spectrophotometrically at 260nm and 280nm using the NanoDrop® (ND-1000 spectrophotometer). A 1μL aliquot of

RNA was placed on the nanodrop pedestal, which is the receiving optic fibre. A second fibre optic cable, the source fibre, is brought into contact with the liquid sample, causing the liquid to bridge the gap between the fibre optic ends. The ND-1000 software automatically calculated the quantity of RNA in the sample based on an OD260 being equivalent to 40mg/mL RNA. The software simultaneously measured the OD280 of the samples, allowing the purity of the sample to be estimated from the ratio of OD260/OD280. This was typically in the range of 1.8-2.0. A ratio of <1.6 indicated that the RNA may not be fully in solution. The RNA was diluted to 1 µg/µl stocks for the reverse transcription (RT).

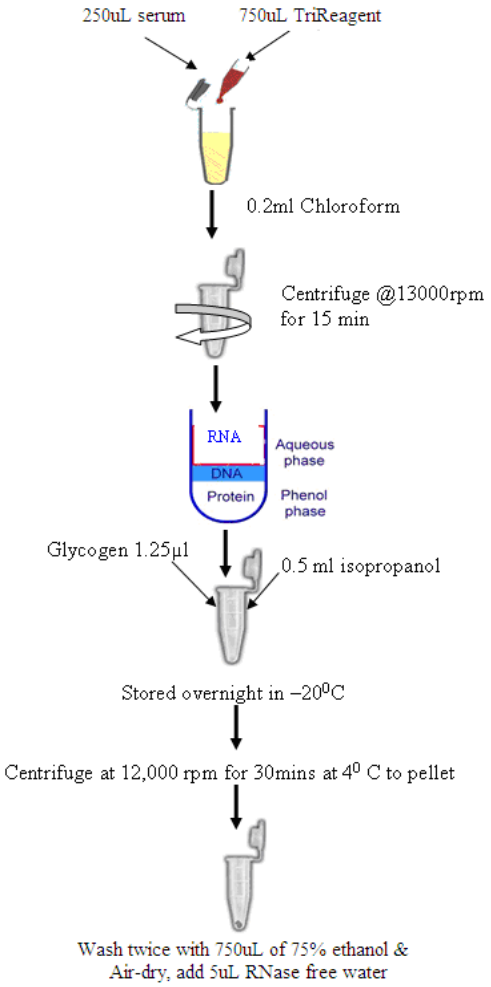

Figure 3.1.1 RNA isolation using TriReagent from serum (Adapted with permission from Sweta Rani's PhD Thesis, Investigation of molecular and cellular events associated with β cell function and elucidation of extracellular RNAs as potential biomarker for diabetes, Dublin City University, 2008)

3.1.4 Quantitative real time reverse transcription-polymerase chain reaction (qRT-PCR)

TaqMan probes are oligonucleotides that have fluorescent reporter dyes attached to the 5' end and a quencher moiety (molecule capable of quenching the fluorescence of the reporter) coupled to the 3' end. Hence, under normal circumstances, the fluorescent emission from the probe is low. During the PCR, the probe binds to the gene of interest and becomes cleaved by the polymerase, hence the reporter and quencher are physically separated and the fluorescence increases (Fig. 3.1.2)

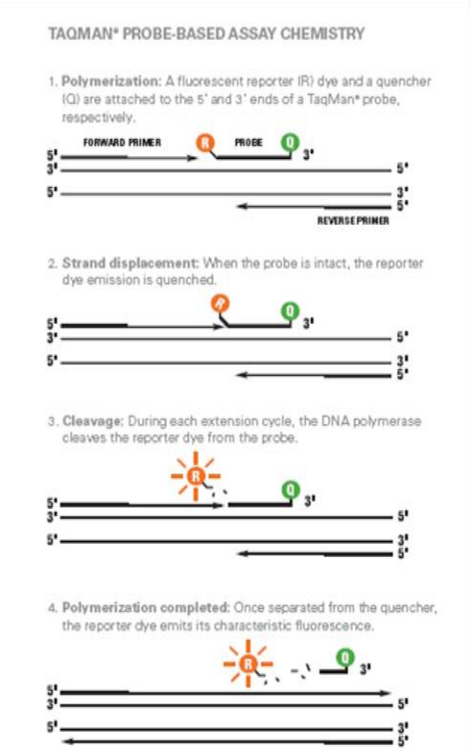

Figure 3.1.2 TaqMan qRT-PCR principle (*Adapted from product insert).*

Messenger RNA was copied to cDNA by reverse transcriptase using an oligo dT primer. First strand cDNA was synthesised by reverse

transcription (RT) by mixing 1 µL of oligodT with 4 µL of RNA in a 0.5 ml Eppendorf tube (Eppendorf, 0030 121 023) and heated at 70°C for 10 min followed by cooling on ice.

In order to exclude any amplification product derived from genomic DNA or any other contaminant that could contaminate the RNA preparation, total RNA without reverse transcription was used as a negative control. Water on its own was amplified as a negative control to rule out presence of any contaminating RNA or DNA.

The TaqMan® Real time PCR analysis was preformed using the Applied BioSystems Assays on Demand PCR Kits, using primer probe pairs as outlined in Table 3.1.1.

Two µl of the cDNA was added to the MicoAmp fast optical 96-well reaction plate (Applied BioSystems, 4346906) followed by 18 µl of reaction master mix (as outlined in Table 3.1.2)

Table 3.1.1 qRT-PCR primer and their assay ID used for serum study

Primer pair	Supplier	Supplier assay ID
Thioredoxin interacting protein	Applied BioSystems	Hs00197750_m1
Egr1	Applied BioSystems	Hs00152928_m1
Chromogranin B	Applied BioSystems	Hs00174956_m1
Pancreatic and duodenal homeobox 1	Applied BioSystems	Hs00426216_m1
Phospholipase D1	Applied BioSystems	Hs00160118_m1
Neuropeptide Y	Applied BioSystems	Hs00173470_m1
Insulin	Applied BioSystems	Hs00355773_m1
Pax4	Applied BioSystems	Mm01159036_m1
B-actin	Applied BioSystems	4352933E

Table 3.1.2 Reagents for Taqman® qRT-PCR reaction.

Reagents	Volume
Nuclease-Free water (Ambion, 9930)	6.8 µl
TaqMan® Fast Universal PCR master mix (2 X) (Applied BioSystems, 4352042)	10 µl
AmpErase® Uracil N-glycosylase (UNG) (Applied BioSystems, N8080096)	0.2 µl
Assay-on-demand	1 µl
Total	18 µl

The PCR protocol followed in this study was: activation, at 50°C for 2 min, followed by denaturation at 95°C for 20 s, followed by 40 cycles of denaturation at 95°C for 3 s and annealing/ extension at 60°C for 30s

Real-time PCR data was analysed using the comparative cycle threshold (Ct) method, which involves comparison of the Ct values of the samples of interest with a control or calibrator sample (such as an untreated sample). The Ct values of both the calibrator and the samples of interest are normalised to an appropriate endogenous control (in our case, β-actin), generating a ΔCt for both the sample of interest and the control/calibrator samples.

ΔCt = Ct [target] – Ct [endogenous control]

ΔΔCt is then calculated as the difference between ΔCt for the sample and calibrator.

ΔΔCt = ΔCt [sample] - ΔCt [calibrator]

Relative quantification (RQ) of target expression is calculated from the equation below as a difference of one Ct is equal to 2 fold change in expression level.

$RQ = 2^{-\Delta\Delta Ct}$

RQ values greater than one indicate an increase in expression (equivalent to fold values), while RQ values between zero and one indicate a reduction in expression levels. To obtain a fold value of RQ between 0 and 1, inversion of RQ is required (1/RQ).

RNA extraction was performed with help and guidance of Drs Sweta Rani and Erica Hennessy.

3.2 Results of mRNA extraction studies

3.2.1 Subjects

We recruited 19 patients (10 male, 9 female) in whom type 2 diabetes (T2DM) has been diagnosed up to 6 months previously, treated either with diet (n=8) or metformin (n=11) and 19 age/sex/BMI-matched controls. Their characteristics are presented in table 3.2.1.

Both patients and controls were instructed to attend having fasted from midnight the night before. Control subjects had oral glucose tolerance test to exclude diabetes.

Table 3.2.1 Characteristics of newly diagnosed type 2 patients (T2DM) and their controls

	T2DM	Controls	P
Age [years (±SD)]	51.2 (±8.2)	48.4(±7.3)	0.39
Sex (F:M)	9:10	9:10	1.0
BMI [kg/m (±SD)]	31.45 ± 3.42	29.64 ± 4.04	0.23
BP systolic [mmHg (±SD)]	137.6 (±16.8)	132.8 (±11.5)	0.45
BP diastolic [mmHg (±SD)]	83.8 (±6.7)	80.7 (±6.3)	0.27
Heart rate (beats/min)	68.5 (±9.6)	71.7 (±10.4)	0.32
Subjects taking beta-blockers	3/19	1/19	0.6
Waist/ hip ratio (±SD)	0.97 (±0.06)	0.93 (0.05)	0.10
Duration of diabetes [months (±SD)]	3 (± 2.4)	--	N/A

	T2DM	Controls	P
Cigarette smoking [pack-years (±SD)	13.2 (±18.9)	9.5 (±10.4)	0.45
Alcohol [units/wk (±SD)	8.32 (±16.13)	11.89 (±10.78)	0.42
Exercise [min/wk (±SD)]	148.68	225.26	0.15
HbA1C [% (±SD)]	7.43 (±1.71)	5.44 (±0.27)	<0.01
Fasting glucose [mmol/L (±SD)]	7.93 (±2.68)	5.12 (±0.37)	<0.01
Fasting insulin [mU/L (±SD)]	10.3 (±5.3)	8.7 (±7)	0.43
HOMA IR (±SD)	1.48 (±0.77)	1.13 (±0.89)	0.20
Total cholesterol [mmol/L (±SD)]	5.13 (±1.05)	5.56 (±0.82)	0.05
LDL [mmol/L (±SD)]	2.85 (±1.27)	3.36 (±1.57)	0.21
HDL [mmol/L (±SD)]	1.18 (±0.31)	1.37 (±0.47)	0.14
Triglyceride	1.80 (±1.44)	1.70 (±1.38)	0.82
Statin use (n, %)	12 (63%)	1(5%)	<0.01
Aspirin use (n, %)	11 (58%)	3 (16%)	0.02
Antihypertensive use (n,%)	5 (19%)	2 (10%)	0.40

3.2.2 Extracellular mRNA

Of the eight mRNA previously detected in the extracellular medium of the extracellular conditioned medium of MIN-6 and monkey kidney fibroblast cells engineered to produce human preproinsulin (Vero-PPI), we found two in the sera of patients with type 2 diabetes and controls: Txnip and Egr1 (45, 91). Expression of both these mRNAs was

compared to expression of endogenous control, β-actin, detected in both patients and healthy controls.

3.2.2.1Thioredoxin-interacting protein (Txnip)

Expression of Txnip in sera of patients with newly diagnosed type 2 diabetes and healthy controls was markedly heterogeneous. There was no significant difference in expression of Txnip, as calculated by independent T-test for ΔCtTxnip of patients with type 2 diabetes and ΔCtTxnip of controls (Figure 3.1.1, p=0.457). Data are presented in table 3.1.2. Matched samples (patients and corresponding healthy controls) are presented in the same row. Expression of Txnip is calculated as explained in section 3.1.4.

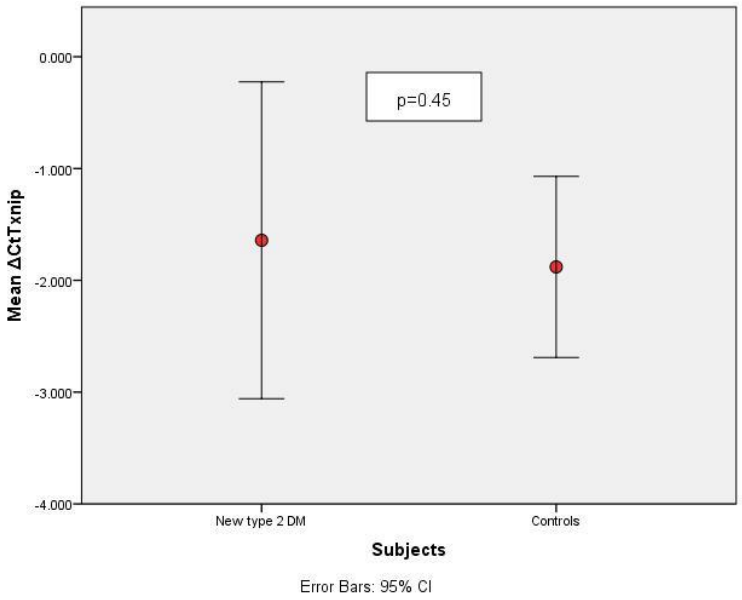

Figure 3.2.1 Expression of Txnip in patients with newly-diagnosed type 2 diabetes and their healthy controls. Error bars represent 95% confidence intervals.

Table 3.2.2 Txnip expression in patients with newly diagnosed type 2 diabetes (T2DM) and their healthy controls.

T2DM					Control					ΔΔ Ct	RQ	Fold
Sample	Code	Ct txnip	Ct b-actin	**Δ Ct**	Sample	Code	Ct Txnip	Ct b-actin	**Δ Ct**			
DS-30	T2N9	37.394	30.997	6.397	DS-32	M6	27.603	29.533	-1.930	8.327	0.003	-321.130
DS-28	T2N8	Undetected	38.432		DS-43	U16	32.596	34.506	-1.910			
DS-10	T2N4	32.716	34.321	-1.605	DS-3	M2	31.589	33.268	-1.679	0.074	0.950	-1.050
DS-9	T2N2	31.419	33.559	-2.140	DS-52	M10	31.320	32.095	-0.775	-1.365	2.576	2.576
DS-59	T2N12	36.253	38.339	-2.086	DS-55	M11	31.246	31.176	0.070	-2.156	4.457	4.457
DS-23	T2N6	31.522	33.305	-1.783	DS-18	U6	32.428	34.116	-1.688	-0.095	1.068	1.068
DS-41	T2N11	33.591	34.750	-1.159	DS-53	M9	35.159	34.835	0.324	-1.483	2.795	2.795
DS-14	T2N3	30.188	34.521	-4.333	DS-2	M1	28.371	29.488	-1.117	-3.216	9.292	9.292

T2DM					Control					ΔΔ Ct	RQ	Fold
Sample	Code	Ct txnip	Ct b-actin	**Δ Ct**	Sample	Code	Ct Txnip	Ct b-actin	**Δ Ct**			
DS-31	T2N10	Undetected	37.946		DS-49	U24	Undetected	39.340				
DS-15	T2N5	28.837	30.788	-1.951	DS-54	U20	Undetected	38.612				
DS-21	T2N7	32.664	35.110	-2.446	DS-16	U5	33.735	35.665	-1.930	-0.516	1.430	1.430
DS-103	T2N20	36.847	36.639	0.208	DS-19	M5	33.766	35.323	-1.557	1.765	0.294	-3.400
DS-106	T2N22	undetected	36.698		DS-51	U19	35.093	39.031	-3.938			
DS-110	T2N23	35.583	38.129	-2.546	DS-37	U13	34.653	39.761	-5.108	2.562	0.169	-5.900
DS-111	T2N24	undetected	38.685		DS-1	U4	36.524	37.104	-0.580			
DS-117	T2N25	34.432	37.268	-2.836	DS-36	U11	35.289	38.317	-3.028	0.193	0.875	-1.100
DS-134	T2N28	36.474	37.247	-0.774	DS-33	U10	36.102	36.144	-0.042	-0.732	1.660	1.700

T2DM					Control					ΔΔ Ct	RQ	Fold
Sample	Code	Ct txnip	Ct b-actin	**Δ Ct**	Sample	Code	Ct Txnip	Ct b-actin	**Δ Ct**			
DS-135	T2N29	34.473	39.437	-4.964	DS-8	M3	35.843	38.260	-2.417	-2.547	5.844	5.800
DS-96	T2N19	32.044	34.656	-2.613	DS-72	M12	34.633	39.294	-4.661	2.049	0.242	-4.100

In correlation analysis, data of the patient with newly-diagnosed type 2 diabetes who was a significant outlier (T2N9) were disregarded as they were skewing the results significantly. It is unclear what is a cause of the significantly different result in T2N9—it is derived both from decreased expression of Txnip in subject T2N9, as well as increased expression of β-actin, when comparing it with other subjects with T2DM. As presence of β-actin demonstrates no issues with RNA extraction or PCR process, it is most likely this result is due to genuinely low Txnip level in this individual, the reason for which is unclear. The clinical characteristics of T2N9 were similar to the other patients with newly diagnosed type 2 diabetes. As inclusion of T2N9 produced statistically significant results, which could potentially be misleading, we decided to exclude this sample from further statistical analysis.

In the remainder of the patients with newly-diagnosed diabetes, there was no correlation between ΔCtTxnip and age of patient, fasting glucose, fasting insulin, BMI, HbA1C, smoking (pack-years), exercise (self-reported in minutes per week), systolic or diastolic blood pressure, waist-hip ratio, HOMA%B, HOMA%S, HOMA-IR, total cholesterol or LDL.

There was no difference in Txnip expression in patients with type 2 diabetes who took metformin, medication postulated to act on hepatic insulin sensitivity through modification of Txnip, compared to patients who were only diet-controlled (Figure 3.2.2)(89, 120).

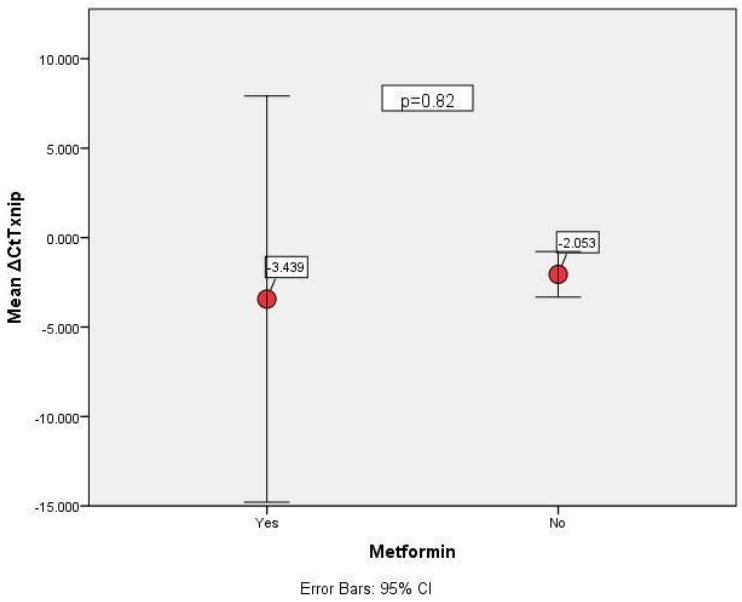

Figure 3.2.2 Expression of mean ΔCtTxnip in patients with newly-diagnosed type 2 diabetes depending on whether they were taking metformin (n=11) or were diet controlled (n=8). Error bars delineate 95% confidence intervals.

ΔCtTxnip was inversely correlated to total cholesterol and HDL level in patients with diabetes who were not on statins (Spearman's ς-0.812, p=0.05 and Spearman's ς -0.841, p=0.036, respectively) (Figures 3.2.3 and 3.2.4)

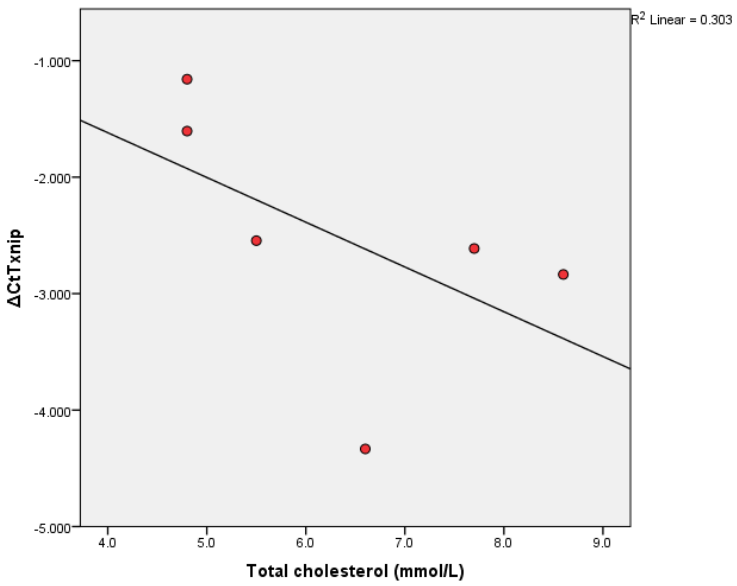

Figure 3.2.3 Correlation between ΔCtTxnip and total cholesterol in patients with newly-diagnosed type 2 diabetes who were not on statin treatment.

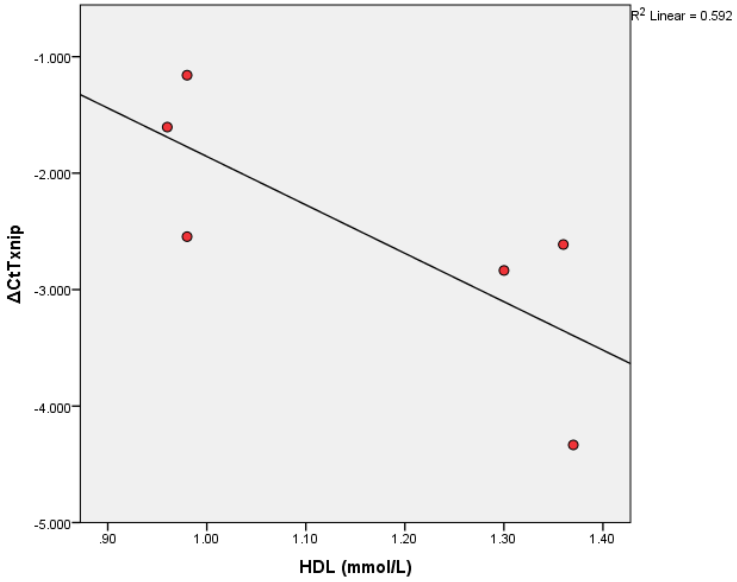

Figure 3.2.4 Correlation between ΔCtTxnip and HDL in patients with newly diagnosed type 2 diabetes who were not taking statins

3.2.2.2 Early growth response 1 (Egr1)

Egr1 was detected in 18 out of 38 samples we analysed. More specifically, it was detected in 9 out of 19 patients with newly diagnosed type 2 diabetes and 9 of 19 healthy controls. The samples were analysed in two separate batches, 11 sample pairs (patients and controls) first and the remaining 8 sample pairs at a later date. No Egr1 was found in the second batch of 8 sample pairs.

It is unclear what caused the non-detection in the entire second batch as the methodology used was the same. In the first batch, in samples in which Egr1 was detected the levels were very low. When the Ct goes beyond 40, it is designated as undetected, as at this point the instrument cannot distinguish between background noise in the system and actual signal from Egr1 detection. The only discernible difference between the batches was the prolonged storage time at -80°C. As there are RNAses present in the serum, prolonged storage time might have led to RNA degradation. We wonder whether prolonged storage time might have pushed the previously low Egr1 levels in both patients and controls into the undetectable range, beyond the level of sensitivity for the instrument.

Here we present data from the first 11 patient/control sample pairs.

The results are presented in table 3.2.3.

Table 3.2.3 Egr1 expression in patients with newly diagnosed type 2 diabetes and their healthy controls.

T2DM					Control							
Sample	Code	Ct Egr 1	Ct β-actin	Δ Ct	Sample	Code	Ct Egr 1	Ct β-actin	Δ Ct	ΔΔ Ct	RQ	fold
DS-30	T2N9	37.930	35.437	2.493	DS-32	M6	Undetected	38.678				
DS-28	T2N8	36.560	31.916	4.644	DS-43	U16	36.008	35.165	0.843	3.801	0.072	-13.940
DS-10	T2N4	37.034	34.464	2.570	DS-3	M2	35.578	33.094	2.484	0.086	0.942	-1.060
DS-9	T2N2	38.036	33.901	4.135	DS-52	M10	34.451	32.249	2.202	1.933	0.262	-3.820
DS-59	T2N12	Undetected	38.779		DS-55	M11	33.059	31.542	1.517			
DS-23	T2N6	Undetected	33.545		DS-18	U6	36.115	33.127	2.988			

T2DM					Control							
Sample	Code	Ct Egr 1	Ct β-actin	Δ Ct	Sample	Code	Ct Egr 1	Ct β-actin	Δ Ct	ΔΔ Ct	RQ	fold
DS-41	T2N11	37.310	33.286	4.024	DS-53	M9	38.134	33.654	4.480	-0.456	1.372	1.370
DS-14	T2N3	38.356	35.221	3.135	DS-2	M1	34.325	32.308	2.017	1.118	0.461	-2.170
DS-31	T2N10	38.741	35.000	3.741	DS-49	U24	37.363	34.951	2.412	1.329	0.398	-2.510
DS-15	T2N5	36.229	33.699	2.530	DS-54	U20	35.072	32.599	2.473	0.057	0.961	-1.040
DS-21	T2N7	38.103	33.242	4.861	DS-16	U5	Undetected	35.030				
DS-103	T2N20	Undetected	36.639		DS-19	M5	Undetected	35.323				
DS-106	T2N22	Undetected	36.698		DS-51	U19	Undetected	39.031				

T2DM					Control							
Sample	Code	Ct Egr 1	Ct β-actin	Δ Ct	Sample	Code	Ct Egr 1	Ct β-actin	Δ Ct	ΔΔ Ct	RQ	fold
DS-110	T2N23	Undetected	38.129		DS-37	U13	Undetected	39.761				
DS-111	T2N24	Undetected	38.685		DS-1	U4	Undetected	37.104				
DS-117	T2N25	Undetected	37.268		DS-36	U11	Undetected	38.317				
DS-134	T2N28	Undetected	37.247		DS-33	U10	Undetected	36.144				
DS-135	T2N29	Undetected	39.437		DS-8	M3	Undetected	38.260				
DS-96	T2N19	Undetected	34.656		DS-72	M12	Undetected	39.294				

Egr1 was significantly more expressed in patients with newly diagnosed type 2 diabetes with ΔCtEgr1 at 3.570 (± 0.922) vs. ΔCtEgr1 of 2.380 (± 1.004) in healthy controls (p=0.019) (Figure 3.2.5).

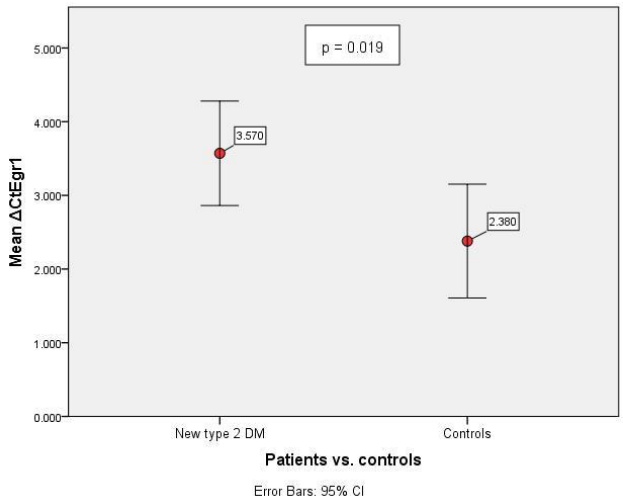

Figure 3.2.5 Mean Egr1 expression in patients with newly diagnosed type 2 diabetes vs. controls.Error bars delineate 95% confidence intervals.

In patients with type 2 diabetes, ΔCtEgr1 was inversely correlated with waist-hip ratio (Spearman's ρ -0.786, p=0.021) (Figure 3.2.6).

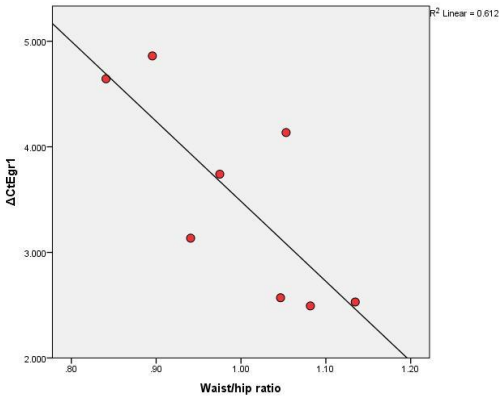

Figure 3.2.6 Correlation between ΔCtEgr1 and waist/hip ratio in patients with newly diagnosed type 2 diabetes.

Apart from the clear relationship between the ΔCtEgr1 and waist/hip ratio, there was no significant correlation between ΔCtEgr1 and any marker of glycaemic/ lipaemic control or metabolic health in patients with newly diagnosed type 2 diabetes (BMI, blood pressure, heart rate, age, smoking in pack-years, exercise level in minutes/week, fasting glucose and fasting insulin level, HOMA%B, HOMA%S, HOMA-IR, total cholesterol, HDL, LDL, triglyceride level)

In healthy controls, ΔCtEgr1 was inversely correlated with systolic blood pressure (Spearman's ρ -0.667, p=0.05; figure 3.2.7) and heart rate (Spearman's ρ -0.765, p=0.016; figure 3.2.8), but it bore no relationship to any other parameter of metabolic health tested.

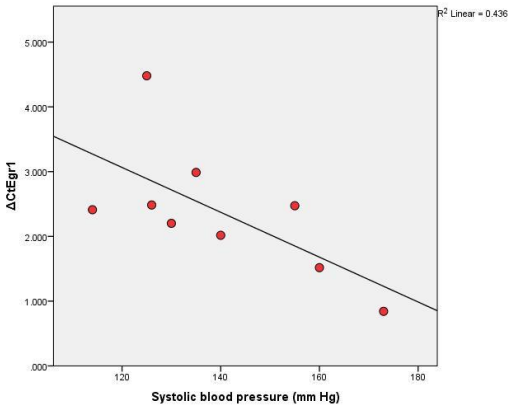

Figure 3.2.7 Correlation of ΔCtEgr1 and systolic blood pressure in healthy controls.

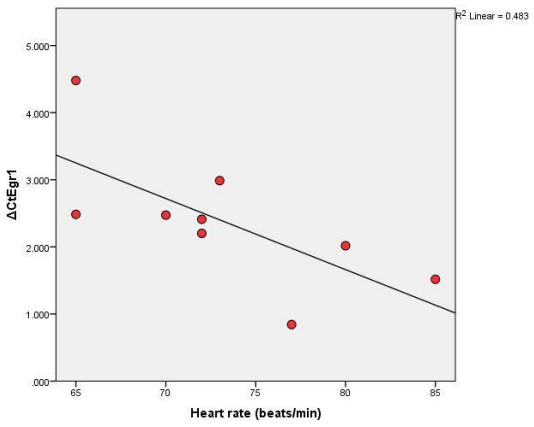

Figure 3.2.8 Correlation between ΔCtEgr1 and heart rate in healthy controls.

3.2.3 Summary of mRNA biomarker studies

There was no significant difference of expression of thioredoxin-interacting protein (Txnip) between patients with newly-diagnosed diabetes and their controls.

In patients with newly-diagnosed diabetes not taking cholesterol-lowering medications, Txnip expression was inversely correlated to total cholesterol, driven by inverse correlation to HDL.

Egr1 was significantly more expressed in patients with newly diagnosed type 2 diabetes, when compared to healthy control subjects.

In patients with newly-diagnosed type 2 diabetes, Egr1 expression was inversely correlated with waist-hip ratio; this was not observed in healthy controls. In healthy controls, Egr1 expression was inversely correlated with systolic blood pressure and heart rate, but there was no relationship with any other metabolic health parameter examined. Relationship between Egr1 and systolic blood pressure was not present in patients with newly diagnosed diabetes type 2.

3.3 Discussion on findings of serum mRNA analysis

3.3.1 Txnip

Thioredoxin-interacting protein, a part of one of the major redox systems in mammals, thioredoxin (TRX) system, binds to the active cysteine residue of thioredoxin and inhibits its antioxidative function (68). Additionaly, Txnip acts independently of its binding to TRX on cell growth inhibition through arrestin domain-mediated suppression of glucose uptake and metabolic reprogramming (72, 121). Txnip appears to regulate both insulin-dependent and insulin-independent pathways of glucose uptake in human skeletal muscle through a phosphorylated G protein-coupled receptor (72, 79). Txnip induces gluconeogenesis in the liver and blocks cellular glucose uptake (74, 122).

In our study, there was no difference between Txnip expression in sera of patients with newly-diagnosed type 2 diabetes and their matched controls (Figure 3.2.1)

The first important question is: how much Txnip will wash off into the serum from tissues in which it is differentially expressed? In the only study known to us which simultaneously looked at Txnip expression in the tissue and Txnip serum levels, the over-expression in the tissue was not reflected in the increased serum level (123). It is therefore possible that the possible differential expression in tissues, observed in other human studies, did not translate into differentially expressed serum levels in our study (79).

We found no significant correlation between serum Txnip expression and fasting glucose or fasting insulin level, or indeed HbA1C.

In various cell studies, glucose increased Txnip expression in tissues: in pancreatic islets, fibroblasts, mesangial kidney cells, rat cardiomyocytes and vascular endothelial and smooth muscle cells, human adipocytes (79, 124-128). In Parikh's study, Txnip expression was increased in muscle biopsies of individuals with impaired glucose tolerance and diabetes, both in fasting samples and samples after 2h of hyperinsulinaemic-euglycaemic clamp, compared to healthy controls (79).

In the same study, when serial muscle biopsies of healthy individuals were analysed before and after 2 hours of hyperinsulinaemic-euglycaemic clamp, Txnip mRNA expression was suppressed in the second sample, i.e. was suppressed by insulin (79).

Parikh points out that in insulin receptor-knockout mice treatment of streptozotocin-treated mice with insulin failed to suppress Txnip expression, indicating that intact insulin signalling was necessary for Txnip suppression by insulin (79).

While we did not have the benefit of the hyperinsulinaemic-euglycaemic clamp to assess paired samples in the same subject and hence could not measure glucose uptake or effect of insulin on Txnip, while keeping glucose level steady, we would have expected an increase of Txnip expression with raised fasting glucose, either as a spill-over from the liver or from the muscle. Txnip over-expression is associated with gluconeogenesis. Liver insulin resistance and, consequently, hyperglycaemia due to gluconeogenesis, is the pathophysiological basis for raised fasting glucose levels (74, 129), but, again, this pattern of relationship was not observed in our study as

reflected in Txnip mRNA. A possible explanation for this again might have arisen from different sample choice: as we studied serum, not tissue Txnip mRNA expression, a possible tissue expression increase, be it liver or muscle, may not have translated into an increased serum level.

We found no difference in Txnip expreession in patients with diabetes who took metformin compared to those who were treatment-naïve (Figure 3.2.2). Metformin acts through improvement of hepatic insulin sensitivity via induction of cAMP kinase, causing enhancement of insulin-mediated suppression of gluconeogenesis and reduction of glucagon-stimulated gluconeogenesis (130-132). While two recent studies suggest that AMP kinase is a regulator of Txnip transcription via modulation of carbohydrate response element-binding protein (ChREBP) and that transcription of Txnip is repressed by metformin, no support for these findings could be found in the sera of our patients (89, 120). This, again, could be due to the increased tissue levels of mRNA not spilling into the sera in amount sufficient for detection.

Another fact which might have affected our results was the absence of difference in insulin resistance between our patients and controls (Table 3.2.1). Our patients were significantly less insulin resistant than previously reported cohorts, with a HOMA-IR of 1.48±0.77. In a study of Mexican American subjects randomly selected from 2000 Census data, HOMA-IR was 3.8 in 39% of subjects; this threshold was taken as a mark of insulin resistance. In a study of subjects with normal glucose tolerance, randomly selected among staff in a Spanish hospital, HOMA-IR 75th percentile was at 2.6 (133, 134). Compared to these population data, our patients with newly diagnosed type 2 diabetes are surprisingly insulin sensitive.

It is difficult to compare our study to any of the above described. Firstly, we analysed Txnip mRNA in the serum, while all of the other data are either from non-human cell studies, cell studies or tissue samples. Our study also has a limitation of being a snapshot of fasting metabolism, rather than a reflection of a dynamic process of glucose handling.

We wonder if it is possible that non-detection of differentially expressed levels of Txnip m RNA in our study could have been, at least in part, due to early stage of the disease in our patients, as evidenced by recent diagnosis, but, even more, by less insulin resistance than in some other studies. We intend to assess if serum expression of Txnip is different in patients with poorly controlled, longer-term diabetes.

3.3.2 Egr1

Egr 1 is a zinc-finger protein, functioning as a transcriptional regulator. In cell cultures, Egr1 expression is reported to be both inducible and repressed by insulin; glucose induces Egr1 mRNA transcription in various β-cell models (83, 92, 94, 135, 136).
In diabetic Zucker rats, Egr1 is up-regulated and this has no effect on glucose-stimulated insulin secretion. Egr1 gene silencing inhibits proliferation of INS-1 cells in a glucose-independent manner, suggesting reduced Egr1 expression may contribute to decreased β-cell proliferation and consequent β-cell failure (82). It has also been proposed that Egr1 overexpression is the mechanism by which

hyperinsulinism induces insulin resistance in adipocytes—by blocking phosphatidylinositide 3-kinases/ protein kinase B (PI3K/Akt) signalling through phosphatase and tensin homologue (PTEN) and augmenting extracellular signal-regulated kinase/ mitogen-activated protein kinase (Erk/MAPK) signalling through geranylgeranyl diphosphate synthase (GGPPS) (137).

In our study, Egr1 was significantly more expressed in patients with newly-diagnosed type 2 diabetes than in their healthy controls. While this may appear expected, considering that insulin increases Egr1 expression, there was no difference in fasting insulin level between patients and their healthy age-, gender- and BMI-matched controls. There was also no correlation between insulin level and Egr1 expression.

There was no correlation between Egr1 expression and any other marker of glycaemic control available to us (fasting glucose, HbA_1C) either when the group was analysed as a whole or when only patients with type 2 diabetes were analysed separately.

There is only one previous Egr1 human serum expression study known to us; this has shown Egr1 increase 1 and 2 hours after 75 g of oral glucose load as part of the oral glucose tolerance test (83). While fasting glucose was higher in the patients with newly diagnosed diabetes than in controls, there was no correlation observed between glucose level and Egr1 expression in our study, so it is possible that other postprandial factors, rather than glucose level per se, influence Egr1 expression.

It is also known that Egr1 is a major transcription factor involved in atherosclerosis (138). Egr1 is five-fold more expressed in human atherosclerotic lesions compared to the adjacent tunica media (139)

and its pro-atherosclerotic action is insulin-induced; once stimulated by insulin, increased transcription of Egr1 entices endothelial cell proliferation and re-growth following mechanical injury (140).

When only patients with newly-diagnosed type 2 were analysed, negative correlation was found between Egr1 expression and waist-hip ratio. Waist-hip ratio is a known parameter of metabolic syndrome and Egr1 is an atherosclerosis marker; it is therefore somewhat surprising that Egr1 expression would be decreasing as the waist-hip ratio increases (141). We cannot find any reasonable hypothesis that would explain the observed phenomenon.

In our study, there was no correlation between Egr1 and cardiovascular history (ischaemic heart disease, stroke disease) or blood pressure values, statin or antihypertensive medications use.

In diabetic mice, Egr1 induces diabetic nephropathy by activating heparanase, an enzyme responsible for decomposition of glomerular basement membrane (142). We have found no relationship between Egr1 and creatinine levels or albumin-creatinine ratio in patients with newly-diagnosed diabetes.

There is a paucity of human in vivo studies of Egr1 expression available for comparison. *In vivo* studies of patients with long-standing type 2 diabetes and vascular complications are needed to assess if serum Egr1 can be used as a non-invasive marker of vascular atherosclerosis. Considering the problems with detection in our second batch, which was stored for a longer time, it may be wise to perform all the analyses as soon to draw time as possible.

4 Proteomics analysis in patients with established type 1 diabetes and newly-diagnosed type 1 diabetes

4.1 Materials and methods

Proteomic analysis was performed on serum samples from patients with newly-diagnosed type 1 diabetes, long-term type 1 diabetes, and two sets of controls: healthy controls (as defined in section 2.1, tables 4.2.1, 4.2.2 and 4.2.3) and a cohort of patients with various autoimmune conditions, whose sera were available from a previous experiment to our colleagues in DCU. The autoimmune group was included in this experiment to allow identification of markers directly related to type 1 diabetes, rather than markers of general autoimmune/inflammatory conditions.

This additional group consisted of serum samples from patients with a range of autoimmune and inflammatory diseases such as rheumatoid arthritis, ulcerative colitis, asthma, eczema, systemic lupus erythematosus, Hashimoto's thyroiditis, psoriatic arthritis and pernicious anaemia. The mean age of these patients was 31.4 ± 4.9 years. Unfortunately, we have no other biometric data or data related to glucose metabolism on them.

4.1.1 Serum pre-treatment with ProteoMiner™

Serum samples were prepared using the ProteoMiner Protein Enrichment Kit (BioRad, 163-3007). ProteoMiner is a column-based technique, with the column containing a highly diverse bead-based library of peptide ligands. High-abundant proteins saturate their high affinity ligands and excess protein is washed away, while low abundant proteins are concentrated on their specific ligands. (Figure 4.1.1)

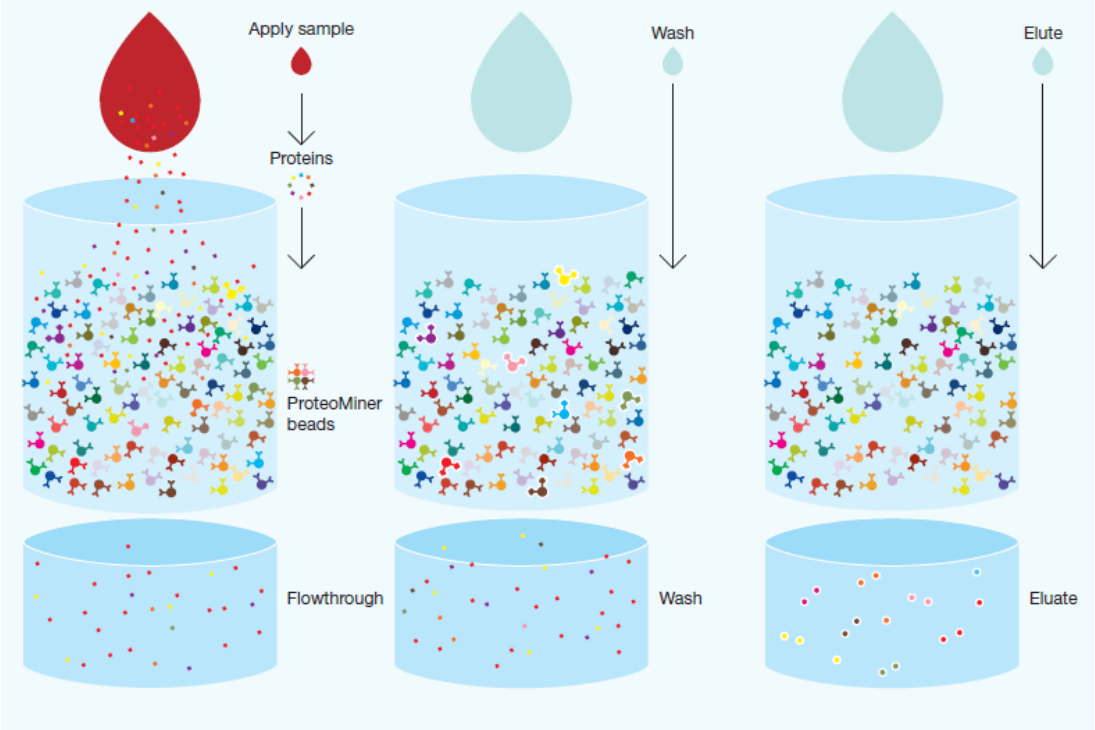

Figure 4.1.1. ProteoMiner™ technology. Each unique hexapeptide binds to a unique protein sequence. Because the bead capacity limits binding capacity, high-abundance proteins quickly saturate their ligands and excess protein is washed out. In contrast, low abundance proteins are concentrated on their specific ligands, thereby decreasing the dynamic range of proteins in the sample. When analysed in downstream applications, the number of proteins detected is dramatically increased. (Adapted from BIORAD ProteoMiner™ kit insert, available at http://wolfson.huji.ac.il/purification/PDF/AlbuminRemoval/BIORAD_ProteoMiner.pdf)

ProteoMiner columns were prepared according to manufacturer's instructions, 1mL of serum was then applied to column and rotated end-on-end for 2 hours to allow binding of protein to ligand. Column was then washed and proteins eluted in 300µL of elution buffer.

50µL of elute was then processed using the ReadyPrep 2D Cleanup Kit (BioRad, 163-2130) according to manufacturer's instructions. This kit allows for precipitation of protein leaving behind salts, detergents and nucleic acid contaminants. Precipitated protein was re-suspended in 100µL of mass-spec grade water. Protein concentration was assessed

using Quick-Start Bradford Dye Reagent 1X (BioRad, 500-0205). Protein samples were diluted 1:4 with water, then 5μL diluted sample was added per well of a 96 well plate. Each sample was analysed in triplicate. 200μL of Bradford reagent was added to sample and incubated for 15 minutes. Absorbance was then read at 595nm. Using the calculated concentration, 20μg of each sample was used for the digestion steps.

To prepare protein samples for digestion, samples were first incubated with 1μL 5mM dithiothreitol reducing agent for 30 minutes at 37°C. 1μL of 25mM iodoacetamide was then added to each sample and incubated in the dark for 20 minutes at room temperature. Digestion of protein samples was performed with Endoproteinase Lys-C (Promega, V1071) at a ratio of 100:1, protein to enzyme, ie. 20μg of protein was digested with 0.2ug of Endoproteinase Lys-C. Samples were incubated at 37°C for 3 hours to allow the digestion to occur. Samples were subsequently digested with trypsin. 7.5μL of trypsin and 80μL of 50mM ammonium bicarbonate was added to each sample and incubated overnight at 37°C. Following overnight incubation, 2% trifluoroacetic acid (TFA) and 20% acetonitrile were added to each sample to stop the trypsin digestion.

4.1.2 Label-free liquid chromatography coupled to tandem mass spectrometry (LC-MS/MS)

Following the preparation of serum samples by ProteoMiner™, label-free liquid chromatography coupled to tandem mass spectrometry (LC-MS/MS) was performed for analysis of peptide composition in

these samples. LC-MS/MS measures the peptide constituents rather than intact proteins, as peptides are more suitable for LC analysis and have better ionization properties.

Label-free LC-MS/MS does not utilise isotopic labelling of proteins. Instead, signal intensities are directly compared between LC-MS/MS runs. Label-free LC-MS/MS is now being used more frequently where previously 2D DIGE (two-dimensional difference in gel electrophoresis) gels were used as standard for biomarker discovery (143). 2D DIGE gels have several limitations, including insufficient resolving power to fully separate peptides in the gel, difficulty in analysing hydrophobic proteins, restricted sample throughput, complex sample preparation, incomplete labelling, as well as high costs (144). Label-free LC-MS overcomes these issues while allowing increased proteome coverage compared to gel based techniques (145).

LC is the most commonly used method for separating peptides before downstream mass spectrometry analysis (144)

The mass spectrometer consists of three main components: the ionisation source which converts the eluting peptides into the gas phase; the mass analyser which separates the ions based on the mass to charge ratio (m/z); the detector which registers relative abundance of ions (144).

In this study, tandem mass spectrometry was employed. This incorporates several mass analysers in series, which enables ions from the first analyser (parent ions) to undergo collision induced dissociation to generate product ions; these are then separated based on m/z in the subsequent mass analysers. Detection of parent and daughter ions allows extra confidence in peptide identification. MS/MS spectral files from the mass spectrometer, containing m/z

information of parent and product ions of each peptide, can be compared to identify differentially abundant ions or peptides which can be directly searched against a database of proteins which have been digested in silico.

To prepare the samples for mass-spectrography analysis, digested peptides were processed using PepClean C-18 Spin Columns (Pierce, 89870) according to manufacturer's instructions to remove interfering contaminants and chemicals. Peptide samples were eluted in 80μL of 80% acetonitrile (ACN) dried down using a speed-vac (MAXI dry plus) and stored at -20°C until required.

When ready for MS analysis, peptide samples were re-solubilised in 80μL of LC-MS grade water with 0.1% TFA and 2% ACN. 40μL was then transferred to glass vials, and then to autosampler on the MS instrument. Peptides were first submitted to the nano-LCMS/MS using an Ultimate 3000 system (Dionex) coupled to an LTQ-Orbitrap XL mass spectrometer (Thermo Fisher Scientific) operating in positive mode with a spray voltage of 1.6kV. 6.5μL of each sample was injected onto a C18 pre-column (300μm inner diameter x 5mm; Dionex) at 25μL/min in 5% ACN, 0.05% TFA. After a 3 minute desalting step, the pre-column was switched on line with the analytical column (75μm inner diameter x 25cm PepMap C18; Dionex) equilibrated in 98% solvent A (2% ACN, 0.05% TFA) and 2% solvent B (98% ACN. 0.04% FA). Peptides were eluted using a 10-35% gradient of solvent B during 150 minutes at a 300nL/min flow rate.

Data were acquired with Xcalibur software version 2.0.7 (Thermo Fisher Scientific). The mass spectrometer was operated in the data-dependent mode and was externally calibrated. Survey MS scans were acquired in the Orbitrap in the 300-2000m/z range with the resolution set to a value of 60,000 at m/z 400. Up to seven of the most

intense multiply charged ions (1+, 2+ and 3+) per scan were CID fragmented in the linear ion trap. A dynamic exclusion window was applied within 40s. All tandem mass spectra were collected using normalised collision energy of 35%, an isolation window of 3m/z, and one microscan.

Data analysis was performed using Progenesis LC-MS software available from Non-Linear Dynamics. Raw MS data files were imported to Progenesis LC-MS software package. A reference run is selected as the sample which is most representative of the data; all additional sample runs are then aligned to the reference sample run. Alignment of sample runs allows correction of variable peptide retention times during chromatographic separation and hence allows comparison of different sample runs. Once sample runs have been aligned, the software is then able to detect features in each run. Detected features are then filtered based on an ANOVA p-value of less than 0.2; this cut-off value was chosen so as not to exclude too many peptides from the analysis, as subsequent identified proteins would be filtered with more stringent criteria at a later stage. From this list of filtered features a principal component analysis (PCA) plot is generated.

Principal component analysis is a statistical technique used for finding patterns in data of high dimension. The MS/MS data from this list of filtered features is then exported into the external search engine MASCOT to match these identified features to known peptides, using the following search criteria: database-Swissprot/UniProt, enzyme-trypsin, allow up to 2 missed cleavages, taxonomy-homo sapiens, fixed modifications carbamidomethyl(C), variable modifications-oxidation (M), peptide tolerance-10ppm, MS/MS tolerance-0.8Da, and peptide charge-2+, 3+ and 4+. Once identifications have been assigned, this information is then imported to progenesis. Various

statistical criteria can then be applied to identified peptides to generate a list of proteins. For this experiment, a statistical criterion of ANOVA p-value less than 0.05, and peptide number greater than one was applied to generate lists of differentially expressed proteins

4.1.3 Validation of proteomic targets

ELISAs were used for validation of targets identified from the proteomic profiling study. Validation was performed on the same 8 newly diagnosed type 1 diabetes (T1DM new), established diabetes (T1DM old), and matched controls (control new and control old) serum specimens used for the profiling experiment, as well as an additional 22 T1DM old and control old specimens.

4.1.3.1 Vitronectin

A vitronectin ELISA kit was sourced from American Diagnostica GmbH (803). Serum specimens were diluted by a factor of 4,000 using dilution buffer. Standards were reconstituted as per manufacturer's instructions using dilution buffer. 100µL of diluted samples or standards were added to each well, and incubated for 1 hour at room temperature on a shaker at 250rpm. The plate was then washed 4 times using wash buffer and excess liquid was removed from the plate by tapping on absorbent paper 4-5 times between each wash step. 100µL of detection antibody was added to each well and incubated for 1 hour at room temperature on a shaker at 250rpm. The plate was then washed 4 times using wash buffer, and excess liquid was removed after each wash step by tapping the plate on absorbent paper. 100µL of substrate was added and incubated for 5 minutes at

room temperature. 50µL stop solution was added and plate was read at 450nm. A polynomial standard curve was plotted using the absorbance of the standards. Using the equation of the line the vitronectin concentration was calculated for each sample.

4.1.3.2 Clusterin

A clusterin ELISA was sourced from Phoenix Pharmaceuticals (EK-018-35). Serum specimens were diluted by a factor of 6,000 using assay buffer. Standards were reconstituted as per manufacturer's instructions using assay buffer. 300µL assay buffer was added to each well of the ELISA plate and allowed to stand for 5 minutes; buffer was then removed and plate tapped on absorbent paper to remove excess liquid. 100µL of diluted samples or standards were added to each well and incubated for 2 hours at room temperature on a shaker at 350rpm. The plate was washed four times using assay buffer and tapped on absorbent paper to remove excess liquid between each wash step. 100µL of detection antibody was added to each well and incubated for 2 hours at room temperature on a plate shaker at 350rpm. The plate was then washed four times, tapping on absorbent paper between each wash. 100µL substrate solution was added and incubated for 30 minutes at room temperature on a shaker at 350rpm. 100µL stop solution was added and absorbance was read at 450nm on a plate reader. A standard curve was plotted as log concentration versus log absorbance. The equation of the line was used for calculation of clusterin concentration in serum specimens.

4.1.3.3 Vitamin K-dependent protein S

A vitamin K-dependent protein S ELISA was sourced from USCN Life Science Inc. (E1971h). Serum specimens were diluted by a factor of 10 using sample diluent. Standards were reconstituted as per the manufacturer's instructions using sample diluent. 50µL of diluted samples or standards were added to each well, followed by 50µL of detection reagent A, and incubated for 1 hour at 37°C. The plate was washed three times using wash buffer, and tapped on absorbent paper after the last wash to remove excess liquid. 100µL of detection reagent B was added and incubated for 45 minutes at 37°C. The plate was washed five times with wash buffer, and tapped on absorbent paper after the last wash. 90µL of substrate solution was added to each well and incubated at 37°C for 30 minutes. 50µL of stop solution was added and absorbance read at 450nm on a plate reader. A 4–parameter logistic standard curve was plotted and using the equation of the line vitamin K-dependent protein S concentration in serum specimens was calculated.

4.1.3.4 Apolipoprotein L1

An apolipoprotein L1 ELISA kit was sourced from USCN Life Science Inc. (E9374Hu). Serum specimens were diluted by a factor of 5 using PBS. Standards were reconstituted as per the manufacturer's instructions using standard diluent. 100µL of diluted samples or standards were added to each well and incubated for 2 hours at 37°C. Liquid was removed from the wells, and without washing, 100µL of detection reagent A was added and incubated for 1 hour at 37°C. The plate was washed three times using wash solution and tapped on absorbent paper after each wash to remove excess liquid. 100µL of detection reagent B was added to each well and incubated for 30

minutes at 37°C. The plate was washed five times using wash solution and tapped on absorbent paper after each wash. 90µL of substrate solution was added to each well and incubated for 15 minutes at 37°C. 50µL stop solution was added to each well and absorbance read at 450nm on a plate reader.

Mass-spectrography instrument was run and lists of differentially expressed proteins generated by Dr. Paul Dowling. ELISAs were run by Dr Erica Hennessy.

4.2 Results

4.2.1 Subjects

4.2.1.1 Patients with newly-diagnosed type 1 diabetes

We recruited 8 patients with type 1 diabetes diagnosed within six months prior to entering the study. They were instructed to come in fasting (defined as no food from midnight on the day before). They were instructed not to take any insulin on the morning of the test. The last 'allowed' insulin dose was the long acting insulin the night before. If they were taking the long-acting insulin in the morning, they were instructed to take it after the test visit. . Their results were compared to their age/sex/BMI-matched controls.

The characteristics of the patients with newly-diagnosed type 1 diabetes and their healthy controls are presented in table 4.2.1.

4.2.1.2 Patients with established type 1 diabetes

From the cohort of patients with established diabetes type 1, we recruited 8 patients with long-term type 1 diabetes, defined as 18 months and more, with average duration of disease of 14±9 years (range 5-26 years). The characteristics of these patients are presented in table 4.2.2.

The patients were instructed to come in fasting (defined as no food from midnight). They were instructed not to take any insulin on the morning of testing. The last 'allowed' insulin dose was long-acting insulin the night before.

The results of proteomic analysis were validated by extending ELISA validation on the whole cohort of 30 patients with established type 1 diabetes, recruited using same inclusion/exclusion criteria. Characteristics of the whole cohort of 30 patients with established type 1 diabetes and their healthy controls are presented in table 4.2.3

Table 4.2.1 Characteristics of patients with newly-diagnosed type 1 diabetes (n=8) and their healthy controls (n=8)

	T1DM new (n=8)	Controls (n=8)	p
Age [years (±SD)]	26 (±5.1)	27.3(± 2.2)	0.49
Sex (F:M)	1:7	1:7	1
BMI [kg/m (±SD)]	24.6 (±4.21)	24.2 (±2.61)	0.86
BP systolic [mmHg (±SD)]	118 (±8.3)	123.7 (±11.3)	0.29
BP diastolic [mmHg (±SD)]	71.8 (±12.8)	81.3 (±9.2)	0.12
Heart rate (beats/min)*	63.6 (±6.5)	63.7 (±10.7)	0.99
Waist/ hip ratio (±SD)	0.84 (±0.05)	0.92 (±0.07)	0.29
Duration of diabetes [months (±SD)]	3 (±2.4)	N/A	--
Cigarette smoking [pack-years (±SD)]	1.38 (±2.26)	0.11 (±0.28)	0.16
Alcohol [units/wk (±SD)	5.88 (±6.55)	14.29 (±12.72)	0.12
Exercise [min/wk (±SD)	188.13 (±201)	120 (±115.4)	0.44
HbA1C [% (±SD)]	7.68 (±1.95)	5.15 (±0.3)	<0.01
Fasting glucose [mmol/L (±SD)]	6.48 (±3.06)	4.48 (±0.37)	0.10

	T1DM new (n=8)	Controls (n=8)	p
Fasting insulin [mU/L (±SD)]	44.45 (±60.78)	5.64 (±2.86)	0.02
HOMA IR (±SD)	-----	1.02 (±0.09)	---
Total cholesterol [mmol/L (±SD)]	4.2 (±0.55)	5.05 (±0.43)	0.01
LDL [mmol/L (±SD)]	2.53 (±0.41)	3.19 (±0.55)	0.02
HDL [mmol/L (±SD)]	1.24 (±0.42)	1.35 (±0.39)	0.62
Insulin daily dose (units)	0-60; 32.75 (± 20.4)	N/A	---
Long-acting insulin daily dose (units)	15.4 (±9.1)	N/A	---
Short-acting insulin daily dose (units)	17.4 (±11.5).	N/A	---
Insulin daily requirement (unit/kg of body weight)	0.81 (±0.44)	N/A	---

Legend: N/A not applicable, HOMA-IR not calculated in T1DM as taking exogenous insulin; *no subjects were taking medications that could affect the heart rate.

Table 4.2.2 Characteristics of patients with established type 1 diabetes (T1DM old, n=8) and their controls (n=8).

	T1DM old (n=8)	Controls (n=8)	P
Age [years (±SD)]	44.7 (±12.84)	42.25 (±4.8)	0.61
BMI [kg/m (±SD)]	28.45 (±4.35)	28.36 (±4.87)	0.97
BP systolic [mmHg (±SD)]	125.3 (±10.9)	126 (±6.2)	0.89
BP diastolic [mmHg (±SD)]	80.5 (±5.8)	78.3 (±8.9)	0.58
Heart rate (beats/min)	73.4 (±5.8)	65.1 (±7.7)	0.03
Subjects taking beta-blockers	1/8	0/8	0.3
Waist/ hip ratio (±SD)	0.89 (±0.1)	0.93 (±0.08)	0.52
Duration of diabetes [years (±SD)]	14.38 (±9.89)	---	n/a
Cigarette smoking [pack-years (±SD)	11.38 (±17.94)	9.88 (±10.32)	0.84
Alcohol [units/wk (±SD)	2.75 (±3.65)	14.63 (±20.96)	0.13
Exercise [min/wk (±SD)	57.5 (±87.1)	224.3 (±361.4)	0.22
HbA1C [% (±SD)]	7.99(±1.28)	5.38(±0.23)	<0.01
Fasting glucose [mmol/L (±SD)]	11 (±5.6)	4.8 (±0.38)	<0.01

	T1DM old (n=8)	Controls (n=8)	P
Fasting insulin [mU/L (±SD)]	5.35 (±6.33)	5.36 (±3.19)	0.99
HOMA IR (±SD)	----	0.81 (±0.51)	---
Total cholesterol [mmol/L (±SD)]	3.95 (±0.66)	5.18 (±0.53)	<0.01
LDL [mmol/L (±SD)]	1.91 (±0.29)	2.74 (±1.09)	0.056
HDL [mmol/L (±SD)]	1.56 (±0.39)	1.45 (±0.17)	0.49
Insulin daily dose (units)	74 (±19.3)	N/A	---
Long-acting insulin daily dose (units)	42.2 (±12.1)	N/A	---
Short-acting insulin daily dose (units)	31.7 (±10.4)	N/A	---
Insulin daily requirement (unit/kg of body weight)	0.86 (±1.71)	N/A	---

Legend: N/A, not applicable

Table 4.2.3 Characteristics of patients with established type 1 diabetes (T1DM old, n=30) and their controls (n=30)

	T1DM old (n=30)	Controls (n=30)	P
Age [years (±SD)]	40.23±10.03	43.17±8.80	0.23
BMI [kg/m (±SD)]	26.52±3.38	27.94±4.18	0.15
BP systolic [mmHg (±SD)]	129.3±19.29	127.87±12.47	0.73
BP diastolic [mmHg (±SD)]	79.53±7.86	80.47±8.72	0.66
Heart rate (beats/min)	74.8 (±12.4)	70.2 (±11.6)	0.14
Waist/ hip ratio (±SD)	0.90±0.09	0.92±0.08	0.35
Duration of diabetes [years (±SD)]	16.86±12.9	---	N/A
Cigarette smoking [pack-years (±SD)	9.34±13.55	11.25±11.58	0.56
Alcohol [units/wk (±SD)	5.38±6.15	11±15.01	0.06
Exercise [min/wk (±SD)	145±179	216±246	0.47
HbA1C [% (±SD)]	7.61±1.08	5.35±0.66	<0.001
Fasting glucose [mmol/L (±SD)]	9.78±4.75	4.94±0.41	<0.001
Fasting insulin* [mU/L (±SD)]	23.98	7.53	N/A*

	T1DM old (n=30)	Controls (n=30)	P
HOMA IR*(±SD)	---	0.91±0.74	N/A*
Total cholesterol [mmol/L (±SD)]	4.39±0.76	5.3±0.66	<0.001
LDL [mmol/L (±SD)]	2.31±0.56	3.09±0.85	<0.01
HDL [mmol/L (±SD)]	1.55±0.46	1.40±o.33	0.18
Insulin daily dose (units)	61.8±27.8	---	N/A
Long-acting insulin daily dose (units)	33.5±19.3	---	N/A
Short-acting insulin daily dose (units)	28.9±14.2	---	N/A
Insulin daily requirement (unit/kg of body weight)	0.75±0.33	---	N/A

Legend: N/A, not applicable, *Even though patients with diabetes were instructed to omit their morning dose, there is an obvious spill-over, most likely from the background insulin; therefore HOMA-IR was not calculated for them.

4.2.2 All-group analysis

Eight serum samples per group (patients with newly-established type 1 diabetes, their matched controls, patients with established type 1 diabetes, and their matched controls) were included in this experiment. One control sample (DS-171/ U30) was incompatible for alignment with any reference sample selected. This may be due to sub-optimal sample handling or a problem associated with the LC-MS run, therefore this sample could not be used in the data analysis. All other sample runs aligned with reference run without any problems.

LC-MS data for all samples from each group were imported to the Progenesis software (excluding control sample DS-171/U30). After successful alignment and filtering of detected features (ANOVA p-value < 0.2), a principal component analysis (PCA) plot was generated.

Figure 4.2.1 shows PCA plot for all sample groups. For brevity, patients with established diabetes are labelled as type 1 old (T1DM old); patients with newly diagnosed diabetes as type 1 new (T1DM new) and their respective controls as controls old and controls new.

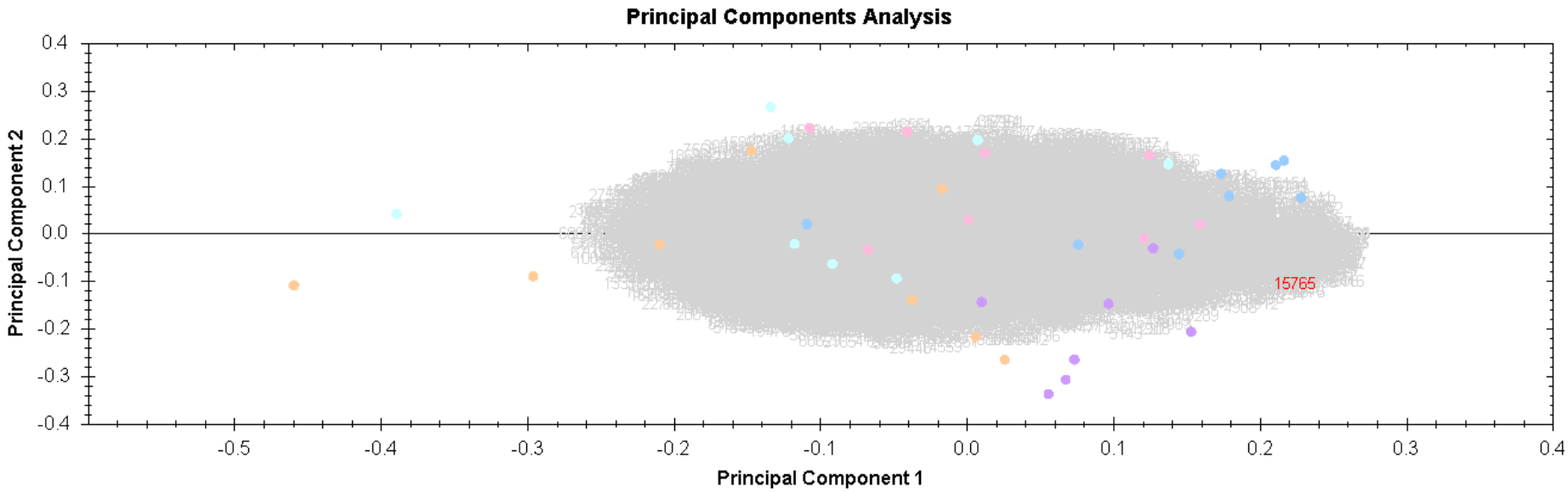

Figure 4.2.1 PCA plot for all sample groups. Pink spots represent T1DM new samples, blue spots represent T1DM old samples, purple spots represent control new samples, orange spots represent control old sample and the cyan spots represent the autoimmune samples

The pink spots represent the samples of patients with newly-diagnosed type 1 diabetes, while the purple spots represent their respective controls. While they did not form distinctly separate clusters, spots belonging to subjects from the healthy control group (those matched to newly diagnosed type 1 diabetes) were clustered quite closely on the bottom right part of the PCA plot.

Spots representing patients with newly-diagnosed type 1 diabetes, while not as closely clustered, were mainly located in the top left corner of the plot.

The autoimmune/ inflammatory disease serum specimens were represented by the cyan spots. These showed a very similar clustering pattern to the samples of patients with newly-diagnosed type 1 diabetes.

The samples from patients with established type 1 diabetes were represented by the blue spots, while their respective healthy controls' samples were represented by the orange spots. Spots belonging to patients with established type 1 diabetes were mainly located in the right portion of the plot while spots belonging to their healthy controls were located in the left of the plot.

While each sample group did not result in the formation of distinctly separate clusters, each sample group clustered in a separate area of the plot. The loose filter criteria for peptide identification (ANOVA p-value 0.2) would also contribute to the samples not clustering as tightly. That said, we did not want to apply so stringent a criterion at this stage as to exclude peptides from the analysis, as identified proteins would be filtered using more stringent criteria at a later stage.

4.2.3 Results of proteomic analysis in patients with newly-diagnosed type 1 diabetes compared to their matched healthy controls

Progenesis analysis was performed in triplicate for all comparisons analysed, using a different reference sample for each replicate. Samples with the highest number of detected features were chosen as reference samples. Therefore, three lists of differentially expressed proteins were generated for each comparison analysed. Proteins common to all three lists were then identified.

For the comparison of patients with newly diagnosed type 1 diabetes and their respective controls, the first replicate was performed with a sample belonging to a newly-diagnosed type 1 diabetes patient (DS-169, T1N8) as reference sample, the second replicate with a 'control new' sample (DS- 175, U35) and the third replicate with another 'control new' sample (DS-178, U36)(Raw data in Appendix A, Tables 1, 2 & 3)

Proteins that were common to all three lists were: complement C5, clusterin, inter-alpha-trypsin inhibitor heavy chain H3, C-reactive protein, POTE ankyrin domain family member E and β-actin-like protein 3 (Table 4.2.4).

A PCA plot was generated for each analysis performed. Figure 4.2.2 shows a very clear distinction between the 'T1DM new' and 'control new' sample clusters, Samples belonging to patients with newly-

diagnosed type 1 diabetes are shown in pink, while their respective control samples are shown in blue.

Table 4.2.4 Summary of proteins differentially expressed in patients with newly-diagnosed type 1 diabetes and their matched healthy controls

						Average normalised abundances	
Accession	Description	Reference run used	Fold	Anova (p)	Peptides	T1DM new	Matched controls
P01031	**Complement C5** OS=Homo sapiens GN=C5 PE=1 SV=4	DS-169	1.65	0.03	20	1.88E+006	1.14E+006
		DS-175	1.74	0.00451	20	2.24E+006	1.28E+006
		DS-178	1.63	0.04	9	4.70E+005	2.88E+005
P10909	**Clusterin**	DS-169	1.72	0.04	13	1.78E+007	1.03E+007

						Average normalised abundances	
Accession	Description	Reference run used	Fold	Anova (p)	Peptides	T1DM new	Matched controls
	OS=Homo sapiens GN=CLU PE=1 SV=1	DS-175	1.68	0.01	12	2.68E+007	1.59E+007
		DS-178	1.57	0.02	4	8.49E+005	5.41E+005
Q06033	**Inter-alpha-trypsin inhibitor heavy chain H3** OS=Homo sapiens GN=ITIH3 PE=1 SV=2	DS-169	2.43	0.01	3	9.40E+004	3.88E+004
		DS-175	2.7	0.00792	5	1.53E+005	5.66E+004
		DS-178	2.5	0.02	2	8.37E+004	3.34E+004
P02741	**C-reactive protein**	DS-169	6.09	0.02	6	1.22E+006	2.00E+005

						Average normalised abundances	
Accession	Description	Reference run used	Fold	Anova (p)	Peptides	T1DM new	Matched controls
	OS=Homo sapiens GN=CRP PE=1 SV=1	DS-175	6.22	0.01	4	1.24E+006	1.99E+005
		DS-178	8.05	0.02	4	4.21E+005	5.23E+004
Q6S8J3	**POTE ankyrin domain family member E** OS=Homo sapiens GN=POTEE PE=1 SV=3	DS-169	1.97	0.02	3	5.39E+004	1.06E+005
		DS-175	1.92	0.03	2	6.34E+004	1.22E+005
		DS-178	2.02	0.03	3	6.91E+004	1.40E+005
Q9BYX7	**B-actin-like protein 3**	DS-169	1.98	0.02	2	4.86E+004	9.63E+004

						Average normalised abundances	
Accession	Description	Reference run used	Fold	Anova (p)	Peptides	T1DM new	Matched controls
	OS=Homo sapiens GN=ACTBL3 PE=1 SV=1	DS-175	1.92	0.03	2	6.34E+004	1.22E+005
		DS-178	2.03	0.03	2	6.31E+004	1.28E+005

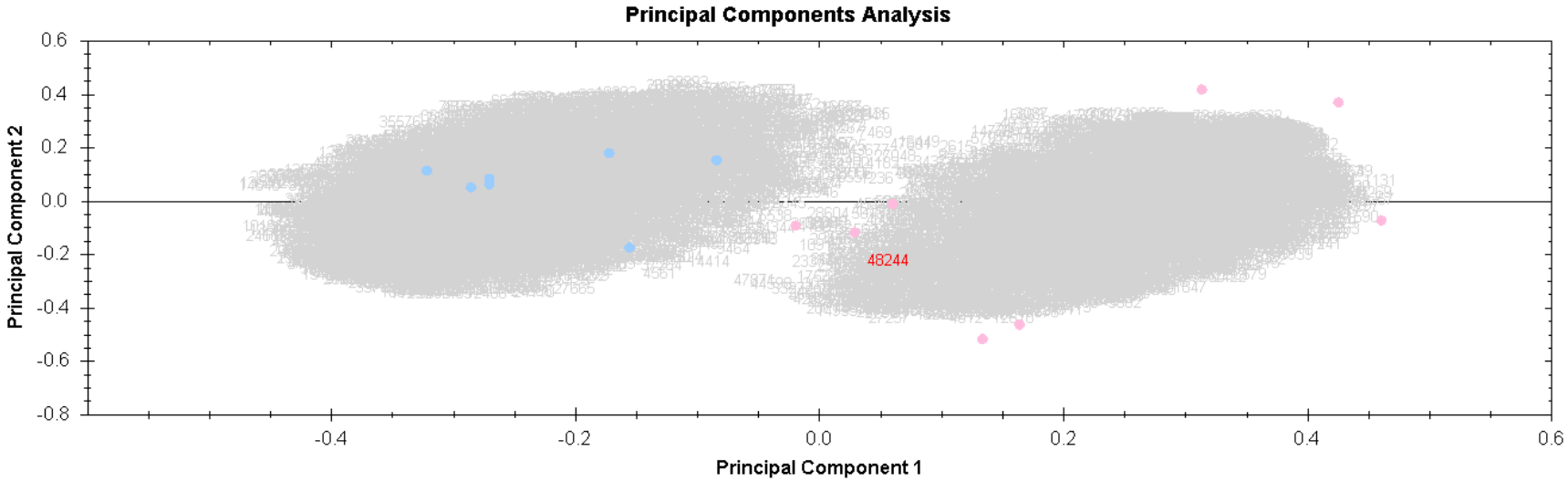

Figure 4.2.2 PCA plot for samples from patients with newly-diagnosed diabetes and their matched healthy controls. DS-175/U35 sample was used as reference run. Pink spots indicate the 'T1DM new' samples while the blue spots indicate the 'control new' samples.

4.2.4 Results of proteomic analysis in patients with established type 1 diabetes compared to their matched healthy controls

The analysis of these groups was performed in triplicate using a different reference sample for each replicate. The first replicate was performed with a sample belonging to a patient with established type 1 diabetes (DS-84/ T1O10) as reference sample, the second replicate with sample from the pool of matched healthy controls with a BMI>30kg/m^2 (DS- 162/M16) and the third replicate with another sample from the pool of matched healthy controls, with a BMI of <30kg/m^2 (DS-39/U14) as reference sample (Raw data in appendix A)

A PCA plot was generated (Figure 4.2.3), showing two distinct clusters. However, one of the samples belonging to a patient with established type 1 diabetes (pink) clustered with the matched controls' samples (blue), rather than with the other established type 1 diabetes samples.

Proteins that were common to all three lists were identified. These included: antithrombin III, apolipoprotein E, apolipoprotein C-II, vitronectin, ficolin-2, ceruloplasmin, vitamin K-dependent protein S, apolipoprotein A-1, transthyretin, C4b binding protein alpha chain, serum amyloid A-4 protein, mannan-binding lectin serine protease 1, apolipoprotein L1,platelet factor 4, apolipoprotein C-IV, von Willebrand factor, complement component C8 β chain, actin-cytoplasmic 2, complement factor H related protein 1, POTE ankyrin domain family member E and β-actin-like protein 3 (Table 4.2.8).

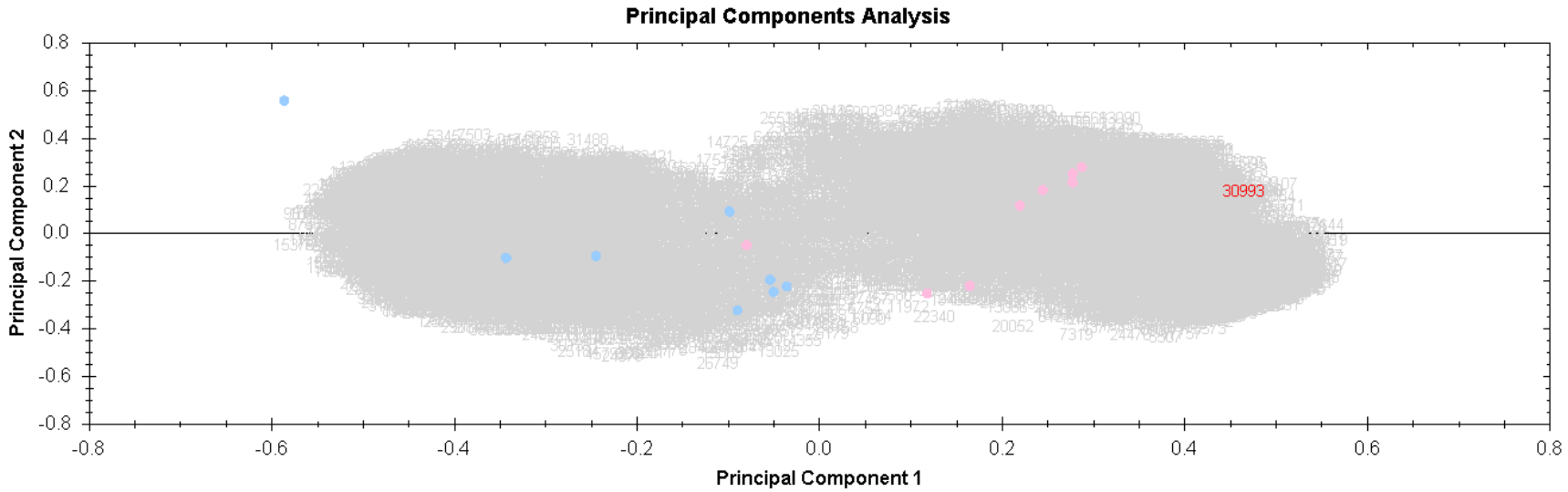

Figure 4.2.3 PCA plot for patients with established type 1 diabetes (T1DM old) and their matched controls' samples. DS-84/ T1O10 'type 1 old' sample was used as reference run. Pink spots indicate the' T1DM old' samples while the blue spots indicate the 'control old' samples

Table 4.2.5 Summary of proteins differentially expressed in patients with established type 1 diabetes versus their matched controls.

						Average normalised abundances	
Accession	Description	Reference run used	Fold	Anova (p)	Peptides	T1DM old	Matched controls
P01008	**Antithrombin-III** OS=Homo sapiens GN=SERPINC1 PE=1 SV=1	DS-84	2.55	0.05	18	6.43E+007	1.64E+008
		DS-162	2.31	0.03	17	3.15E+007	7.27E+007
		DS-39	2.37	0.03	16	2.79E+007	6.63E+007
P02649	**Apolipoprotein E** OS=Homo sapiens GN=APOE PE=1 SV=1	DS-84	2.19	0.02	12	1.46E+007	3.20E+007
		DS-162	2.05	0.02	15	1.07E+007	2.19E+007

						Average normalised abundances	
Accession	Description	Reference run used	Fold	Anova (p)	Peptides	T1DM old	Matched controls
		DS-39	2.05	0.02	15	1.05E+007	2.16E+007
P02655	**Apolipoprotein C-II** OS=Homo sapiens GN=APOC2 PE=1 SV=1	DS-84	2.41	0.01	4	4.06E+006	9.79E+006
		DS-162	2.25	0.01	5	3.13E+006	7.05E+006
		DS-39	2.5	7.13E-003	5	2.76E+006	6.88E+006
P04004	**Vitronectin** OS=Homo sapiens GN=VTN PE=1 SV=1	DS-84	1.72	0.03	5	2.55E+007	4.39E+007
		DS-162	1.62	0.03	5	1.71E+007	2.77E+007
		DS-39	1.57	0.03	6	1.76E+007	2.77E+007

						Average normalised abundances	
Accession	Description	Reference run used	Fold	Anova (p)	Peptides	T1DM old	Matched controls
Q15485	**Ficolin-2** OS=Homo sapiens GN=FCN2 PE=1 SV=2	DS-84	3	0.02	5	5.81E+005	1.75E+006
		DS-162	2.81	0.02	7	4.37E+005	1.23E+006
		DS-39	2.88	0.02	6	4.10E+005	1.18E+006
P00450	**Ceruloplasmin** OS=Homo sapiens GN=CP PE=1 SV=1	DS-84	1.7	0.03	6	5.53E+005	3.25E+005
		DS-162	1.44	0.04	8	4.51E+005	3.13E+005
		DS-39	1.6	0.03	7	5.17E+005	3.23E+005
P07225	**Vitamin K-dependent protein S**	DS-84	2.47	0.05	7	1.52E+006	3.75E+006

						Average normalised abundances	
Accession	Description	Reference run used	Fold	Anova (p)	Peptides	T1DM old	Matched controls
	OS=Homo sapiens GN=PROS1 PE=1 SV=1	DS-162	2.13	6.32E-003	4	4.03E+005	8.59E+005
		DS-39	2.24	5.34E-003	6	4.03E+005	9.04E+005
P02647	**Apolipoprotein A-I** OS=Homo sapiens GN=APOA1 PE=1 SV=1	DS-84	1.9	0.05	5	2.66E+007	5.06E+007
		DS-162	1.76	0.04	4	1.99E+007	3.50E+007
		DS-39	1.75	0.05	5	1.96E+007	3.44E+007
P02766	**Transthyretin** OS=Homo sapiens GN=TTR PE=1 SV=1	DS-84	2.69	0.04	4	2.14E+006	5.74E+006
		DS-162	2.39	0.03	3	1.63E+006	3.91E+006

						Average normalised abundances	
Accession	Description	Reference run used	Fold	Anova (p)	Peptides	T1DM old	Matched controls
		DS-39	2.46	0.04	3	1.51E+006	3.71E+006
P04003	**C4b-binding protein alpha chain** OS=Homo sapiens GN=C4BPA PE=1 SV=2	DS-84	2.62	0.04	3	5.67E+006	1.49E+007
		DS-162	2.39	0.03	3	4.23E+006	1.01E+007
		DS-39	2.4	0.03	4	4.16E+006	9.97E+006
P35542	**Serum amyloid A-4 protein** OS=Homo sapiens GN=SAA4 PE=1 SV=1	DS-84	2.34	0.02	2	8.40E+005	1.97E+006
		DS-162	2.25	0.02	2	5.16E+005	1.16E+006
		DS-39	2.37	0.01	3	5.00E+005	1.19E+006

						Average normalised abundances	
Accession	Description	Reference run used	Fold	Anova (p)	Peptides	T1DM old	Matched controls
P48740	**Mannan-binding lectin serine protease 1** OS=Homo sapiens GN=MASP1 PE=1 SV=3	DS-84	1.97	5.95E-003	4	4.04E+005	7.95E+005
		DS-162	1.95	2.11E-003	4	2.82E+005	5.49E+005
		DS-39	1.91	2.59E-003	4	2.79E+005	5.35E+005
O14791	**Apolipoprotein L1** OS=Homo sapiens GN=APOL1 PE=1 SV=5	DS-84	4.07	3.71E-003	2	7.27E+004	2.96E+005
		DS-162	2.44	0.03	3	7.75E+004	1.89E+005
		DS-39	2	0.02	3	1.25E+005	2.49E+005
P02776	**Platelet factor 4**	DS-84	2.1	0.05	2	7.12E+005	1.49E+006

						Average normalised abundances	
Accession	Description	Reference run used	Fold	Anova (p)	Peptides	T1DM old	Matched controls
	OS=Homo sapiens GN=PF4 PE=1 SV=2	DS-162	1.98	0.05	2	5.30E+005	1.05E+006
		DS-39	1.97	0.05	2	5.22E+005	1.03E+006
P63261	**Actin, cytoplasmic 2** OS=Homo sapiens GN=ACTG1 PE=1 SV=1	DS-84	3.42	0.03	4	1.28E+005	4.38E+005
		DS-162	3.14	0.02	4	1.45E+005	4.56E+005
		DS-39	3.09	0.03	4	1.52E+005	4.71E+005
Q9BYX7	**B-actin-like protein** 3 OS=Homo sapiens GN=ACTBL3 PE=1 SV=1	DS-84	3.99	0.01	3	6.77E+004	2.70E+005
		DS-162	3.72	9.51E-003	3	4.79E+004	1.78E+005

						Average normalised abundances	
Accession	Description	Reference run used	Fold	Anova (p)	Peptides	T1DM old	Matched controls
		DS-39	3.63	0.02	3	5.17E+004	1.88E+005
Q6S8J3	**POTE ankyrin domain family member E** OS=Homo sapiens GN=POTEE PE=1 SV=3	DS-84	3.99	0.01	3	6.77E+004	2.70E+005
		DS-162	3.72	9.51E-003	3	4.79E+004	1.78E+005
		DS-39	3.63	0.02	3	5.17E+004	1.88E+005
P55056	**Apolipoprotein C-IV** OS=Homo sapiens GN=APOC4 PE=1 SV=1	DS-84	2.9	0.02	2	5.04E+004	1.46E+005
		DS-162	3.53	3.89E-03	2	2.86E+004	1.01E+005
		DS-39	3.03	4.00E-003	2	3.58E+004	1.08E+005

						Average normalised abundances	
Accession	Description	Reference run used	Fold	Anova (p)	Peptides	T1DM old	Matched controls
P04275	**von Willebrand factor** OS=Homo sapiens GN=VWF PE=1 SV=3	DS-84	4.42	0.02	2	1.76E+004	7.80E+004
		DS-162	3.51	0.01	2	1.67E+004	5.87E+004
		DS-39	3.9	0.01	2	1.41E+004	5.50E+004
Q03591	**Complement factor H-related protein 1** OS=Homo sapiens GN=CFHR1 PE=1 SV=2	DS-84	1.88	6.65E-003	3	2.30E+006	4.34E+006
		DS-162	1.74	0.02	3	1.42E+006	2.47E+006
		DS-39	1.74	0.03	2	1.34E+006	2.33E+006
P07358	**Complement component C8 β chain**	DS-84	1.46	0.01	3	8.24E+004	5.64E+004

						Average normalised abundances	
Accession	Description	Reference run used	Fold	Anova (p)	Peptides	T1DM old	Matched controls
	OS=Homo sapiens GN=C8B PE=1 SV=3	DS-162	1.86	1.57E-003	2	6.35E+004	3.41E+004
		DS-39	1.91	5.89E-004	2	6.34E+004	3.31E+004

4.2.5 Results of proteomics analysis in patients with newly-diagnosed type 1 diabetes compared to patients with established type 1 diabetes

The analysis of this comparison was performed in triplicate using a different reference sample for each replicate. The first replicate was performed with a sample belonging to a patient with newly-diagnosed diabetes (DS-169/T1N8) as reference sample, the second replicate with sample belonging to a patient with established type 1 diabetes (DS-74/T1O7) and the third replicate with another sample belonging to a patient with established type 1 diabetes (DS-90/T1O12). A list of differentially expressed proteins was also generated for each replicate analysis performed (Raw data presented in Appendix A)

PCA plot was generated for this comparison (Figure 4.2.4.), showing two distinct clusters. However, one of the samples belonging to a patient with established type 1 diabetes,- DS-29/T1O4 (blue), clustered slightly closer to the samples belonging to patients with newly-diagnosed type 1 diabetes (pink), rather than with the other samples from patients with established diabetes.

Proteins that were common to all three lists were identified in table 4.2.6. These included: complement C4-B, prothrombin, clusterin, Ig mu chain C region, antithrombin III, Ig kappa chain C region, vitronectin, vitamin K-dependent protein and apolipoprotein C-1.

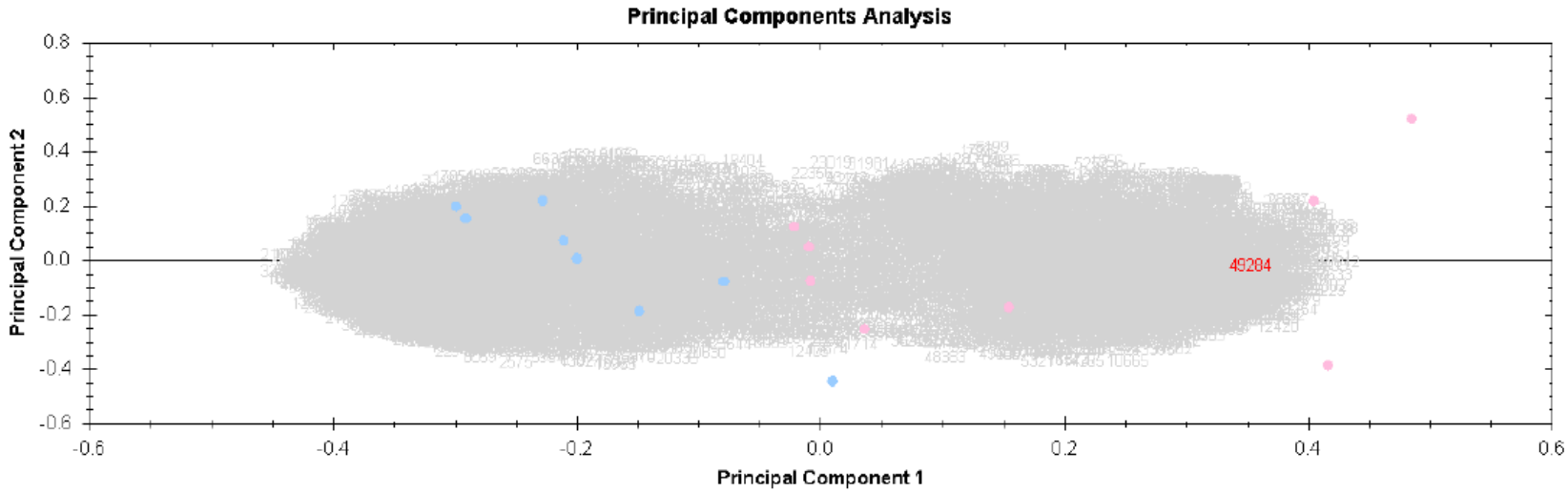

Figure 4.2.4 PCA plot for T1DM new and T1DM old. DS-169 control sample was used as reference run. Pink spots indicate the T1DM new samples while the blue spots indicate the T1DM old samples.

Table 4.2.6 Summary of proteins differentially expressed in patients with newly-diagnosed type 1 diabetes compared to patients with established type 1 diabetes.

						Av normalised abundances	
Accession	Description	Reference run used	Fold	Anova (p)	Peptides	T1DM new	T1DM old
P0C0L5	**Complement C4-B** OS=Homo sapiens GN=C4B PE=1 SV=1	DS-169	1.35	0.02	47	1.11E+08	8.23E+07
		DS-74	1.45	0.01	46	1.56E+08	1.08E+08
		DS-90	1.48	0.01	44	1.62E+08	1.09E+08
P00734	**Prothrombin** OS=Homo sapiens GN=F2 PE=1 SV=2	DS-169	1.39	0.05	19	3.08E+07	2.22E+07
		DS-74	1.4	0.05	15	4.57E+07	3.27E+07
		DS-90	1.42	0.03	17	4.69E+07	3.31E+07

						Av normalised abundances	
Accession	Description	Reference run used	Fold	Anova (p)	Peptides	T1DM new	T1DM old
P10909	**Clusterin** OS=Homo sapiens GN=CLU PE=1 SV=1	DS-169	1.43	0.005	7	2.10E+07	1.47E+07
		DS-74	1.42	3.88E-03	9	3.31E+07	2.34E+07
		DS-90	1.45	3.08E-03	10	3.35E+07	2.31E+07
P01871	**Ig mu chain C region** OS=Homo sapiens GN=IGHM PE=1 SV=3	DS-169	1.57	0.04	4	6.61E+06	4.21E+06
		DS-74	1.57	0.04	5	1.26E+07	8.04E+06
		DS-90	1.55	0.03	6	1.43E+07	9.25E+06

						Av normalised abundances	
Accession	Description	Reference run used	Fold	Anova (p)	Peptides	T1DM new	T1DM old
P01008	**Antithrombin-III** OS=Homo sapiens GN=SERPINC1 PE=1 SV=1	DS-169	1.44	6.47E-03	10	2.35E+07	1.63E+07
		DS-74	1.43	0.01	13	3.12E+07	2.18E+07
		DS-90	1.46	7.92E-03	13	4.18E+07	2.87E+07
P01834	**Ig kappa chain C region** OS=Homo sapiens GN=IGKC PE=1 SV=1	DS-169	1.54	0.03	4	6.15E+06	4.00E+06
		DS-74	1.55	0.02	5	9.42E+06	6.07E+06
		DS-90	1.58	0.02	4	9.56E+06	6.06E+06

						Av normalised abundances	
Accession	Description	Reference run used	Fold	Anova (p)	Peptides	T1DM new	T1DM old
P04004	**Vitronectin** OS=Homo sapiens GN=VTN PE=1 SV=1	DS-169	1.45	0.03	4	1.72E+07	1.18E+07
		DS-74	1.46	0.03	5	2.57E+07	1.76E+07
		DS-90	1.42	0.03	4	3.39E+07	2.38E+07
P07225	**Vitamin K-dependent protein S** OS=Homo sapiens GN=PROS1 PE=1 SV=1	DS-169	1.71	7.49E-03	4	6.27E+05	3.67E+05
		DS-74	1.49	9.13E-04	5	6.24E+05	4.18E+05
		DS-90	2.2	3.38E-03	2	6.16E+05	2.80E+05

						Av normalised abundances	
Accession	Description	Reference run used	Fold	Anova (p)	Peptides	T1DM new	T1DM old
P02654	**Apolipoprotein C-I** OS=Homo sapiens GN=APOC1 PE=1 SV=1	DS-169	1.55	4.51E-03	4	2.59E+06	1.67E+06
		DS-74	1.56	2.43E-03	2	3.78E+06	2.42E+06
		DS-90	1.59	2.83E-03	3	3.88E+06	2.45E+06

4.2.6 Target protein selection for follow-up

Proteins for follow up were selected based on their potential interest in both newly-diagnosed type 1 diabetes and established type 1 diabetes studies.

Clusterin was identified as being up-regulated in samples of patient with newly-diagnosed type 1 diabetes relative to their matched healthy controls and relative to patients with established type 1 diabetes (tables 4.2.4and 4.2.6)

Vitronectin was down-regulated in samples of patients with established type 1 diabetes relative to their matched healthy controls, as well as relative to patients with newly-diagnosed diabetes (tables 4.2.5 and 4.2.6). Vitronectin was also up-regulated in two of the three replicates for comparison of samples from patients with newly-diagnosed diabetes and their matched healthy controls (Appendix A).

Vitamin K-dependent protein S levels showed the same pattern as vitronectin. This protein was down-regulated in samples of patients with established type 1 diabetes relative to their healthy controls (table 4.2.5) and to patients with newly-diagnosed diabetes (table 4.2.6). It was also up-regulated in two of the three replicate comparisons of samples from patients with newly-diagnosed diabetes and their matched healthy controls (Appendix A).

Apolipoprotein L1 was down-regulated in samples of patients with established type 1 diabetes relative to their healthy controls (table

4.2.5), while it was also down-regulated in one of the replicates for T1DM old versus T1DM new comparisons (Appendix A)

These proteins were also selected on the basis that they had no conflicting identified peptides. Conflicting peptides are peptides that are not unique to the named protein, and may be present in a number of other different proteins. Performing each comparison in triplicate with different reference samples, assigning filter criteria of ANOVA p-value less than 0.05, as well as analysing proteins with no conflicting peptides allowed identification of the most robustly differentially expressed proteins in the samples analysed.

Using these criteria, clusterin, vitronectin, apolipoprotein L1 and vitamin K-dependent protein S were selected for follow-up validation in a larger cohort of patient samples.

Samples from healthy controls matched to newly-diagnosed patients and controls matched to patients with established type 1 diabetes were compared to determine if protein changes seen in disease vs. control samples were related to disease phenotype or to control samples' variation.

A PCA plot of 'control new' and 'control old' samples was generated (Figure 4.2.5). This indicated that DS-7/U3 was a slight outlier for the 'control old' group. Differentially expressed protein lists were generated with and without the DS-7 outlier sample (Apendix A)

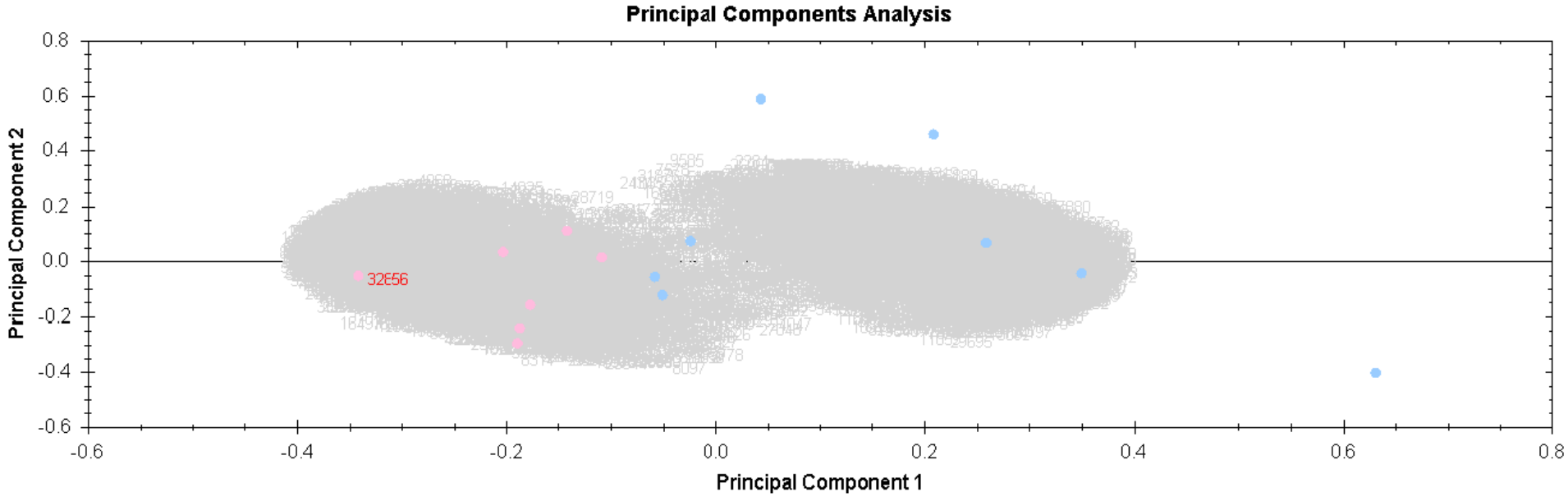

Figure 4.2.5 PCA plot for comparison of controls matched to newly-diagnosed patients with controls matched to patients with established type 1 diabetes. Sample DS-178/U36 was used as reference run. Blue spots indicate the 'control old', while pink spots indicate 'control new' samples. 'Old control' sample DS-7 is a slight outlier relative to the rest of the control old group.

Apolipoprotein L1 and vitronectin were unchanged in the comparison of two control samples' sets with and without outlier DS-7 sample included in analysis. This indicates that changing levels of these proteins are due to the disease phenotype.

Clusterin and vitamin K-dependent protein S were seen to be up-regulated in the 'control old' samples relative to the 'control new' samples in comparisons including and excluding outlier sample DS-7 (Appendix A). However, as these proteins were also identified as being differentially expressed in samples belonging to patients with newly-diagnosed type 1 diabetes versus samples belonging to patients with established type 1 diabetes, (table 4.2.6), we conclude that their differential expression is not due only to the difference in control samples.

Protein changes between autoimmune (n=8) and control samples (n=16) were also analysed, to determine if protein targets identified in the T1DM study were type 1 diabetes-related, or if they were related to autoimmunity or inflammation per se. This analysis was limited by the fact that we unfortunately had no data on glucose values or medication use in autoimmune subjects. Various medications used for treatement of autoimmune conditions have an effect on insulin sensitivity and glucose handling in those subjects.

Three lists of differentially expressed proteins were generated for comparison of samples from patients with autoimmune diseases vs healthy controls used in our studies. Samples DS-175/U35, DS-178/U36 and DS-39/U14 were used as a reference run (complete lists shown in Appendix A)

No changes in vitronectin, clusterin or vitamin K-dependent protein S were seen in any of the 'autoimmune' versus 'control' comparisons, indicating that changes in these protein levels in the type 1 diabetes study could be specifically diabetes-related.

One of the three comparisons (where control sample DS-178 was used as reference run, Appendix A.) showed decreased levels of apolipoprotein L1 in 'autoimmune' samples. Therefore, it is possible that decreased levels of apolipoprotein L1 in samples of patients with established type 1 diabetes could be related to a general autoimmune or inflammatory response. However, as apolipoprotein L1 was increased in patients with newly-diagnosed type 1 diabetes, this protein was selected for validation studies.

4.2.7 ELISA validation of target proteins

Protein targets identified in label-free LC-MS study were validated using ELISA technology. Validation was performed on the same samples of 8 patients with newly-diagnosed type 1 diabetes (T1DM new), 8 patients with established type 1 diabetes (T1DM old) and the samples of their respective controls (8 subjects in each, 'control new', 'control old') which were used in the label-free study, as well as in additional 22 samples of patients with established type 1 diabetes (T1DM old) and their respective healthy controls (control old) samples.

4.2.7.1Vitronectin

4.2.7.1.1 Vitronectin in samples of patients with newly-diagnosed type 1 diabetes compared to their healthy controls

Label-free proteomics analysis showed vitronectin levels to be significantly increased in samples of patients with newly-diagnosed type 1 diabetes compared to their respective controls by approximately 1.44 fold.

An ELISA kit was sourced from American Diagnostica GmbH (catalogue number 803) for validation of this target protein (protocol outlined in section 4.1.3.1).

ELISA detection of vitronectin in the same samples from patients with newly-diagnosed type 1 diabetes and their matched controls showed no significant difference in vitronectin levels between the groups (116.54±21.18 vs. 113.63±15.95 µg/mL, respectively, p=0.76), with a fold change of 1.02 (Figure 4.2.6).

Looking at each individual matched pair separately (Figure 4.2.7), vitronectin levels were higher in the T1DM new specimens in four of the eight matched pairs.

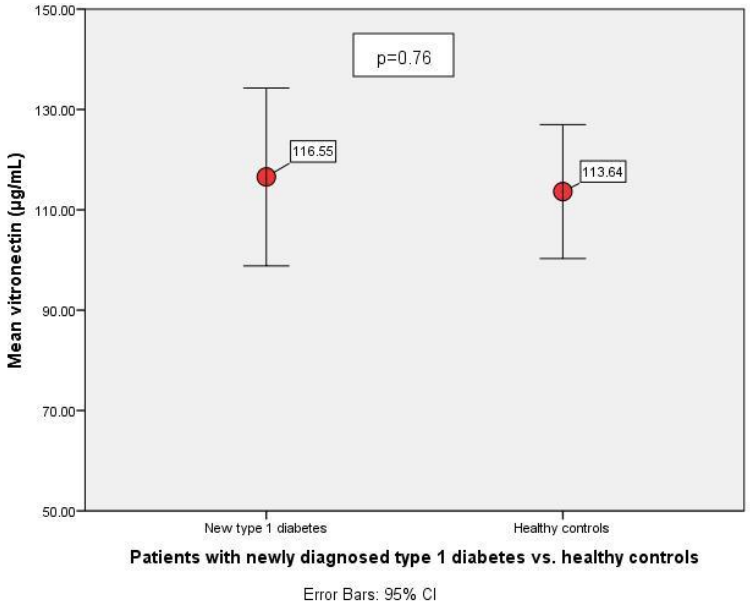

Figure 4.2.6 Mean vitronectin concentration (µg/mL) in patients with newly diagnosed type 1 diabetes and their healthy controls. Error bars delineate 95% confidence intervals.

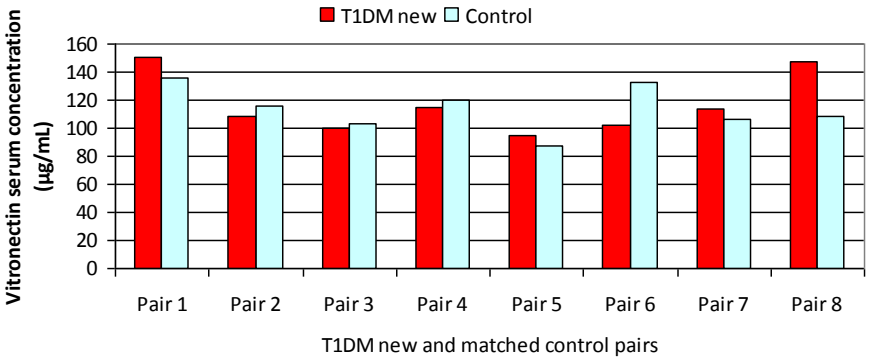

Figure 4.2.7.Vitronectin serum concentration shown for pairs of patients with newly-diagnosed type 1 diabetes (T1DM new) and their respective healthy controls.

4.2.7.1.2 Vitronectin in samples of patients with established type 1 diabetes compared to their healthy controls

In the label-free proteomic experiment, vitronectin was shown to be significantly reduced in patients with established type 1 diabetes compared to their healthy controls by approximately 1.64 fold.

Validation of this target was performed in a larger cohort of 30 T1DM old samples, including the samples used for the label-free proteomics experiment.

ELISA validation confirmed reduced vitronectin levels (1.14 fold) in samples of patients with established type 1 diabetes compared to matched controls (119.52±28.27 vs. 135.94±32.82 µg/mL, p=0.038) (Figure 4.2.8).

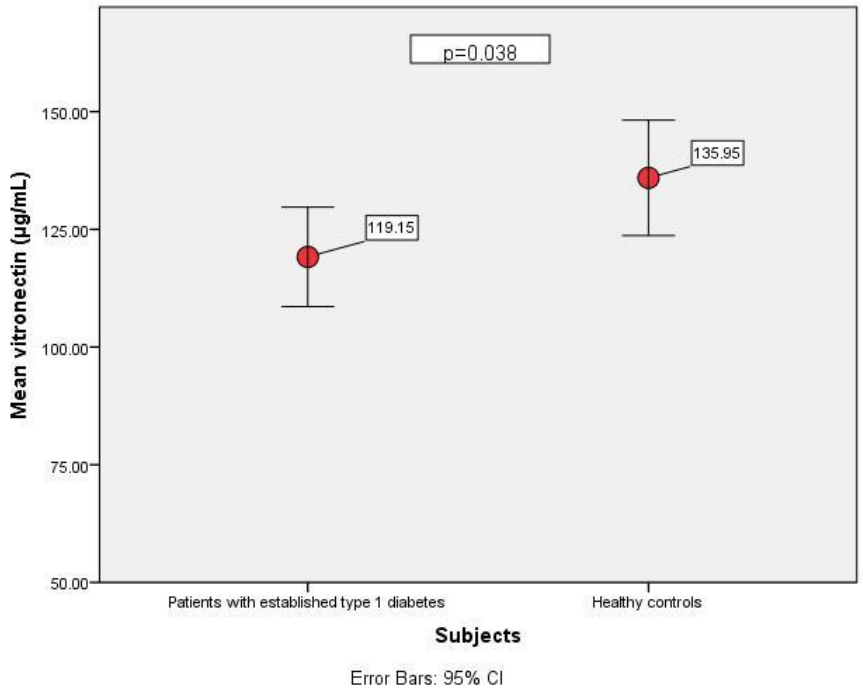

Figure 4.2.8. Mean vitronectin concentration in patients with established type 1 diabetes and their healthy controls. Error bars delineate 95% confidence intervals.

Looking at each individual matched pair, reduced vitronectin levels in patients with established T1DM is seen in 23 of the 30 matched pairs (figure 4.2.9).

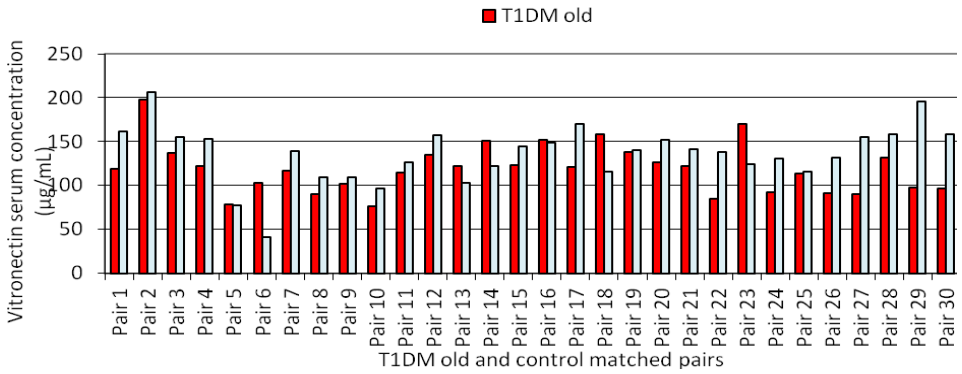

Figure 4.2.9 Vitronectin levels in matched pairs of patients with established type 1 diabetes (T1DM old) and their healthy controls.

There was no correlation between vitronectin levels and markers of inflammation (ESR, FBC) or markers of glycaemic control (HbA_1C).

4.2.7.1.3 Vitronectin in samples of patients with newly-diagnosed type 1 diabetes compared to patients with established type 1 diabetes

In the label-free proteomics experiment vitronectin levels were significantly decreased in samples of patients with established type 1 diabetes compared to patients with newly-diagnosed specimens by approximately 1.44 fold.

On expansion of the T1DM old sample cohort to 30 specimens, vitronectin levels were not significantly different between patients

with established type 1 diabetes (T1DM old) and newly-diagnosed type 1 diabetes (119.15±28.28 vs. 116.55±21.18 µg/mL, p=0.81) (Figure 4.2.10).

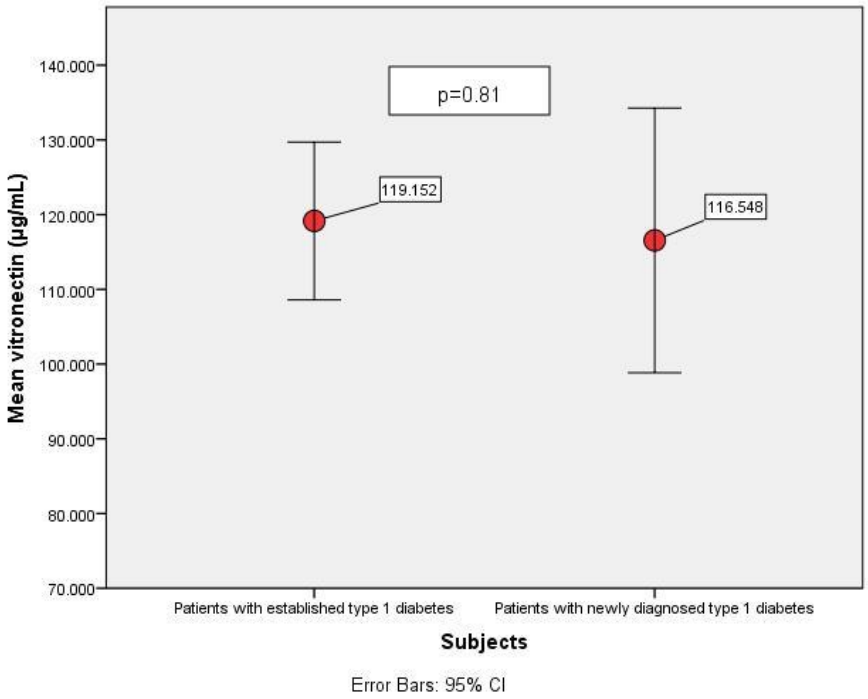

Figure 4.2.10 Vitronectin levels in patients with with established type 1 diabetes (T1DM old, n=30) and in patients with newly-diagnosed type 1 diabetes (T1DM new, n=8). Error bars delineate 95% confidence intervals.

4.2.7.2 Clusterin

4.2.7.2.1 Clusterin in samples of patients with newly-diagnosed type 1 diabetes compared to their healthy controls

Clusterin protein levels were found to be significantly up-regulated (1.66 fold) in samples from patients with newly-diagnosed type 1 diabetes (n=8) when compared to their healthy controls (n=8) in the label-free proteomics experiment.

Attempted validation of this target was performed using a clusterin ELISA sourced from Phoenix pharmaceuticals (catalogue number EK-018-35) in the same samples used in label-free proteomics experiment (protocol outlined in section 4.1.3.2). There was no up-regulation of clusterin in samples from newly-diagnosed type 1 diabetes when compared to healthy controls (186.77±80.19 vs. 212.94±31.09 µg/mL, p=0.40) (Figure 4.2.11).

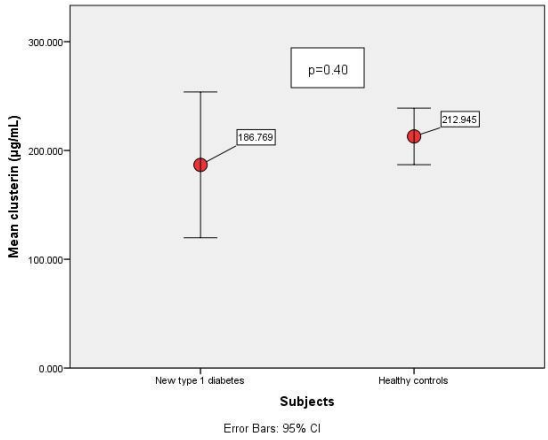

Figure 4.2.11 Clusterin concentration in patients with newly-diagnosed type 1 diabetes compared to the healthy controls. Error bars delineate 95% confidence intervals.

Looking at the ELISA results of each matched pair individually (Figure 4.2.12), 6 of the 8 sets of matched pairs show reduced clusterin levels in T1DM new sample compared to control.

The increased clusterin expression detected in the label-free experiment may have been skewed by the outlier T1DM new sample in pair 1 (Figure 4.2.12), which shows almost double the level of clusterin compared to the other T1DM new samples analysed.

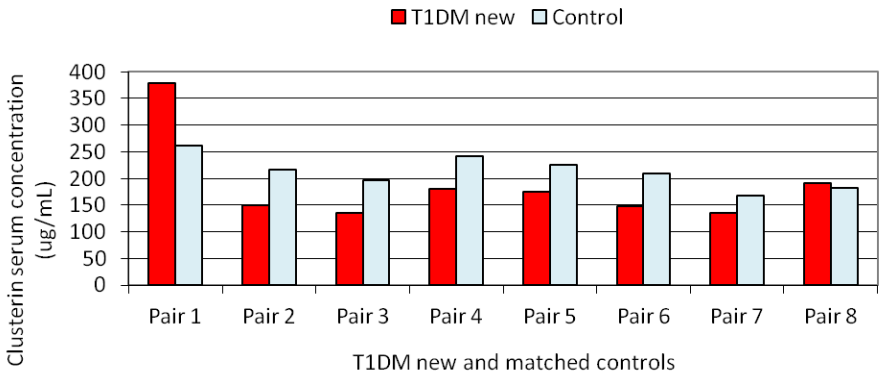

Figure 4.2.12 Clusterin serum concentrations in matched pairs of patients with newly-diagnosed type 1 diabetes and their healthy controls.

As clusterin shows an association with inflammation and lipid transport and its expression appears to be stimulated by glucose in the liver, we investigated correlations of clusterin level and parameters of metabolic health in our patients with newly diagnosed type 1 diabetes (BMI, blood pressure, smoking in pack-years, exercise in minutes/week, heart rate, waist/hip ratio, fasting glucose, insulin, HbA1C, HOMA indices and lipid levels). There was no significant correlation found with any parameter of metabolic health (146).

4.2.7.2.2 Clusterin in samples of patients with established type 1 diabetes compared to their healthy controls

In label-free proteomic analysis, there was no significant difference in clusterin levels between patients with established type 1 diabetes and their healthy controls. This bore true in ELISA validation as well. The levels in patients with established type 1 diabetes did not differ significantly when compared to their healthy controls (215.59±59.20 vs. 231.48±60.01 µg/mL, p=0.30; Figure 4.2.13).

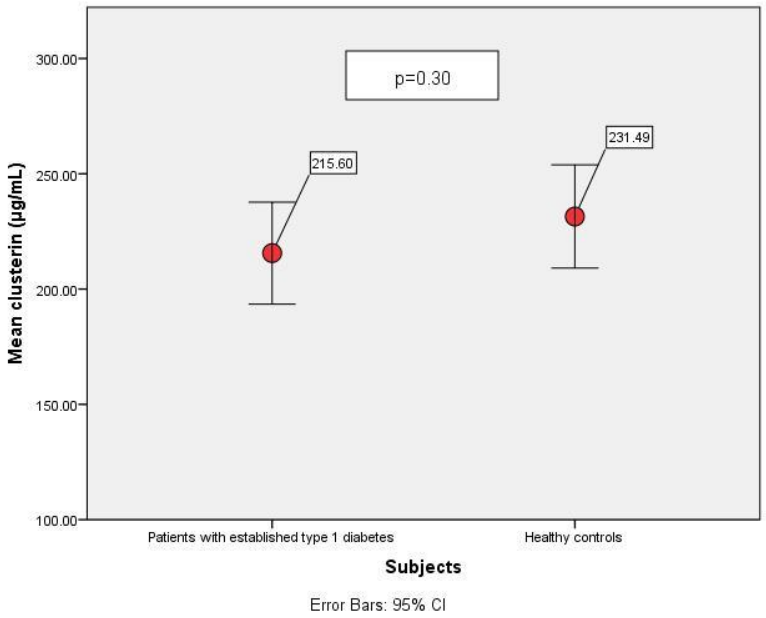

Figure 4.2.13 Levels of clusterin serum concentration in patients with established type 1 diabetes (T1DM old, n=30) and their matched controls (n=30). Error bars delineate 95% confidence intervals.

Looking at the matched pairs individually (Figure 4.2.14), large variation in clusterin expression was seen in both control and T1DM old

serum specimens. Sixteen out of thirty matched pairs showed lower clusterin levels in samples of patients with established type 1 diabetes relative to their healthy controls, with the remaining 14 pairs showing higher clusterin levels in the T1DM old samples (Figure 4.2.14).

There was no significant correlation between clusterin levels and markers of dyslipidaemia (levels of total cholesterol, HDL, LDL, triglycerides), BMI or markers of glycaemic control (fasting glucose, HbA1C).

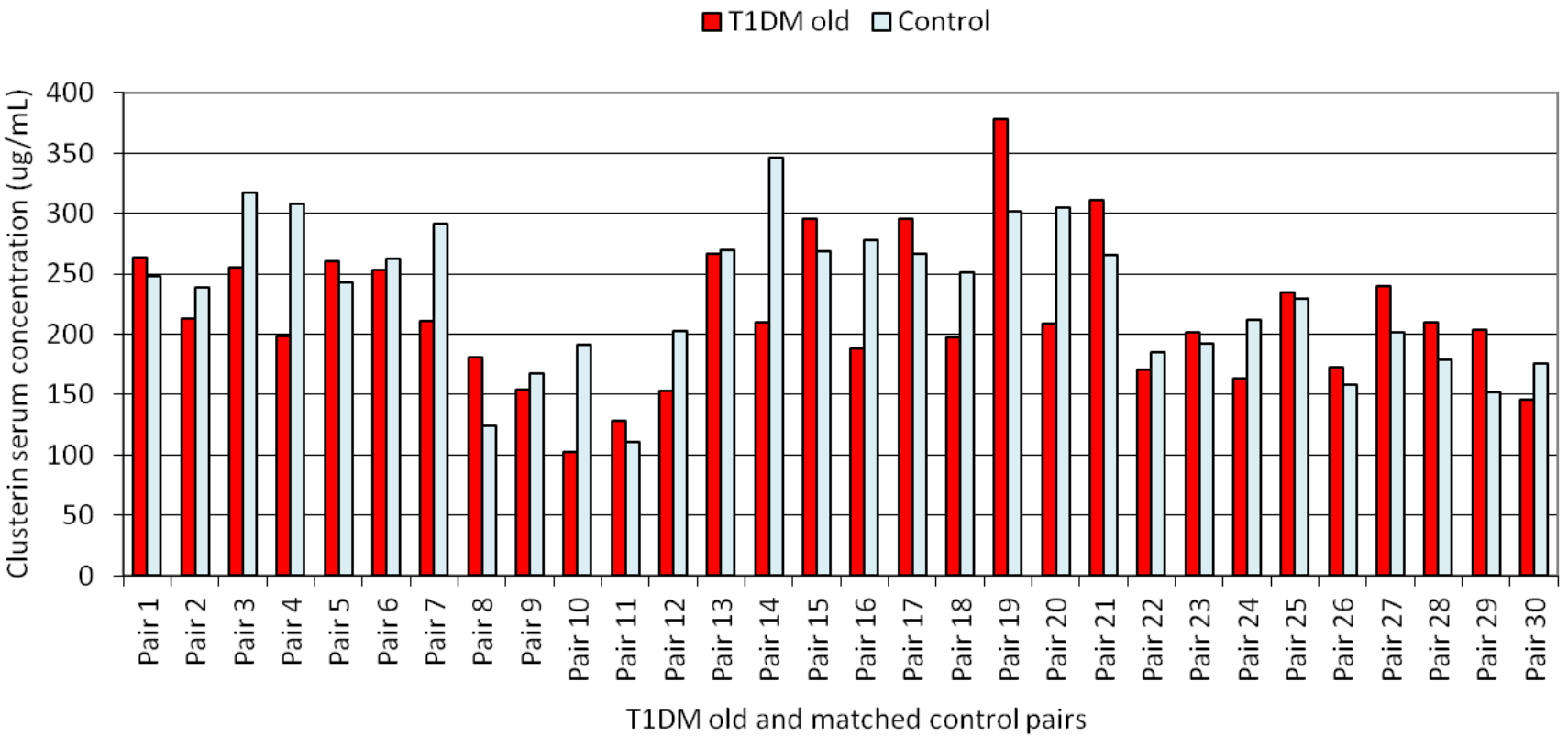

Figure 4.2.14 Levels of clusterin in matched pairs of patients with established type 1 diabetes and their healthy controls.

4.2.7.2.3 Clusterin in samples of patients with newly diagnosed type 1 diabetes compared to patients with established type 1 diabetes

Clusterin expression was significantly up-regulated by 1.43 fold in patients with newly-diagnosed type 1 diabetes compared to patients with established type 1 diabetes, as established by the label-free proteomics analysis. Attempted validation of clusterin expression by ELISA in 30 samples of patients with established type 1 diabetes and the same 8 samples from patients with newly-diagnosed type 1 diabetes used in the initial analysis showed no significant difference in clusterin expression (215.59±59.2 VS. 186.76±80.19 µg/mL, p=0.26) (Figure 4.2.15).

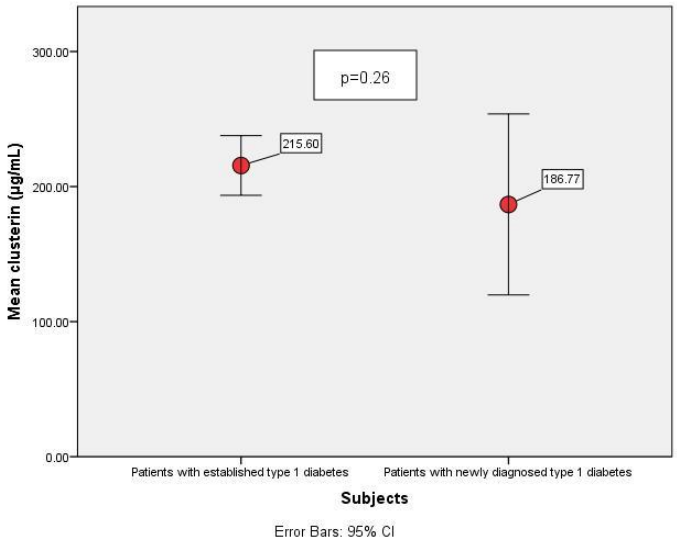

Figure 4.2.15 Clusterin levels in patients with established type 1 diabetes vs. patients with newly-diagnosed type 1 diabetes. Error bars delineate 95% confidence intervals.

4.2.7.3 Vitamin K-dependent protein S

4.2.7.3.1 Vitamin K-dependent protein S in samples of patients with newly-diagnosed type 1 diabetes compared to their healthy controls

Vitamin K-dependent protein S was found to be significantly up-regulated in serum of patients with newly diagnosed type 1 diabetes, compared to their matched healthy controls, by approximately 1.42 fold, in the label free proteomics experiment.

An ELISA kit was sourced from USCN Life Science Inc. (catalogue number E1971h) for attempted validation of this target protein (protocol outlined in section 4.1.3.3).

On ELISA in the same eight samples of patients with newly-diagnosed type 1 diabetes and their eight healthy controls, vitamin K-dependent protein S was significantly down-regulated in samples of patients with newly-diagnosed type 1 diabetes by 1.24 fold when compared to their healthy controls (360.93±79.92 vs. 448.48±68.13 ng/mL, p= 0.03; Figure 4.2.16).

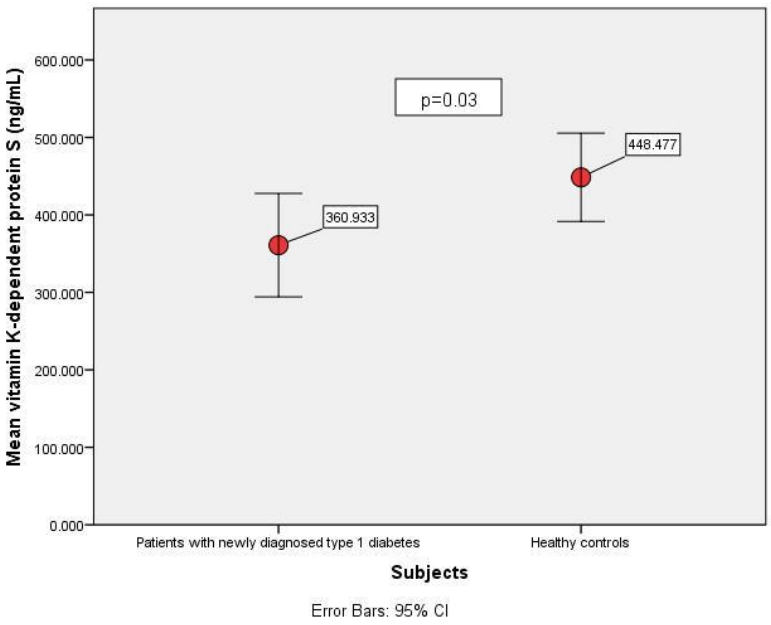

Figure 4.2.16 Vitamin K-dependent protein S concentration in patients with newly-diagnosed type 1 diabetes (T1DM new) and their healthy controls. Error bars delineate 95% confidence intervals.

Figure 4.2.17 shows the individual levels of vitamin K-dependent protein S in each of the matched pairs. Lower levels of vitamin K-dependent protein S are seen in samples of patients with newly diagnosed type 1 diabetes for 6 of the 8 matched pairs. One matched pair shows no change, while one pair shows higher vitamin K-dependent protein S levels in the T1DM new specimen.

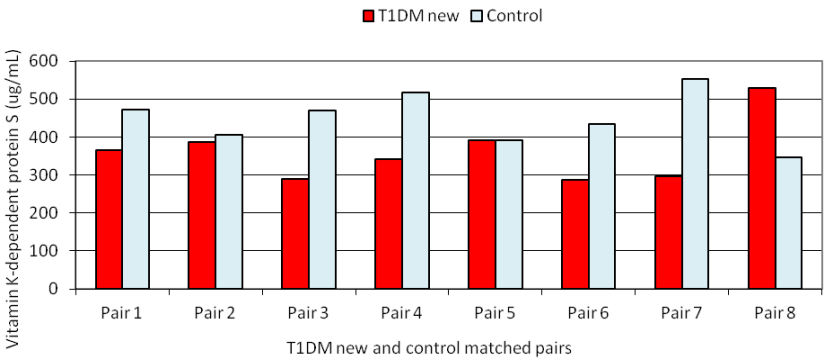

Figure 4.2.17 Concentration of vitamin K-dependent protein S in patients with newly-diagnosed type 1 diabetes (T1DM new) and their matched controls.

There was no significant correlation between vitamin K-dependent protein S and markers of glycaemic control (fasting glucose, HbA1C) or markers of lipaemic control (total cholesterol, HDL, LDL, Tg).

4.2.7.3.2 Vitamin K-dependent protein S in samples of patients with established type 1 diabetes compared to their healthy conrols

Vitamin K-dependent protein S was significantly down-regulated in patients with established type 1 diabetes when compared to their healthy controls in label free proteomic analysis, by approximately 2.28 fold.

ELISA validation of this target was performed using an expanded cohort of 30 T1DM old and 30 control old samples, but no significant

difference in vitamin K-dependent protein S was found between the groups (358.49±118.22 vs. 388.44±122.16 ng/mL, p=0.33; Figure 4.2.18)

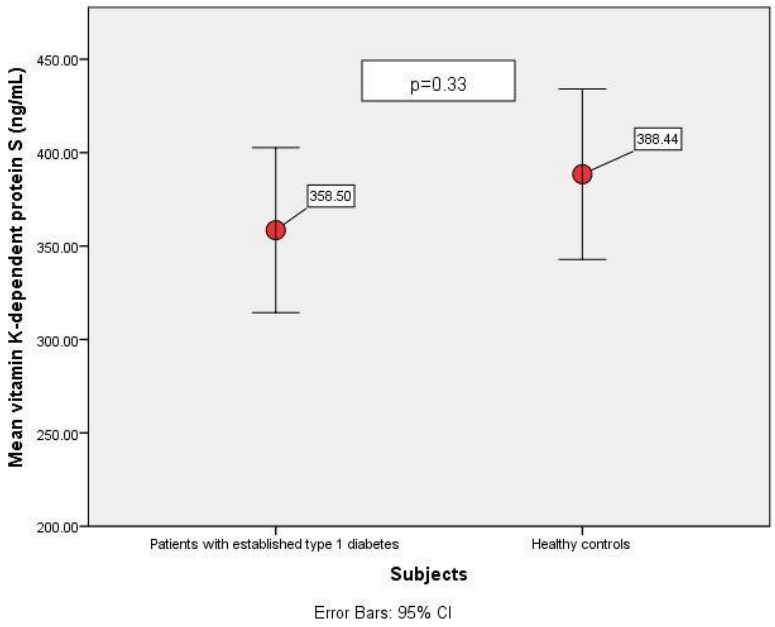

Figure 4.2.18 Vitamin K-dependent protein S in patients with established type 1 diabetes (n=30) and their matched controls (n=30). Error bars delineate 95% confidence interval.

Looking at each matched pair individually (Figure 4.2.19), no consistent change was seen in vitamin K-dependent protein S expression. This target was present at lower levels in serum of patients with established type 1 diabetes in 15 of the 30 matched pairs, in higher levels in 14 of 30 matched pairs, and no change in one pair.

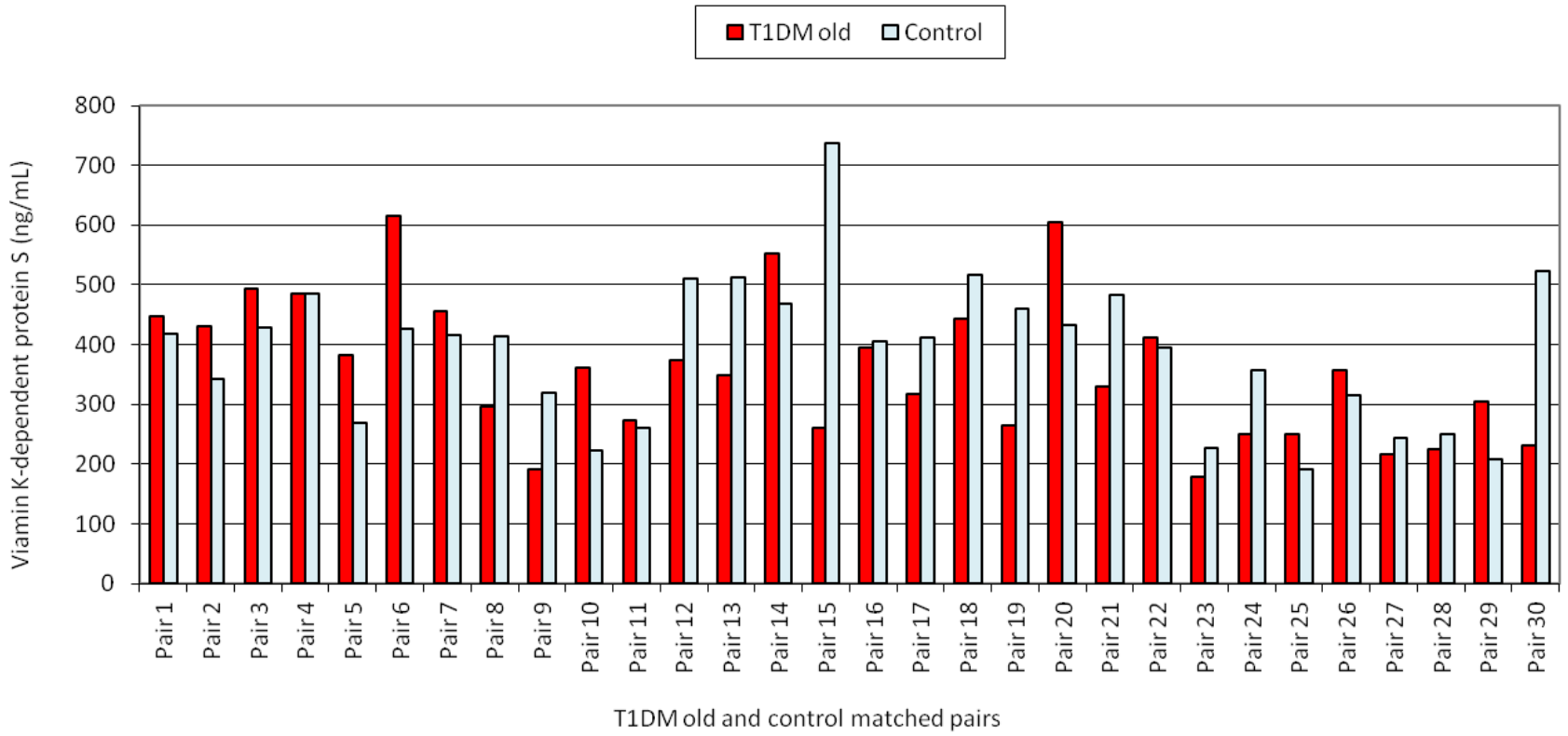

Figure 4.2.19 Vitamin K-dependent protein S in patients with established type 1 diabetes and their matched healthy controls.

4.2.7.3.3 Vitamin K-dependent protein S in samples of patients with newly-diagnosed type 1 diabetes compared to patients with established type 1 diabetes

Label-free proteomics analysis identified vitamin K-dependent protein S as being significantly up-regulated in serum of patients with newly-diagnosed type 1 diabetes, compared to patients with established type 1 diabetes. However, on expansion of the established type 1 diabetes cohort, ELISA quantification of vitamin K-dependent protein S found no significant difference in levels of this target between sera of patients with newly-diagnosed and established type 1 diabetes (358.49 vs. 360.79 ng/mL, p=0.95; Figure 4.2.20)

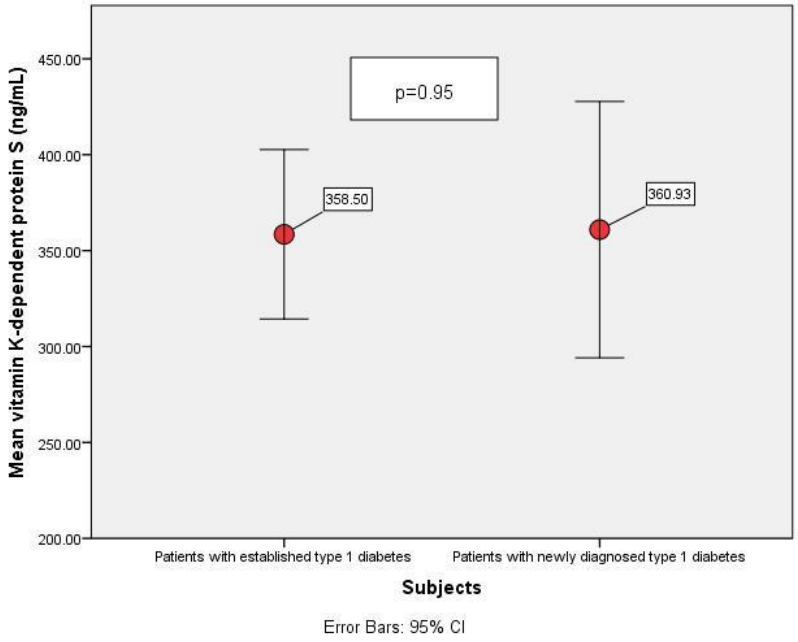

Figure 4.2.20 Vitamin K-dependent protein S concentration in patients with established type 1 diabetes (n=30) compared to patients with newly-diagnosed type 1 diabetes (n=8).

4.2.7.4Apolipoprotein L1

Label free proteomics analysis showed a significant 2.84 fold decrease in apolipoprotein L1 in sera of patients with established type 1 diabetes when compared to their matched healthy controls. It also showed a 1.88 fold decrease when sera of patients with established type 1 diabetes were compared to sera of patients with newly-diagnosed type 1 diabetes.

The human apolipoprotein L1 ELISA used for this validation study was sourced from USCN Life Science Inc. (catalogue number E9374Hu). However, no suggested serum dilutions were included in this kit. Therefore, an apolipoprotein L1 concentration estimation was performed using two serum samples (T1DM old sample DS-100 and T1DM new sample DS-170), and three dilutions of each sample, at 1:10, 1:500 and 1:5,000, as well as the lowest and highest points of the standard curve. The apolipoprotein L1 ELISA used for this experiment is based on a sandwich ELISA technique (protocol outlined in section 2.2.6.4). Therefore higher concentrations of apolipoprotein L1 should lead to high absorbance readings at 450nm. For each sample analysed, the 1:10 dilution showed the highest absorbance, with a lower absorbance reading for the 1:500 dilutions, as expected. However, absorbance readings for 1:5,000 dilutions showed higher absorbance reading than the 1:500 dilutions for both samples tested (Table 4.2.7). As the lowest dilution (1:10) absorbance readings were only marginally above the lowest standard curve reading, therefore a 1:5 dilution was chosen to perform ELISA on all remaining samples.

Samples from eight patients with newly diagnosed type 1 diabetes and their controls as well as thirty samples from patients with established type 1 diabetes and their controls were diluted at 1:5 before performing the apolipoprotein L1 ELISA.

Table 4.2.7 Apolipoprotein L1 serum concentration estimation. Absorbance values measured at 450nm for two serum samples (DS-100 and DS-170), serially diluted to 1:10, 1:500 and 1:5000

Sample	Absorbance
1.25ng/mL standard	0.21
80ng/mL standard	Too high
DS-100 1:10 dilution	0.349
DS-100 1:500 dilution	0.120
DS-100 1:5000 dilution	0.262
DS-170 1:10 dilution	0.297
DS-170 1:500 dilution	0.138
DS-170 1:5000 dilution	0.251

All sample absorbances were below the lowest point on the standard curve, therefore apolipoprotein L1 concentrations could not be deduced. DS-100 and DS-170 samples which were used for the concentration estimation were also diluted 1:5 and assayed again with all other samples. However, the absorbance reading was lower than the lowest point on the standard curve for DS-170, and

the DS-100 absorbance reading was lower than the blank absorbance reading of the standard diluent solution.

The low absorbance readings of serum samples may indicate that apolipoprotein L1 levels were below the level of detection. However, as more dilute samples showed higher absorbance readings during the concentration estimate, this may indicate that these pre-coated ELISA plates may not have been uniformly coated with the anti-apolipoprotein L1 capture antibody.

4.2.8 Summary of proteomic biomarker study

Label-free proteomics and ELISA validation results for each target analysed are shown in table 4.2.23. Only two comparisons reached statistical significance when validated using ELISA technology, 1) vitamin K-dependent protein S, in the comparison of sera from patients with newly-diagnosed type 1 diabetes and their matched controls and 2) vitronectin, in the comparison of sera from patients with established type 1 diabetes with their matched controls.

ELISA validation experiments were performed by Dr Erica Hennessy.

Table 4.2.8 Summary of proteomic studies. Legend:' T1DM new', patients with newly-diagnosed type 1 diabetes; 'control new' healthy controls matched to patients with newly-diagnosed type 1 diabetes; 'T1DM old', patients with established type 1 diabetes; 'control old', healthy controls matched to patients with established type 1 diabetes

	T1DM new vs control new		T1DM old vs control old		T1DM new vs T1DM old	
	Proteomics (n=8)	ELISA (n=8)	Proteomics (n=8)	ELISA (n=30)	Proteomics (n=8)	ELISA (T1DM N=8, T1DMO=30)
Vitronectin	1.45 fold up in T1DM new (2/3)	No change	1.64 fold down in T1DM old	**1.14 fold down in T1DM old (significant)**	1.44 fold up in T1DM new	No change
Clusterin	1.66 fold up in T1DM new	No change	No change	No change	1.43 fold up in T1DM new	No change
Vitamin K-dependent protein S	1.42 fold up in T1DM new (2/3)	**1.24 fold down in T1DM new (significant)**	2.28 fold down in T1DM old	No change	1.80 fold up in T1DM new	No change
Apolipoprotein L1	No change	Unmeasurable	2.84 fold down in T1DM old	Un-measurable	1.88 fold up in T1DM new (1/3)	Unmeasurable

4.3 Discussion on findings of proteomics serum analysis

While in the past the majority of research was hypothesis-driven, hypothesis-free global approaches, such as microarray-based transcriptional profiling or quantitative proteome analysis, have the advantage of investigating the whole complexity of an organism. Thus, evidence for patterns of changes can be provided and, potentially, new hypotheses generated. The transcriptomic and proteomic approaches are complementary as changes in mRNA levels do not necessarily mirror changes in the abundance of the proteins encoded by these genes, and potentially important post-translational modifications can only be detected by proteomics (107).

Serum is an obvious choice for proteomic profiling due to ease of access. As initial proteomic investigations in diabetes were on tissues, we are comparing our data to those.

In our study, from the four proteins identified on label-free serum proteomic analysis as being differentially expressed in type 1 diabetes (vitronectin, clusterin, apolipoprotein 1 and vitamin K-dependent protein S), only two proteins were significantly differentially expressed when validated by ELISA studies (Table 4.2.8). Vitronectin was down-regulated by 1.14 fold in established type 1 diabetes patients compared to their healthy controls, while vitamin K-dependent protein S was 1.24 fold down-regulated in patients with newly-diagnosed type 1 diabetes compared to their healthy controls.

4.3.1 Vitronectin

Vitronectin was 1.45 fold up-regulated in two thirds of patients with newly diagnosed type 1 diabetes in initial label-free proteomic experiment; this was not confirmed on ELISA. It was 1.64 down-regulated in patients with established type 1 diabetes compared to their healthy controls and that was upheld by ELISA validation.

Vitronectin is an adhesive glycoprotein which plays a role in attachment of cells to their surrounding matrix and may be involved in regulation of cell differentiation, proliferation, migration and morphogenesis (147). Vitronectin expression on angiogenic endothelial retinal cells contributes to diabetic retinopathy (148). In our group, there was no difference in vitronectin levels between patients with type 1 diabetes who had retinopathy when compared to those who did not have retinopathy (data not shown).

Vitronectin levels are increased in regulation of complement activation and blood coagulation (147). It is possible that an elevation in newly-diagnosed type 1 diabetes on label-free proteomics, albeit not confirmed on ELISA, is a remnant of autoimmune destructive processes as our patients were recruited on average around three months after diagnosis. Unfortunately, no coagulation testing was performed in our patient cohort.

4.3.2 Clusterin

Clusterin was 1.66 fold increased in newly diagnosed patients with type 1 diabetes, when compared to healthy controls on label-free proteomic analysis, but this did not hold on ELISA validation. There was no difference in clusterin between samples of established type 1 diabetes and their controls, or between the samples of patients with newly-diagnosed and established diabetes.

Clusterin is a stress-response protein involved in various biological processes, including cell proliferation, apoptosis, tissue differentiation, inflammation and lipid transport (146). Clusterin gene polymorphisms were found to be associated with type 2 diabetes in Japanese population and hepatic clusterin expression is increased by glucose stimulation (146, 149). It is also associated with metabolic changes of type 2 diabetes: high levels of circulating clusterin and LDL-bound clusterin were found in patients with type 2 diabetes (150). In another study of men only with type 2 diabetes, clusterin level was increased when LDL-associated proteins were analysed with mass spectrometry, 2-DIGE and ELISA (151). Same positive association between clusterin and LDL and total cholesterol was found in healthy young males (152) . Clusterin was also found to be low in the protein HDL of men with reduced insulin sensitivity and higher BMI (153) . In our study there was no association of clusterin with BMI, total cholesterol, LDL, HDL or triglycerides.

Reduced levels of clusterin were found in the vitreous fluid of patients with proliferative diabetic retinopathy in type 2 diabetes (112).

In type 1 diabetes, there is a significant paucity of data on clusterin. In the only available previous serum study, serum levels of clusterin were lower in patients with newly-diagnosed type 1 diabetes (within 14 days of starting insulin treatment) when compared to controls, while in our study, higher levels initially identified on label-free proteomics were not confirmed on ELISA validation (103).

4.3.3 Vitamin K-dependent protein S

Vitamin K-dependent protein S is an anticoagulant factor. It is a cofactor to activated protein C in the degradation of coagulation factors Va and VIIIa (154). It is secreted by hepatocytes, megakaryocytes and endothelial cells as well as osteoblasts; it stimulates fibrinolysis and is involved in serum-stimulated phagocytosis of apoptotic cells (155, 156). About 40% of the protein S in plasma is in the free form, whereas the remaining 60% is associated in a 1:1 complex with C4b-binding protein (C4bBP). Both forms bind strongly to negatively charged phospholipids exposed on the surface of activated platelets. Free protein S (although having no strong inhibitory effect on FVa or FVIIIa itself) forms a calcium- dependent complex with activated protein C, helping to orient its active site above the phospholipid surface and enhancing its anticoagulant activity (157).

Increased coagulation was described in type 1 diabetes, due to increased concentration of coagulation factor VII and to increased platelet adhesiveness, activation of the coagulation system, and decreased plasma fibrinolytic potential (158, 159). It is known that

hypoglycaemia activated the coagulation system, partly by increasing the concentration of von Willebrand antigen (160).

In our study, vitamin K-dependent protein S was down-regulated in patients with newly-diagnosed type 1 diabetes (which would be expected to promote coagulation) and up-regulated in patients with established type 1 diabetes (which would be expected to promote anticoagulation) on label-free proteomics. Only the down-regulation in newly-diagnosed type 1 patients was confirmed by ELISA validation.

There was no history of thrombotic events or family history of thrombosis in our cohort of patients with newly-diagnosed type 1 diabetes. Unfortunately, we have not collected any coagulation data on our patients. It is also known that hypoglycaemia promotes thrombosis; unfortunately, we have not collected data on hypoglycaemic episodes in this patient population.

Increased levels of protein S have been described in poorly controlled newly diagnosed patients type 1 diabetes, with no evident clinical consequence (161). Decreased levels of protein S have been described in patients with type 2 diabetes and microvascular complications, in particular diabetic nephropathy, while conflicting data exists on patients with type 1 diabetes with various degrees of diabetic nephropathy—increased protein S levels were found in patients with increased urinary albumin excretion and yet, a surgical study analysing prothrombotic defects in patients with type 1 diabetes undergoing pancreas/kidney transplant found a significant number of patients suffering from protein S deficiency (12/47, 25%); this had not affected their surgical thrombosis risk (162, 163).

It would certainly be interesting to assess the vitamin K-dependent protein S level in a larger sample of patients with newly-diagnosed

and established type 1 diabetes, particularly with detailed assessment of coagulation function.

4.3.4 Apolipoprotein L1

Apolipoprotein L1 is a HDL-associated lipoprotein. While label-free proteomics showed a down-regulation in established type 1 diabetes, apolipoprotein L1 was not measurable on ELISA validation. A different method would be needed to establish if there is a real difference in apolipoprotein L1 in established type 1 diabetes.

5 Metabolomic analysis in patients with newly-diagnosed type 1 diabetes

5.1 Materials and methods

Metabolites can vary greatly in their physical properties; as of yet no single technique is capable of detecting and quantifying such a diverse range of compounds.

The diagnostic company Metabolon incorporate three independent analysis platforms in their procedure for metabolite profiling, in order to get maximum separation of the different types of biochemicals present in the samples (164, 165).

Two separate ultra-high performance liquid chromatography / tandem mass spectrometry (UHPLC/MS/MS) injections and one gas chromatography/mass spectrometry (GC/MS) injection are performed per sample. One UHPLC/MS/MS injection was optimised for detection of positive ions while the second injection was optimised for negative ion detection; GC/MS platform allows for better separation of carbohydrates which are difficult to detect with LC methods.

Each detected biochemical is automatically compared to a reference standard in the company's database, using retention index and mass spectrum. The result is a broad range of biochemicals identified including amino acids, carbohydrates, lipids, nucleic acids and cofactors. The service provides two types of data: 1)biochemical data file, which contains information about each sample processed: biochemical name, super pathway, sub pathway, KEGG ID (Kyoto Encyclopaedia of Genes and Genomes) , HMDB ID (Human Metabolome Database ID), and amount detected; the data is provided in two forms, raw and imputed, and 2) statistical heat map--

statistical analysis of the data, which shows the fold change of each biochemical, grouped by super and sub pathway, and colour coded in terms of increase or decrease relative to control (164).

This type of metabolomic profiling is a non-targeted one, meaning that it allows for detection of new metabolites, not yet documented in the reference library (166).

Following an overnight fast, whole blood specimens were collected from newly diagnosed type 1 diabetes patients (n=8) and age/BMI/gender matched healthy controls (n=8). Samples were processed as detailed in the introduction. Resulting serum specimens were stored at -80°C until required. Serum specimens (500µL) were shipped on dry ice to Metabolon Inc., North Carolina, USA, where the metabolomic profiling was performed.

The samples were re-labelled by Metabolon, ED for patients with newly-diagnosed diabetes ('disease') and EN ('control').

Metabolon incorporates three independent complimentary analysis platforms to maximise the number of small molecules and metabolites that the combined systems can identify and measure. Two independent ultra-high performance liquid chromatography / tandem mass spectrometry (UHPLC/MS/MS2) injections (one optimised for basic compounds, and the other for acidic compounds) and one GC/MS injection per sample are performed.

Firstly, small molecules were extracted from serum specimens using methanol to allow precipitation of proteins. The extract supernatant was then split into four equal aliquots; two for UHPLC/MS, one for GC/MS and one reserve aliquot. Aliquots were then dried overnight to

remove solvent. For the UHPLC methods, one aliquot was reconstituted in 50µL 0.1% formic acid and the other in 50µL 6.5mM ammonium bicarbonate pH 8.0. For GC/MS analysis, aliquots were derivatised using equal parts N,O-bistrimethylsilyltrifluoroacetamide and a solvent mixture of acetonitrile:dichloromethane:cyclohexane (5:4:1) with 5% triethylamine at 60ºC for 1 hour. All reconstitution solvents contained instrument internal standards used to monitor instrument performance.

UHPLC/MS was carried out using a Waters Acquity UHPLC coupled to an LTQ mass spectrometer equipped with an electrospray ionization source. Two independent UHPLC/MS injections were performed on each sample. The acidic injections were monitored for positive ions and the basic injections were monitored for negative ions. The derivatised samples for GC/MS were analyzed on a Thermo-Finnigan Trace DSQ fast-scanning single-quadrupole MS.

The resulting MS/MS2 data was then searched against Metabolon's reference standard library. This library was generated from 1500 standards and contains the retention time/index, mass to charge (m/z), and MS/MS spectral data for all molecules in the library, including their associated adducts, in-source fragments, and multimers. The library allows identification of experimentally detected metabolites based on a multiparameter match basis. All identifications and quantifications were subjected to QC to verify the quality of the identification and peak integration.

An internal standard was added to each sample before injection onto the mass spectrometers. Instrument variability was determined by calculating the median relative standard deviation (RSD) for the internal standard; median of measured RSD was 4%. A small amount of each study sample was also used to create a homogenous pool

called the client matrix. Technical replicates of this client matrix were used to determine overall process variability by calculating the median relative standard deviation of all endogenous metabolites, which amounted to 11%. Process variability as measured by median RSD passed Metabolon's quality control criteria. Metabolon recommend an RSD cut off value of 13% to ensure minimum process variability.

5.1.1 Validation of metabolomic target fibrinopeptide A

ELISA validation of metabolite target was performed on the same eight samples of patients with newly-diagnosed type 1 diabetes and their controls as well as 30 samples of patients with established type 1 diabetes and their matched controls.

Fibrinopeptide A (FPA) ELISA was sourced from Hyphen BioMed (catalogue number RK016A). Serum specimens to be analysed were diluted by a factor of 1500 using sample diluent. Standards were reconstituted as per the manufacturer's instructions using sample diluent. 100µL of anti-FPA antibodies were added to 1mL diluted samples or standards in an Eppendorf tube, and incubated at 37°C for 1 hour. 200 µL of sample/antibody or standard/antibody mix was added to each well of the ELISA plate, and incubated for 1 hour at room temperature. The plate was washed five times using wash solution. 200µL antibody conjugate solution was added to each well and incubated for 1 hour at room temperature. The plate was washed five times using wash solution. 200µL substrate solution was added to each well and incubated for 5 minutes at room temperature. 50µL stop solution was added and incubated for 10 minutes, and then

absorbance was read at 450nm. The standard curve was plotted as log concentration versus log absorbance, and the FPA concentration of samples was calculated using the equation of the line.

5.2 Results of metabolomic profiling

In this study, we sent the samples from eight patients with newly-diagnosed type 1 diabetes and their matched healthy controls (characteristics described in section 2.1.3 and table 4.2.1) on dry ice (sample preparation described in section 5.1) to Metabolon Inc., North Carolina, USA, for metabolic profiling. The samples were re-labelled by Metabolon, ED for patients with newly-diagnosed diabetes ('disease') and EN ('control').

Overall, 302 biochemicals were detected in the serum samples. Biochemical data was analysed using two different methods--Welch's two-sample t-test was used to compare disease group versus control group as a whole, while matched pairs t-test was used to analyse the individual matched pairs. A p-value of less than or equal to 0.05 was used as a cut-off for identification of significantly different biochemicals.

Comparing disease group to control group, 19 biochemicals reached statistical significance, with 5 biochemicals at higher levels and 14 biochemicals at lower levels in the disease group relative to control. A further 13 biochemicals were just beyond the level of significance and were termed 'approaching significance', with p-value greater than 0.05 but less than 0.1. Of the 13 biochemicals approaching significance, 4 were present at higher levels and 9 at lower levels in disease versus control specimens (Table 5.2.1).

The matched pairs' analysis showed very similar results to the group analysis. 21 biochemicals were significantly different, 5 of which were at higher levels and 16 at lower levels in disease versus control. 11 biochemicals were in the approaching significance group, 6 of which were at higher levels and 5 at lower levels in disease group (Table 5.2.1)

Table 5.2.1 Biochemicals detected at significantly altered levels in patients with newly-diagnosed type 1 diabetes and their matched healthy controls.

	Welch's two-sample t-test	Matched pairs t-test
Biochemical with $p \leq 0.05$	19	21
Biochemicals (↑↓)	5|14	5|16
Biochemicals approaching significance 0.05<p>0.10	13	11
Biochemicals (↑↓)	4|9	6|5

Table 5.2.2 lists all biochemicals which were identified as significantly different either by Welch's two-sample analysis or by matched pair analysis. The fold change for the matched pair analysis is reported as the average fold changes for each of the individual matched pairs. Direction of fold change for all biochemicals in table 5.2.2 is consistent, whether analysed with Welch's two sample analysis or

matched pair analysis, although in a limited number of cases the biochemical only reaches statistical significance with one of analysis methods. Box and whisker plots of all significantly different biochemicals are shown in figure 5.1.1.

Table 5.2.2 Significantly altered biochemicals in newly diagnosed type 1 diabetes specimens compared to healthy controls. : Red boxes indicate biochemicals which are present at significantly higher levels in newly diagnosed type 1 diabetes serum specimens. Green boxes indicate biochemicals which are present at lower levels in type 1 diabetes serum specimens compared to control specimens (derived from the 'heat map' produced by Metabolon Inc.)

	Group analysis		Matched pairs analysis	
Metabolite	Fold change	P-value	Average fold change	P-value
1,5-anhydroglucitol	2.85	0.0036	2.7	0.0063
Fibrinogen cleavage peptide	2.67	0.0085	5.01	0.012
Caffeine	2.5	0.0439	1.96	0.0156
Isovalerylcarnitine	1.92	0.0081	1.69	0.0138
Theophylline	1.89	0.059	1.61	0.0316

Metabolite	Group analysis		Matched pairs analysis	
	Fold change	P-value	Average fold change	P-value
1-pentadecanoylglycerophosphocholine	1.82	0.0038	1.67	0.0053
Paraxanthine	1.78	0.0962	1.51	0.0358
Malate	1.72	0.0036	1.61	0.0022
3-carboxy-4-methyl-5-propyl-2-furanpropanoate	1.72	0.0847	1.67	0.0176
1,7-dimethylurate	1.67	0.0424	1.43	0.0474
2-methylbutyroylcarnitine	1.64	0.0214	1.41	0.0469
Glucose	1.58	0.0162	1.59	0.0175

Metabolite	Group analysis		Matched pairs analysis	
	Fold change	P-value	Average fold change	P-value
Arginine	1.56	< 0.001	1.59	< 0.001
N-acetyl threonine	1.54	0.0337	1.35	0.0659
Hexanoylcarnitine	1.49	0.0256	1.33	0.0746
Catechol sulphate	1.49	0.0099	1.59	0.0027
Sebacate	1.47	0.0081	1.41	0.0239
Propionylcarnitine	1.39	0.0335	1.33	0.0209
Succinylcarnitine	1.37	0.0445	1.33	0.0441

Metabolite	Group analysis		Matched pairs analysis	
	Fold change	P-value	Average fold change	P-value
1,3-dimethylurate	1.37	0.0345	1.28	0.0223
Urate	1.23	0.0758	1.22	0.0281
5-oxyproline	1.16	0.0225	1.16	0.0082
Glutamine	1.14	0.0339	1.14	0.0361

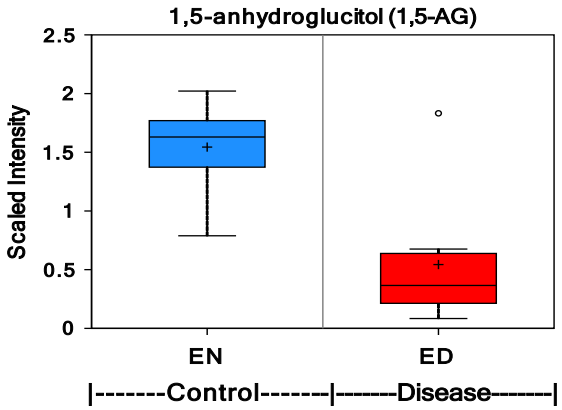
1,5-anhydroglucitol (1,5-AG)
Scaled Intensity
2.5
2
1.5
1
0.5
0
EN
ED
|-------Control-------|-------Disease-------|

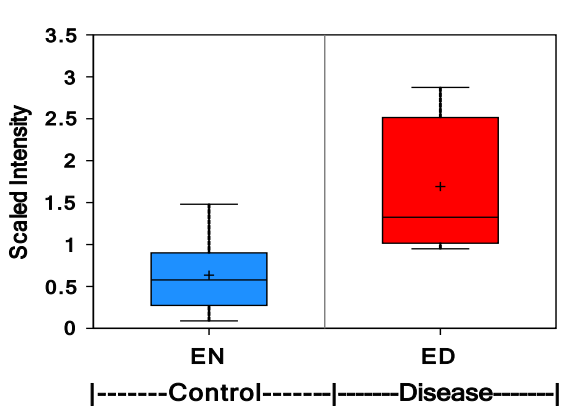
Scaled Intensity
3.5
3
2.5
2
1.5
1
0.5
0
EN
ED
|-------Control-------|-------Disease-------|

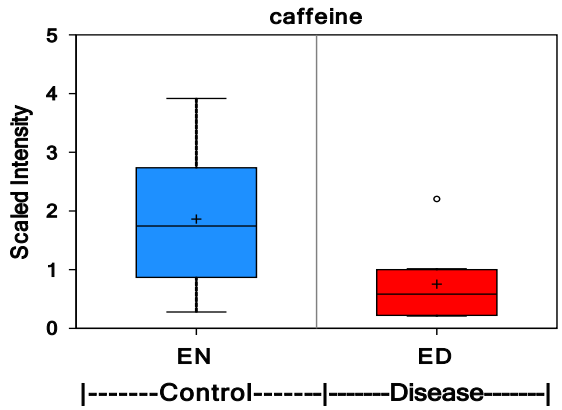
caffeine
Scaled Intensity
5
4
3
2
1
0
EN
ED
|-------Control-------|-------Disease-------|

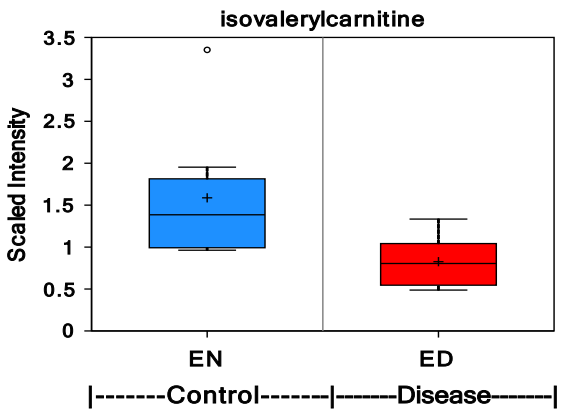
isovalerylcarnitine
Scaled Intensity
3.5
3
2.5
2
1.5
1
0.5
0
EN
ED
|-------Control-------|-------Disease-------|

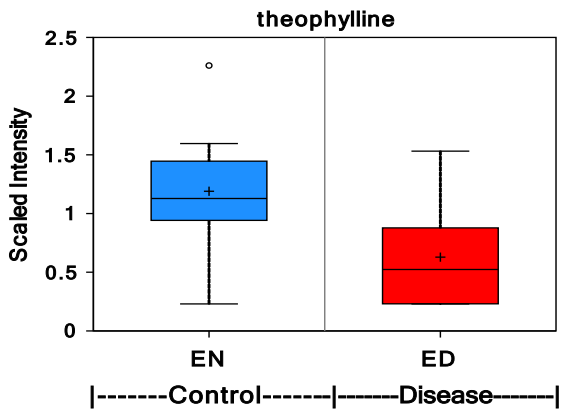
theophylline
Scaled Intensity
2.5
2
1.5
1
0.5
0
EN
ED
|-------Control-------|-------Disease-------|

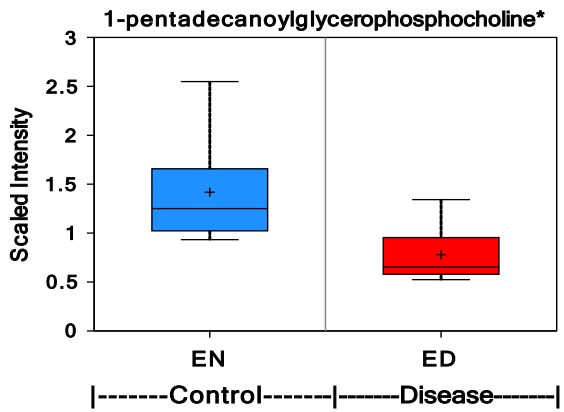
1-pentadecanoylglycerophosphocholine*
Scaled Intensity
3
2.5
2
1.5
1
0.5
0
EN
ED
|-------Control-------|-------Disease-------|

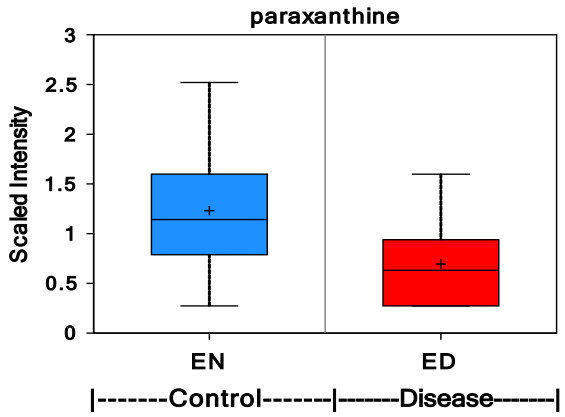
paraxanthine
Scaled Intensity
3
2.5
2
1.5
1
0.5
0
EN
ED
|-------Control-------|-------Disease-------|

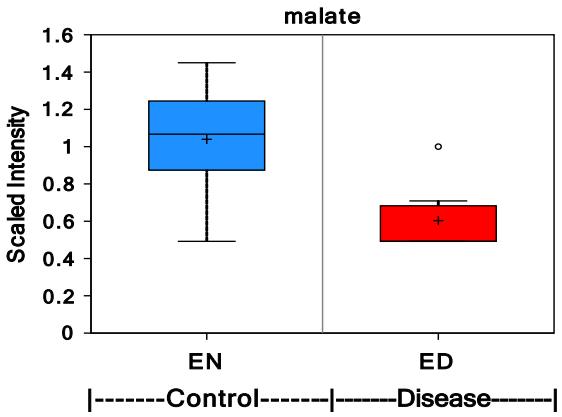
malate
Scaled Intensity
1.6
1.4
1.2
1
0.8
0.6
0.4
0.2
0
EN
ED
|-------Control-------|-------Disease-------|

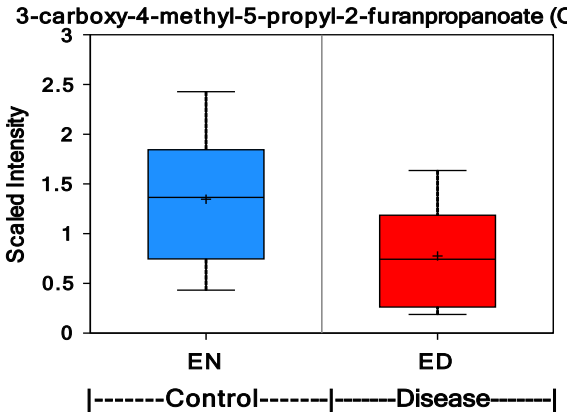
3-carboxy-4-methyl-5-propyl-2-furanpropanoate (C
Scaled Intensity
3
2.5
2
1.5
1
0.5
0
EN
ED
|-------Control-------|-------Disease-------|

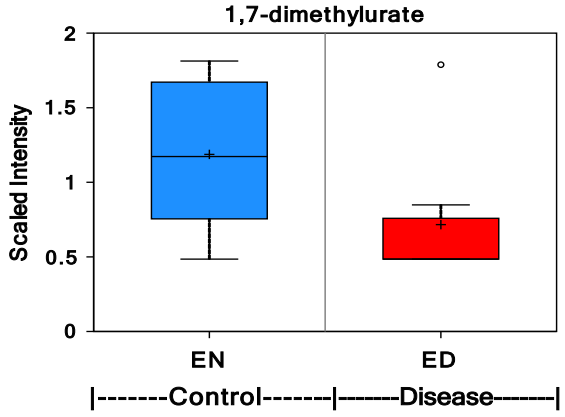
1,7-dimethylurate
Scaled Intensity
2
1.5
1
0.5
0
EN
ED
|-------Control-------|-------Disease-------|

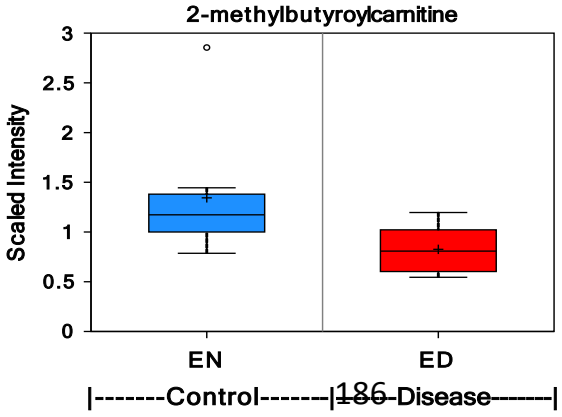
2-methylbutyroylcarnitine
Scaled Intensity
3
2.5
2
1.5
1
0.5
0
EN
ED
|-------Control-------|-------Disease-------|

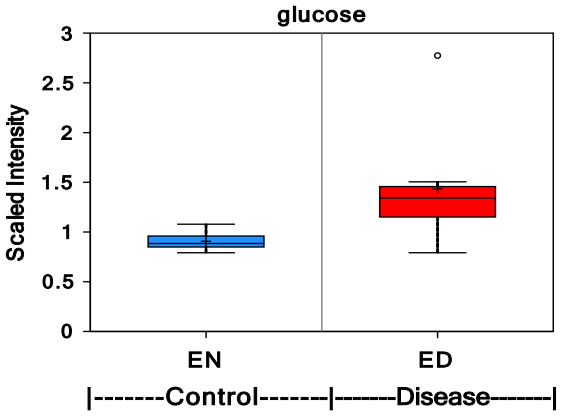
glucose
Scaled Intensity
3
2.5
2
1.5
1
0.5
0
EN
ED
|-------Control-------|-------Disease-------|

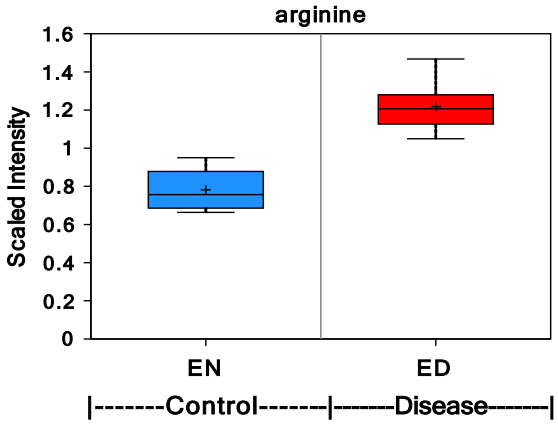
arginine
Scaled Intensity
1.6
1.4
1.2
1
0.8
0.6
0.4
0.2
0
EN
ED
|-------Control-------|-------Disease-------|

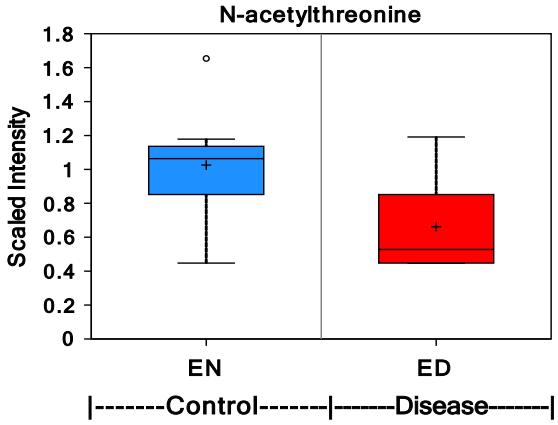
N-acetylthreonine
Scaled Intensity
1.8
1.6
1.4
1.2
1
0.8
0.6
0.4
0.2
0
EN
ED
|-------Control-------|-------Disease-------|

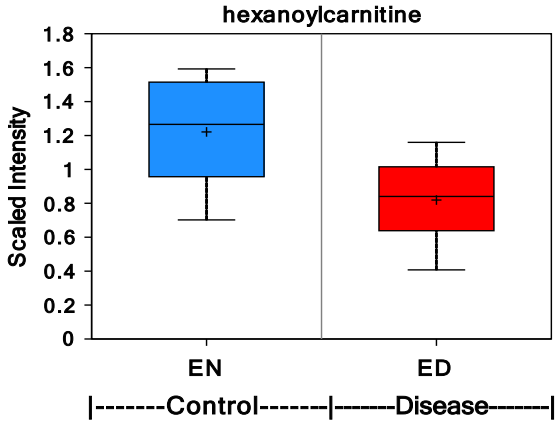
hexanoylcarnitine
Scaled Intensity
1.8
1.6
1.4
1.2
1
0.8
0.6
0.4
0.2
0
EN
ED
|-------Control-------|-------Disease-------|

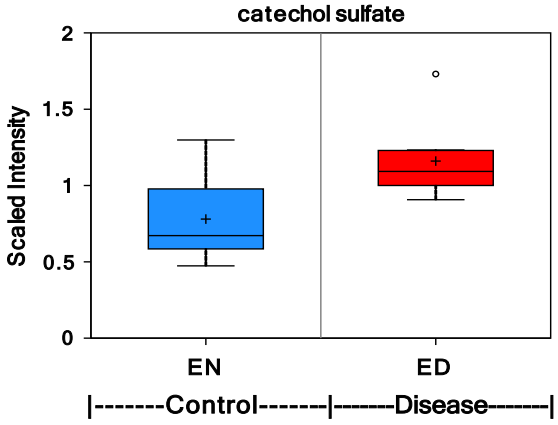
catechol sulfate
Scaled Intensity
2
1.5
1
0.5
0
EN
ED
|-------Control-------|-------Disease-------|

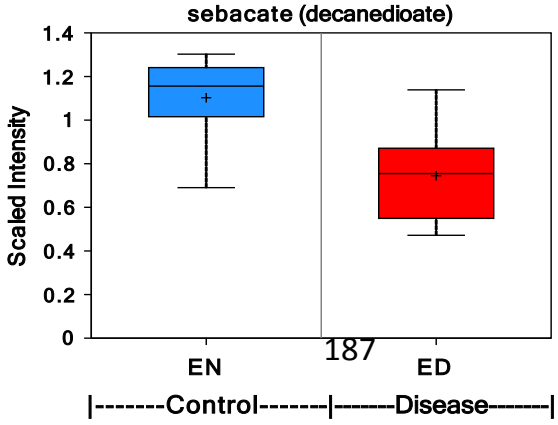
sebacate (decanedioate)
Scaled Intensity
1.4
1.2
1
0.8
0.6
0.4
0.2
0
EN
ED
|-------Control-------|-------Disease-------|

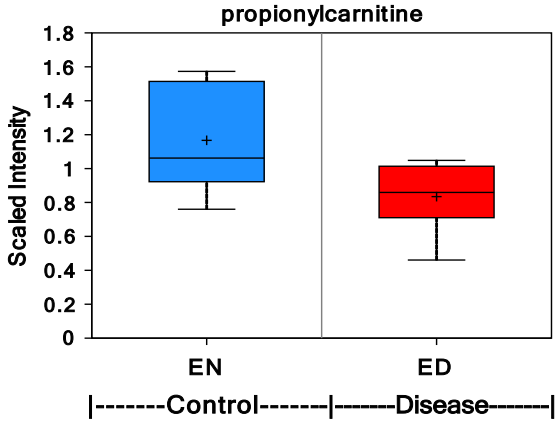
propionylcarnitine
Scaled Intensity
1.8
1.6
1.4
1.2
1
0.8
0.6
0.4
0.2
0
EN
ED
|-------Control-------|-------Disease-------|

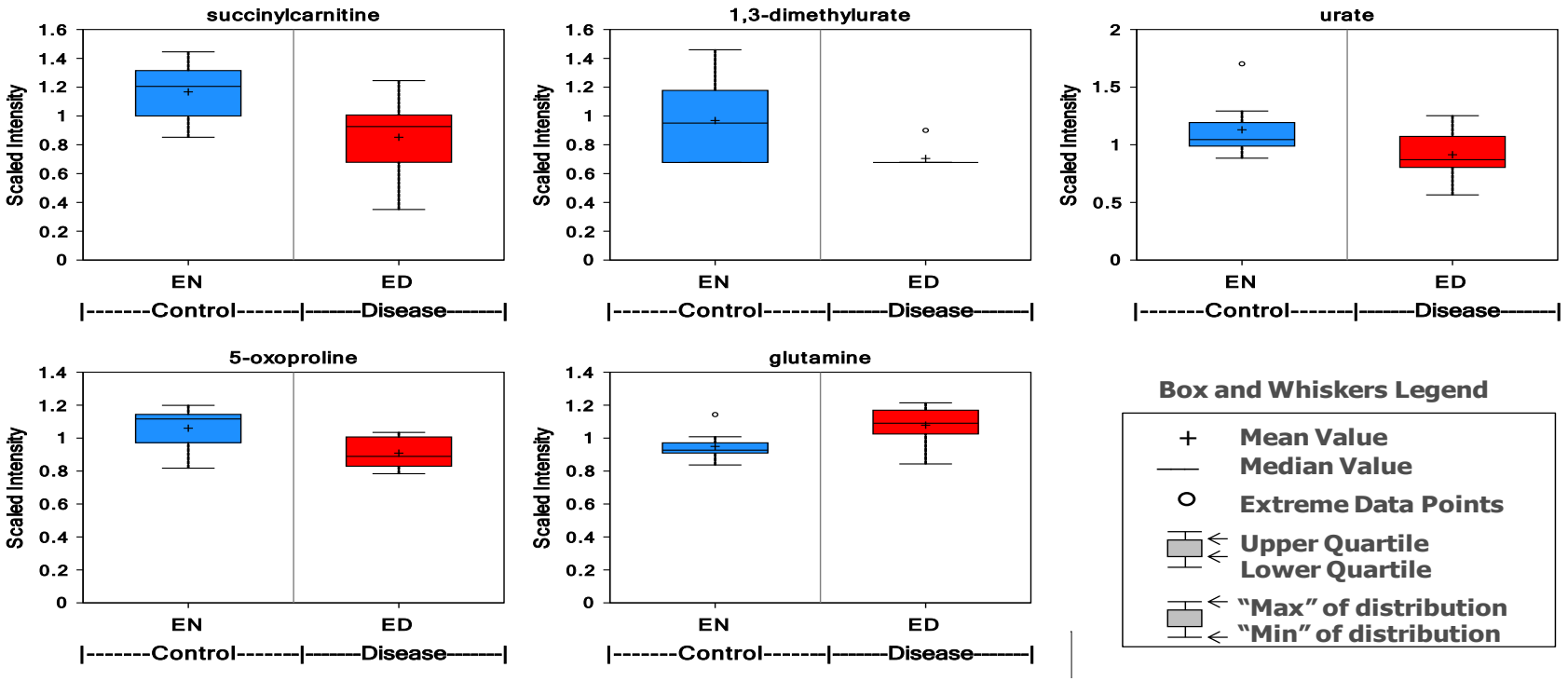

Figure 5.2.1. Box and whisker plots of all significantly different biochemicals in disease- newly diagnosed type 1 diabetes, compared to control- healthy specimens. Box and whisker plots show the distribution of the dataset. The median indicates the middle of the data, with 50% of the data being above and 50% below this value. Upper quartile indicates 25% of the data is above this value, while the lower quartile indicates that 25% of the data is below this value.

5.2.1 Validation of metabolomic targets

We picked the metabolite with the strongest fold difference in expression on metabolomic studies, fibrinogen cleavage peptide/ fibrinopeptide A, and attempted to validate it with ELISA studies.

Fibrinogen cleavage peptide/ fibrinopeptide A (FPA) levels were increased in T1DM new samples according to the metabolomics analysis by 2.67 and 5.01 fold in the groups and matched pairs' analysis, respectively. Levels of this peptide were assessed in the same samples of patients with newly-diagnosed type 1 diabetes and their matched controls using an ELISA (Hyphen BioMed catalogue number RK016A) (protocol outlined in section 2.2.7.1). ELISA confirmed a significant increase (1.8 fold) in FPA levels in samples of patients with newly-diagnosed type 1 diabetes when compared to samples of healthy controls (31.035 ± 6.058 vs 17.536 ± 4.819 µg/mL, p<0.001) (figure 5.2.2).

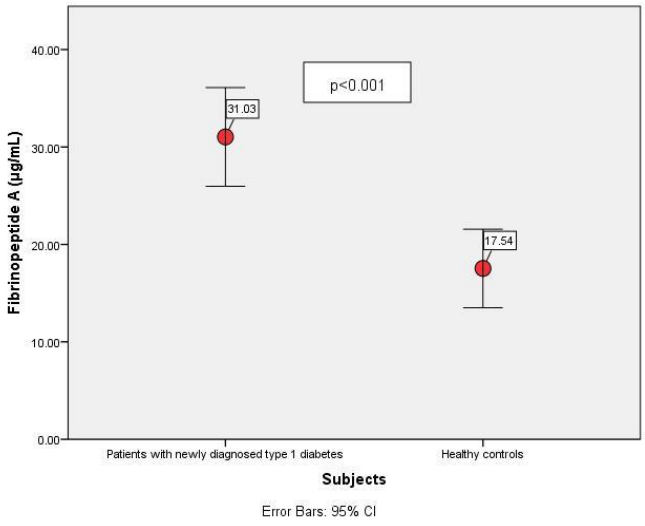

Figure 5.2.2 Fibrinopeptide A concentrations in patients with newly-diagnosed type 1 diabetes (T1DM new) and their matched controls. Error bars delineate 95% confidence intervals.

Figure 5.2.3 shows ELISA quantification of FPA in individual matched pairs. Fold change for pair 2 and pair 3 was 10 and 14 fold, respectively, according to metabolomics analysis. However, according to ELISA quantification, fold changes for these pairs was 1.37 and 1.49, respectively.

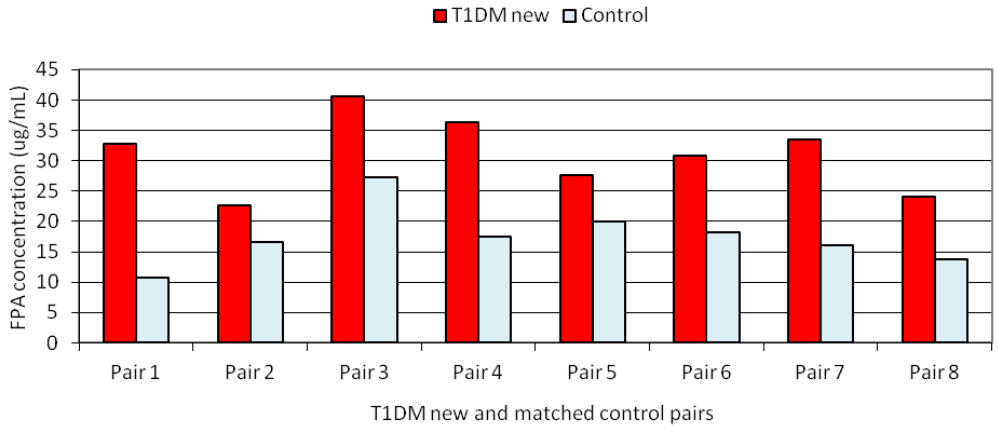

Figure 5.2.3. FPA concentrations in matched pairs of patients with newly-diagnosed type 1 diabetes (T1DM new) and their matched controls.

To test whether increased FPA levels was specifically seen in patients with newly-diagnosed type 1 diabetes or this was a more general diabetes-related event, FPA levels were assessed in patients with established type 1 diabetes. No difference in FPA levels was seen in patients with established type 1 diabetes (n=30) when compared to their matched controls (n=30) (Figure 5.2.4.).

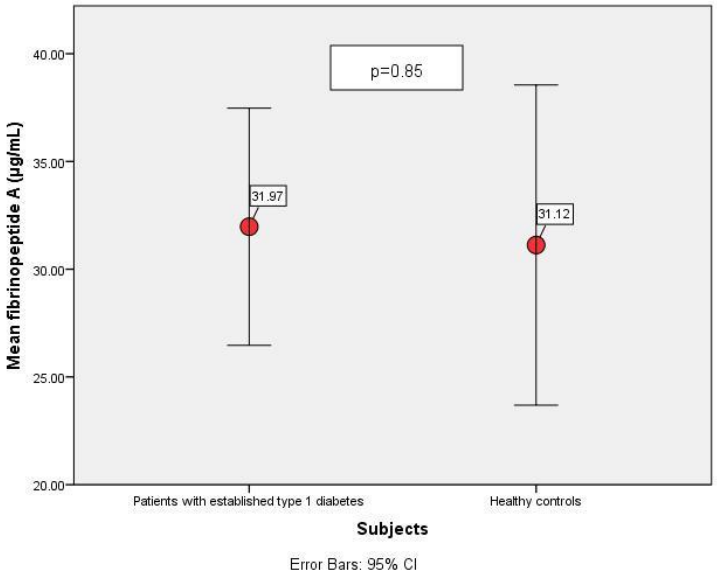

Figure 5.2.4. Fibrinopeptide A levels in patients with established type 1 diabetes and their matched controls. Error bars delineate 95% confidence intervals.

Figure 5.2.5. shows FPA levels in individual matched pairs of patients with established type 1 diabetes and their controls. FPA was down-regulated in patients with established type 1 diabetes in 11 of 30 matched pairs, while it was up-regulated in 17 of 30 matched pairs.

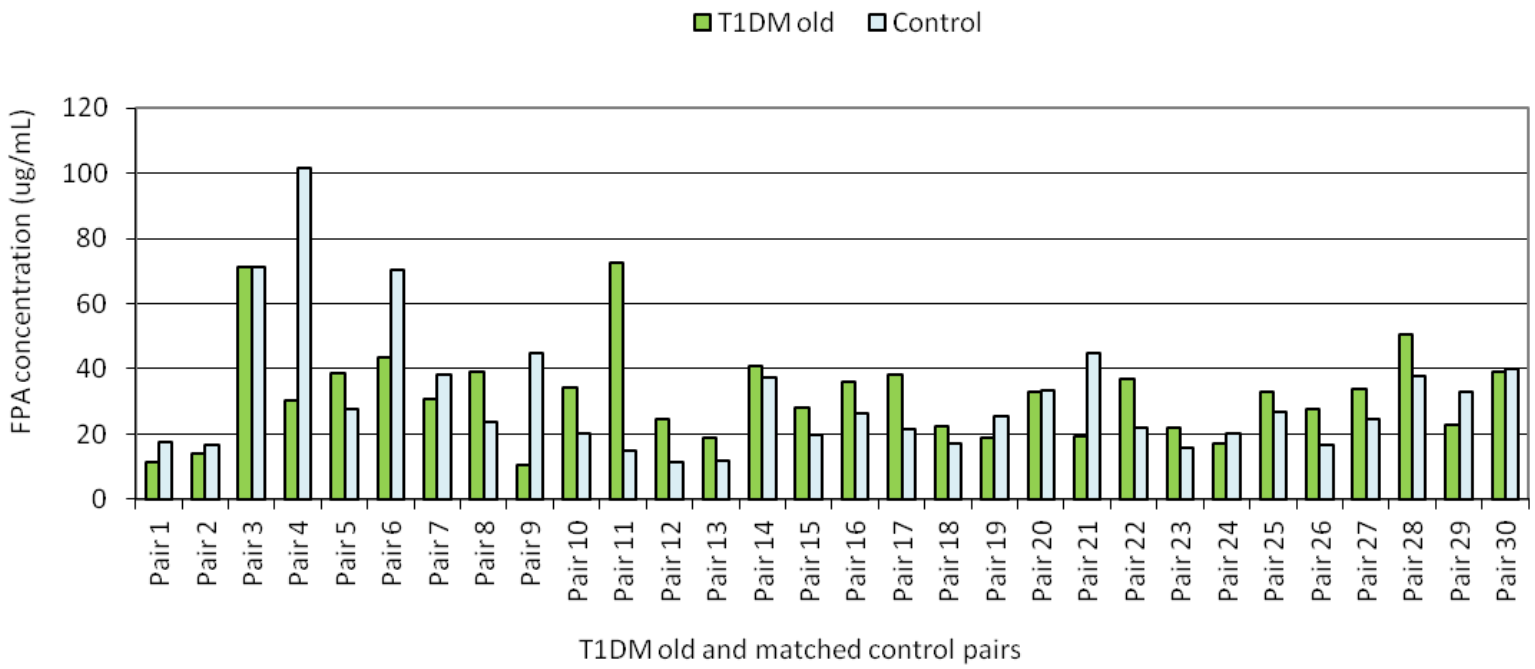

Figure 5.2.5. FPA concentration in patients with established type 1 diabetes (T1DM old) and their matched controls.

FPA levels were assessed in T1DM new (n=8) compared to T1DM old (n=30) serum specimens, however, no significant change in expression levels was seen in these groups (Figure 5.2.6).

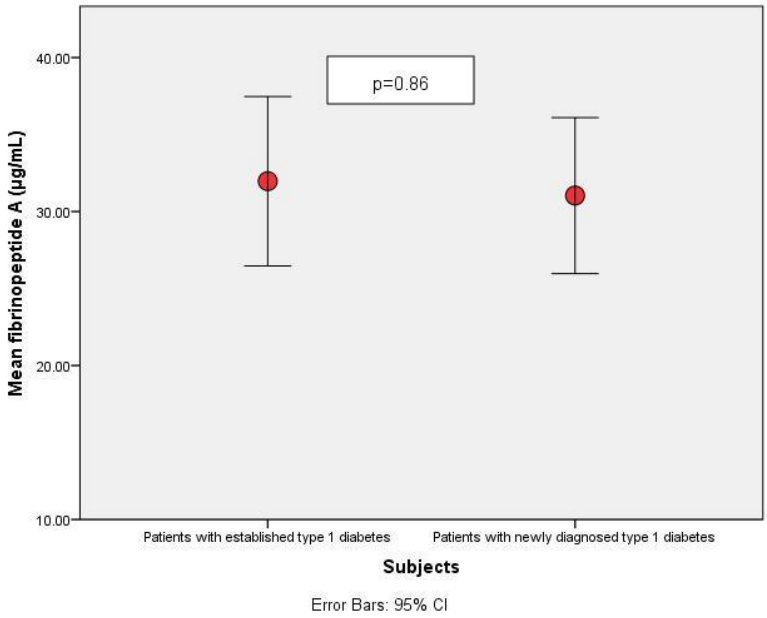

Figure 5.2. 6 . FPA concentration in patients with newly-diagnosed type 1 diabetes and patients with established type 1 diabetes. Error bars delineate 95% confidence intervals.

Fibrinopeptide levels were decreased significantly in samples of healthy controls of patients with newly-diagnosed type 1 diabetes when compared to patients with newly-diagnosed diabetes (17.536 ± 4.819 vs. 31.035 ± 6.058 µg/mL, $p<0.001$) and controls to patients with established type 1 diabetes samples (17.536 ± 4.819 vs. 31.120 ± 19.907, $p<0.001$) (Figure 5.2.7). Therefore, differential expression seen between samples of patients with newly-diagnosed type 1 diabetes and their controls seems to be related to the control samples used rather than change due to the disease.

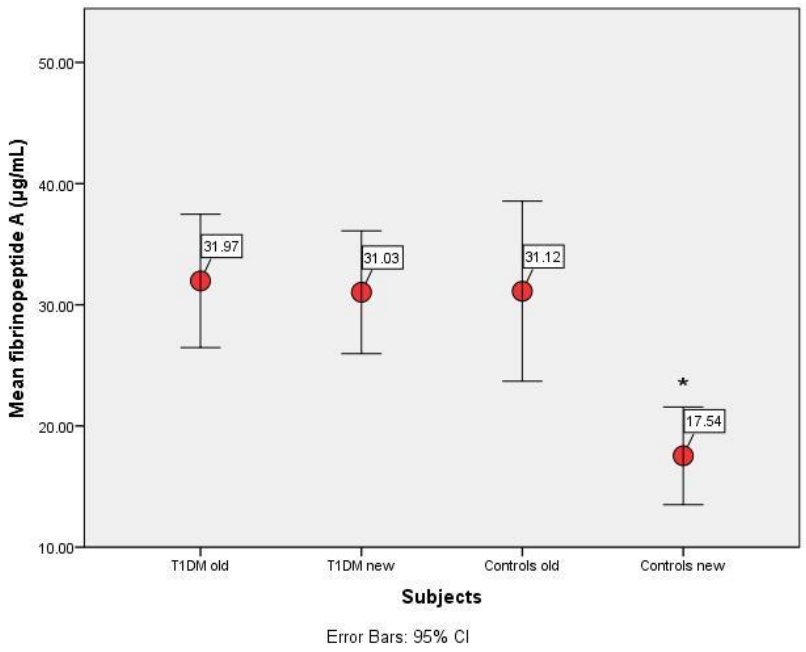

Figure 5.2.7. Concentrations of fibrinopeptide A in patients with established type 1 diabetes IT1DM old), their matched controls (control old), patients with newly-diagnosed diabetes (T1DM new) and their matched controls (control new), *p<0.01

ELISA validation experiment was performed by Dr Erica Hennessy.

5.2.2 Summary of metabolomic biomarkers study results

Twenty-one different metabolites were differentially expressed in metabolomic studies; five metabolites were higher in patients than in controls and sixteen were lower in patients with newly-diagnosed type 1 diabetes than in controls. However, the strongest differential expression of a metabolite, fibrinogen cleavage peptide/ fibrinopeptide A, was found to be due to a difference in the samples of the healthy controls, rather than in levels in patients with newly-diagnosed type 1 diabetes.

5.3 Discussion

Overall, 19 substances were significantly differentially expressed between patients with newly-diagnosed type 1 diabetes and their matched controls. Of those, 5 were more expressed in patients and 14 were less expressed in patients.

5.3.1 Carbohydrate metabolism

1.5-anhydroglucitol (1,5-AG) was the most significantly differentially expressed metabolite from the carbohydrate metabolism; it was 2.85-fold lower in group analysis and 2.7-fold lower in matched pair analysis.

This was an expected change: 1,5-anhydroglucitol is a serum monosaccharide that is excreted in the urine at an accelerated rate in the presence of glycosuria (167) (Figure 5.3.1).

1,5-AG is a naturally occurring 1-deoxy form of glucose, discovered in 1888 (168). Most of 1,5-AG is thought to originate from the diet, soy being the largest food source, while rice and pasta contain smaller quantities (169). A negligible amount is produced de novo (169). Its function in the human metabolism is still unknown.

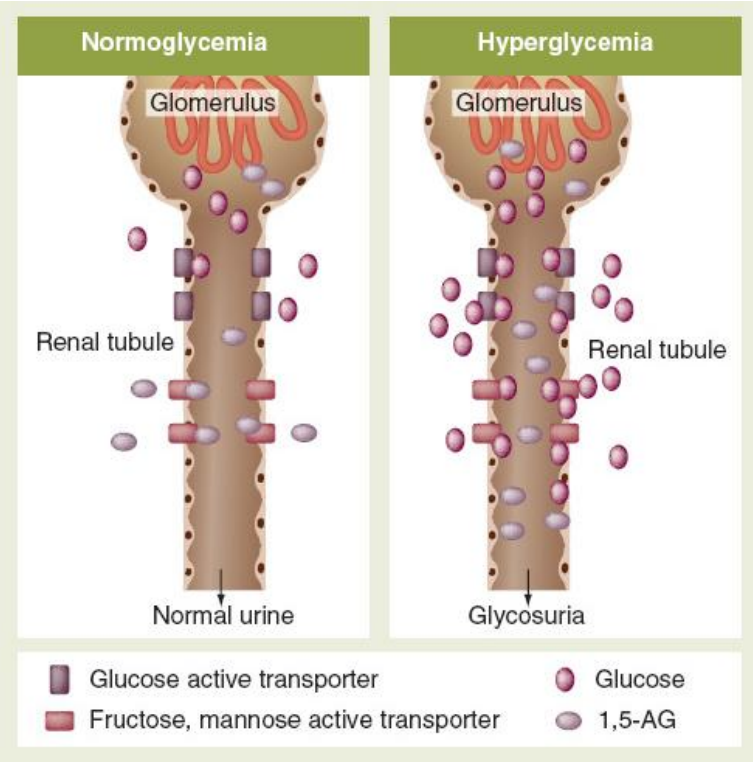

Figure 5.3.1 Competitive tubular reabsorption of glucose and 1, 5-anhydroglucitole (1,5-AG) in hyperglycaemia [*Adapted from Dungan, 2008 (169)*].

1, 5-AG intake is balanced by urinary excretion and nearly 99.9% is absorbed by the kidney (170). It appears to be transported through the SGLT4 transporter (sodium-glucose co-transporter 4) (169). After 1,5-AG is filtered through the kidney, it competes with glucose for reabsorption in the kidney tubule (168). When circulating levels of glucose increase the above the renal threshold for glucose (around 10 mmol/L) even temporarily, 1,5-anhydroglucitol is lost in the urine and circulating levels fall, hence poor glycaemic control is associated with low serum levels of 1,5-AG (169).

1,5-AG reflects glycaemic status over the preceding 48 hours to 2 weeks and it has been used in Japan for over a decade to ascertain short-term diabetes control (168). 1, 5-AG appears to correlate better than HbA1C with extent of glycaemic excursions and to be more successful at identifying patients with great fluctuations in glucose

levels despite similar HbA1C levels (170). It is not, however, as good as fasting glucose and HbA1c at establishing the diagnosis of diabetes due to poor sensitivity and specificity (168, 171). Recently it was successfully used to identify people at risk of cardiovascular disease development (172).

There were no other metabolites involved in glucose metabolism which were significantly differently expressed.

Malate and succynilcarnitine, metabolites from the Krebs cycle (citric acid cycle, tricarboxylic acid cycle, TCA) were less expressed in patients with newly-diagnosed type 1 diabetes (Figure 4.3.2). Succynilcarnitine is derived from succinyl-coenzyme A, which is derived from pyruvate in the Krebs cycle, while malate is part of the Krebs cycle metabolites (Figures 5.3.2 & 5.3.3). We hypothesise that reduction of levels of these two metabolites was due to a possible relative pyruvate deficiency in patients with type 1 diabetes, as pyruvate level reduction per se did not reach statistical significance in our study. It was previously shown in a study with radiolabelled carbon on Krebs cycle metabolites in type 1 diabetes that relative contribution of pyruvate oxidation to TCA cycle flux was decreased by approximately 30% in patients with type 1 diabetes (173).

Pyruvate, the starting point of the Krebs cycle, is the end product of glycolysis. While glucose levels were high in our patients with newly-diagnosed type 1 diabetes (table 5.2.1), in order for glucose to enter the cell and enter the glycolytic pathway, insulin needs to be present. Our patients were fasting and had very variable levels of insulin on board, having been instructed not to take any insulin that morning; the only insulin present being the long-acting preparation taken the

night before. Hence, their insulin levels may not have been high enough to transport sufficient amount of glucose across the cell membrane at the time of testing. This would account for lower pyruvate and consequently lower succinylcarnitine and malate. This pattern of reduced citric acid cycle metabolites was previously described in proteomic analyses of sera of patients with type 2 diabetes (174).

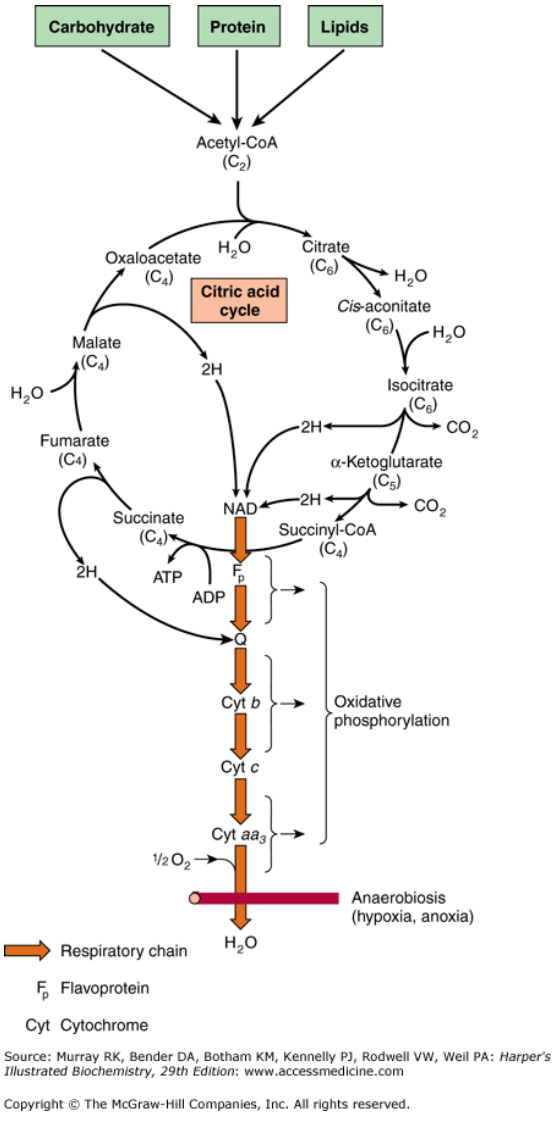

Figure 5.3.2 Citric acid cycle, positions of malate and succynil-coenzyme A visible *(Adapted from Murray et al. Harper's Illustrated Biochemistry, 29th ed.)*

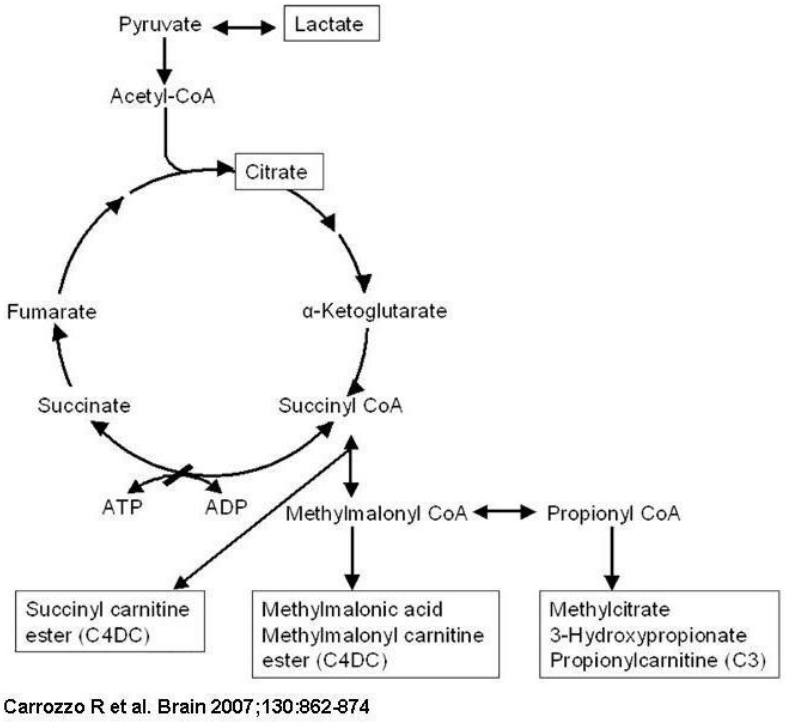

Figure 5.3.3 Citric acid cycle, pathway to synthesis of succinylcarnitine ***[Adapted from Carrozo et al (175)]***

5.3.2 Lipid metabolism

On routine blood tests, controls had higher total cholesterol and higher LDL; this was despite the fact that none of our patients with type 1 diabetes was on statin treatment (Table 4.2.1). Considering that both patients and controls were rather young, there is most likely no pathological reason and it is due to chance that controls have less healthy lipid profiles. That said, controls to newly-diagnosed type 1 diabetes patients were all medical interns; we could possibly extrapolate that being a medical intern is not the healthiest of lifestyles.

When the metabolome was analysed, several components of lipid metabolism were differentially expressed: sebacate, 3-carboxy-4-methyl-5-propyl-2-furanpropanoate (CMPF) (only on matched pairs mean ratio analysis), propionylcarnitine, hexanoylcarnitine (Welch two-sample T-test only), and 1-pentadecanolglycerophosphocholine (Table 5.2.2).

Sebacate and CMPF, both fatty acid dicarboxylates, were decreased in serum of patients with newly-diagnosed diabetes (Table 5.2.2). This is, at least in part, great news for our patients as CMPF is a known uremic toxin, which induces cell damage to proximal tubular cells via the generation of a radical intermediate (176).

Reduced levels of fatty acids in fasting patients with type 1 diabetes could be connected to decreased lipolysis, which would fit in with relatively good glycaemic control of our patients (mean HbA1C of 7.68%), meaning that they were mostly able to satisfy the energy metabolism requirements from glucose metabolism, rather than

needing to recruit energy creation from fat. Reduced levels of fatty acids could be also due to inappropriately high insulin from their basal (background, long acting) insulin

Lipolysis involves the hydrolysis of triglycerides stored in adipose tissue into free fatty acids (FFA) in the fasted state, when hormone-sensitive lipase is stimulated by glucagon and cortisol. FFAs can then pass into the blood stream and travel to sites of energy requirements. β-oxidation is the breakdown of FFAs to acetyl coenzyme-A (CoA), which can enter the TCA cycle to generate energy. β-oxidation of FFAs occurs in the mitochondrial matrix and in order for FFAs to access the mitochondrial matrix they must be transported via a carnitine shuttle (Figure 5.3.4). Firstly FFAs undergo conjugation to CoA generating fatty acyl-CoA. Fatty acyl-CoA is then transiently attached to carnitine via a transesterification reaction to form fatty acyl-carnitine, which can then be translocated into the mitochondrial matrix via the acyl-carnitine transporter. Once inside the mitochondrial matrix, the fatty acyl-CoA is regenerated, while the carnitine molecule is released and transported back into the intermembrane space ready to transport the next fatty acyl-CoA molecule (177).

In this study, a number of fatty acylcarnitine compounds were present at lower levels in the patients with newly-diagnosed type 1 diabetes compared to controls. Propionylcarnitine and hexanoylcarnitine levels were significantly lower 1.39 and 1.47 fold, respectively. A decrease in free carnitine and increase of acylcarnitine has previously been reported in sera of young patients with poorly controlled type 1 diabetes (178).

The decrease in fatty acylcarnitine compounds could be related to reduced β-oxidation in our patients—as carnitine shuttle-mediated

transportation of fatty acyl-CoA molecules into the mitochondrial matrix is the rate limiting step of fatty acid β-oxidation, lower levels of free carnitine would lead to lower levels of fatty acid β-oxidation, and subsequently lower levels of fatty acid dicarboxylates. This could also be due to the lower level of fatty acids due to decreased lipolysis.

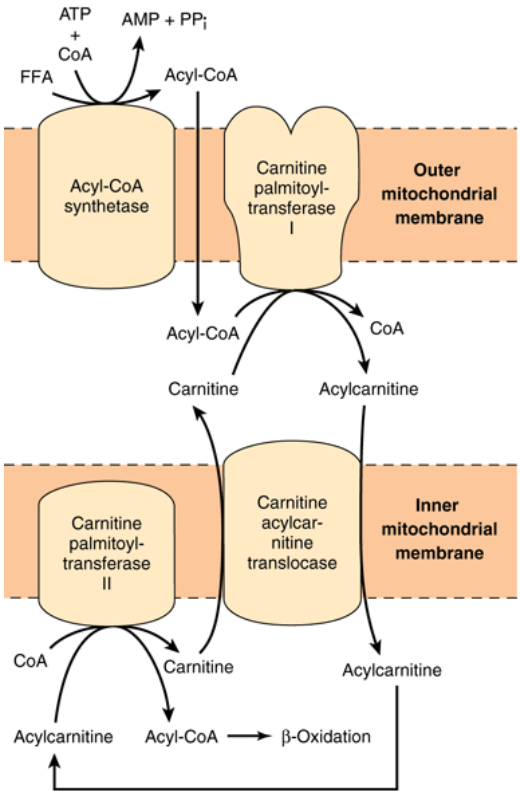

Figure 5.3.4 Transport of fatty acids through carnitine shuttle and link to FFA β oxidation, Krebs cycle and respiratory chain *(Adapted from Murray et al, Harper's Illustrated Biochemistry, 29th e d(177)*

The lysolipid- 1-pentadecanolglyerophosphocholine was also present at significantly lower levels (1.82 fold) in serum of patients with newly-diagnosed type 1 diabetes compared with controls. Lysolipids are involved in the formation of lipid bilayers of cell membranes.

Of the 16 lysolipids detected in this study, 1-pentadecanoylglycerophosphocholine is the only lysolipid which is significantly reduced in sera of patients with newly diagnosed diabetes. No obvious trend was seen in the other lysolipids analysed and the patophysiology behind this result remains a mystery to us.

Lipid metabolite changes identified in this study cannot be conclusively determined to be related to type 1 diabetes. As control subjects' cholesterol was significantly higher than that of patients with type 1 diabetes and the control subjects overall exhibited a less healthy cholesterol profile, with higher LDL cholesterol, it is plausible that results of our lipid metabolism analysis were thus skewed.

5.3.3 Amino acid metabolism

The aminoacids arginine and glutamine were present at increased levels in samples of patients with newly diagnosed diabetes compared to control, 1.56 and 1.14 fold respectively.

Arginine and glutamine are gluconeogenic aminoacids; after degradation of gluconeogenic amino acids, their carbon skeleton is diverted to gluconeogenesis (Figure 5.3.5). Arginine is also a urea cycle intermediate further indicating an increase in proteolysis, as the urea cycle functions to convert ammonia from amino acid oxidation to urea for excretion (Figure 5.3.6 A). Glutamine is also a major component of amino acid oxidation (Figure 5.3.6 B). Ammonia generated from amino acid oxidation is toxic to tissues; therefore, it is combined with glutamate to yield glutamine, which can then be transported safely to the liver or kidneys for excretion. Increased levels

of glutamine therefore also suggest increased activity of the amino acid degradation pathway.

Newly presenting patients with type 1 diabetes and patients with poorly controlled established diabetes typically exhibit increased protein catabolism and muscle wasting (30). As our patients were well controlled, this would explain a small difference in gluconeogenic amino acid level between patients and controls, indicating they were not suffering from significant levels of muscle wasting and proteolysis.

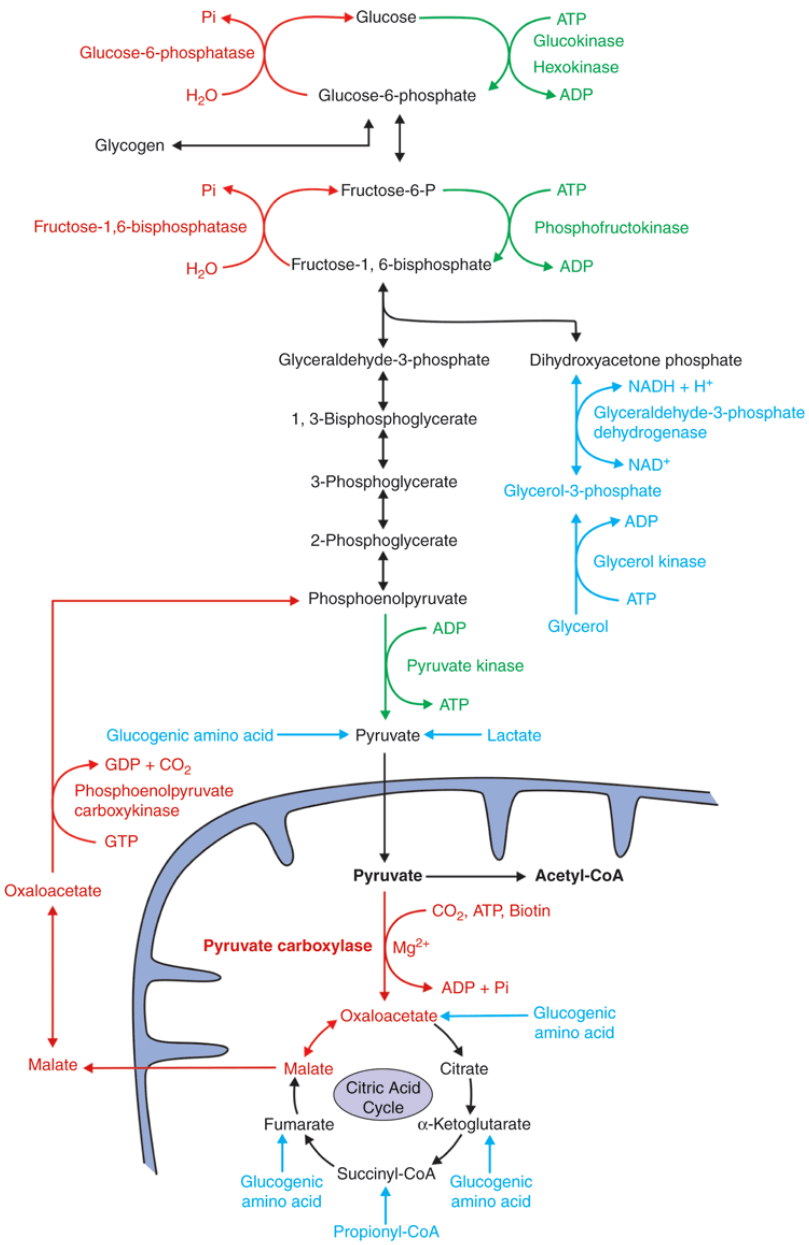

Source: Janson LW, Tischler ME: *The Big Picture: Medical Biochemistry*: www.accessmedicine.com

Figure 5.3.5 The pathway of gluconeogenesis includes 11 enzymatic steps, which form one molecule of glucose from two molecules of pyruvate. Reactions and enzymes specific only to gluconeogenesis are shown in red. Irreversible reactions specific for glycolysis are shown in green. Additional substrates for gluconeogenesis are shown in blue and may also enter gluconeogenesis as denoted by the associated arrows. *(Adapted from Naik P: Biochemistry, 3rd edition, Jaypee Brothers Medical Publishers Ltd, 2009, published in Janson (179))*

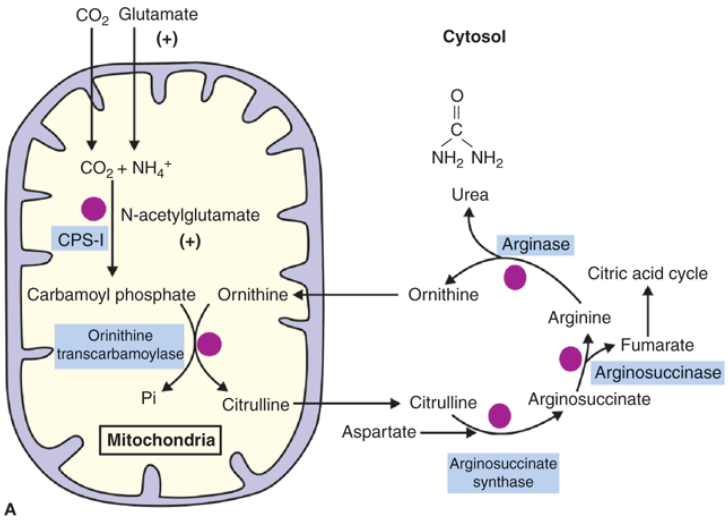

Figure 5.3.6 A. The urea cycle converts two amino groups (NH3) from glutamate and aspartate into urea as part of the body's nitrogen balance. Glutamate donates the first nitrogen atom via the molecule carbamoyl phosphate that is synthesized via the regulated enzyme carbamoyl phosphate synthetase (CPS-1). This enzyme is activated by increased glutamate, N-acetylglutamic acid, and/or arginine concentrations [indicated by (+)]. Carbamoyl phosphate then enters the urea cycle by combination with ornithine via ornithine transcarbamoylase. Aspartate donates the second nitrogen. Other amino acids contribute amino groups after conversion into glutamate or aspartate. *Adapted from Janson et al, (179).*

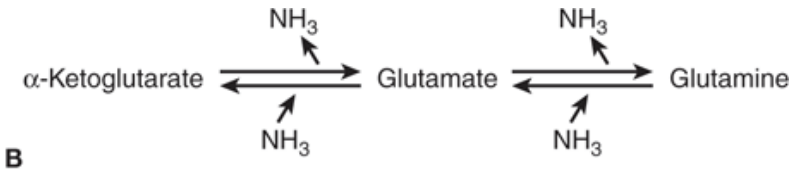

Figure 5.3.6 B. α-ketoglutarate/glutamate/glutamine Ammonia Buffering System. The interconversion of -ketoglutarate to/from glutamate to/from glutamine offers the body an important system to utilise, generate, and/or store ammonia. *Adapted from Janson et al (179).*

Other amino acid-related metabolites less expressed in sera of patients with newly-diagnosed type 1 diabetes were isovalerylcarnitine, 2-methylbutyorylcarnitine, N-acetilthreonine. Isovalerylcarnitine and 2-methylbutyorylcarnitine come from the valine/leucine/isoleucine metabolism pathway.

As valine, leucine and isoleucine are essential amino acids, and cannot by synthesised in the body, metabolites of these amino acids are an indication of amino acid oxidation rather than amino acid synthesis. Valine, leucine and isoleucine amino acids contain aliphatic side chains and are therefore known as the branched chain amino acids (BCAA). BCAAs have previously been reported to be of significance in diabetes, with raised BCAA levels presenting prior to autoantibody positivity in children which later develop type 1 diabetes (18). Similar pattern of reduced alanine, leucine, isoleucine, valine, ,methionine, proline, lysine, tyrosine, histine and glutamine was previously seen in metabolomic analysis of sera of type 2 diabetes patients (174). Increased levels of BCAAs have previously been seen in studies of patients with poorly controlled type 1 diabetes (180, 181). The reduced level of BCAAs in our well patient cohort could be due to good metabolic and glycaemic control.

N-acetyl threonine, involved in threonine metabolism, another essential amino acid, was also down regulated in samples of patients with newly-diagnosed type 1 diabetes. 5-oxyproline, involved in glutathione metabolism was also down regulated in patients with newly diagnosed type 1 diabetes. There is no known association between these amino acid metabolites and diabetes. .

5.3.4 Peptide metabolism

On metabolomic analysis, the only significantly differently expressed peptide between patients with newly-diagnosed type 1 diabetes and controls was fibrinogen cleavage peptide/fibrinopeptide A (FPA). FPA was significantly increased in samples of patients with newly-diagnosed type 1 diabetes. This was proven during ELISA validation to be due to the differentially expressed FPA in control samples matched to patients with type 1 diabetes, rather than to up-regulation in patients with newly diagnosed type 1 diabetes (Section 5.2.1)

FPA is produced during the clotting process, when thrombin cleaves fibrinogen to produce fibrin and fibrinopeptide. Up-regulation of FPA has previously been reported in type 1 diabetes (182). Raised levels of FPA have previously been linked to increased alcohol consumption (183). While control subjects consumed more alcohol per week than patients with type 1 diabetes in our study, the difference was not statistically significant.

5.3.5 Nucleotide metabolism

Urate levels were significantly decreased in samples of patients with newly diagnosed type 1 diabetes when compared to control subjects, by 1.23 fold.

Urate is formed from the degradation of purine-containing nucleotides (adenine and guanine), and is excreted in the urine (36). Low levels of urate could indicate reduced activity of nucleotide catabolism, due to either reduced purine intake in the diet, or reduced proteolysis. Increased uric acid levels have been reported to be associated with

increased risk of microvascular complications in patients with type 1 diabetes (184). Our patients were newly diagnosed and hence, complication-free.

As urate was the only differently expressed metabolite of eleven nucleotide-related metabolites detected, we conclude that changes in nucleotide metabolism were minor.

5.3.6 Xenometabolites

Caffeine, paraxantine, theophylline, cathecol sulphate and 1,3 dimethylurate are xenometabolites, meaning that they are substances with no role in organism's metabolism.

In our study, caffeine, paraxantine and 1, 3-dimethylurate were present at a lower level in patients with type 1 diabetes than in control subjects.

They are all caffeine metabolites, which would indicate that the control subjects, medical interns, consumed a lot more caffein-containing products than the patients with type 1 diabetes

Cafestol, the diterpene present in coffee, previously described as the most potent cholesterol-elevating compound in human diet, was not found in sera of patients or controls.

Cathecol sulphate was increased in patients with newly-diagnosed type 1 diabetes. Cathecol sulphate is a benzoate metabolite and benzoates are food preservatives used in acidic juices and soft drinks, indicating that patients with type 1 diabetes consumed more soft drinks than medical interns.

5.3.7 Summary of metabolomic studies

In the snapshot of metabolome, our patients with newly-diagnosed type 1 diabetes were found to have less 1,5-anhydroglucitol, consistent with higher glucose levels than controls.

Krebs cycle metabolites malate and succinylcarnitine were less expressed in patients with newly-diagnosed type 1 diabetes, possibly due to relative pyruvate deficiency, or decreased flux of pyruvate into TCA cycle.

Fatty acylcarnitine compounds were present at lower levels in patients with newly-diagnosed type 1 diabetes when compared to controls; this may be related to reduced β-oxidation of fatty acids in our patients.

Gluconeogenic aminoacids arginine and glutamine were present at significantly increased levels in sera of patients with newly-diagnosed type 1 diabetes, most likely due to increased muscle catabolism in patients with diabetes in fasting state.

Branched chain aminoacids were also less expressed in patients with newly-diagnosed type 1 diabetes.

Peptide and nucleotide metabolism were not significantly different between patients and controls.

Xenometabolites derived from caffeine were more expressed in control subjects, while xenometabolites derived from sodium benzoate were more expressed in control subjects.

6 Conclusion

6.1 Serum mRNA studies

Based on previous cell line work from our Dublin City University colleagues, several mRNA targets were investigated with qRT-PCR. Of those, two were found in the sera of our patients with newly diagnosed type 2 diabetes and their healthy controls, thioredoxin-interacting protein (Txnip) and early growth factor 1 (Egr1). No significant difference of expression was found in Txnip expression levels between patients with newly-diagnosed diabetes and their controls, contrary to findings of previous muscle biopsy studies.

Considering Txnip's mode of action through arrestin-mediated supression of glucose uptake, it would be interesting ot extend this study to other groups of patients, particularly those with impaired fasting glucose and impaired glucose tolerance as well as patients with poorly controlled diabetes mellitus, as initially planned when devising this study. We hope that financial constraints which prevented us from performing these analyses at the time will be overcome in the future.

Egr1 mRNA was significantly more expressed in patients with newly diagnosed type 2 diabetes when compared to controls. In cell cultures, Egr1 expression is reported to be both inducible and repressed by insulin and glucose induces Egr1 mRNA in various β-cell

models; in the only human serum study known to us, it was inducible by oral glucose load (83). It has been proposed that Egr1 overexpression is the mechanism by which hyperinsulinism induces insulin resistance in adipocytes (185).

In our study, no relationship between Egr1 expression and insulin or fasting glucose levels was observed, so we have no data to support or refute the above theory.

As Egr1 is a major transcription factor in atherosclerosis, even though our patients had no history of atherosclerosis or atherosclerosis-related events, it would be interesting to follow this cohort in the future and record the occurance of cardiovascular events, to investigate if increased Egr1 transcription could have had pathological consequences (138).

6.2 Serum proteomics studies

Proteomic profiling was performed on sera of patients with newly diagnosed type 1 diabetes and their healthy controls as well as patients with established type 1 diabetes and their healthy controls.

Initial label-free proteomic analysis identified four targets as differentially expressed: vitronectin, clusterin, vitamin K-dependent protein S and apolipoprotein A.

Label-free proteomics results were validated by ELISA for each target analysed. Only two comparisons reached statistical significance when validated using ELISA technology: vitamin K-dependent protein

S, which was decreased in sera from patients with newly-diagnosed type 1 diabetes when compared to their matched controls; and vitronectin, which was decreased in sera from patients with established type 1 diabetes when compared with their matched controls.

While the decrease in anticoagulant protein S in our patients with type 1 diabetes would have reasonably been expected to have a prothrombotic effect, no such events were reported by patients with newly diagnosed type 1 diabetes. While we had not performed any coagulation testing, the usual screening tests, prothrombin time and activated partial thromboplastin time, would not have been much use as they do not assess the propensity of organism to clotting adequately. It would be interesting to perform additional detailed thrombophilia studies on patients with newly diagnosed type 1 at diagnosis, including protein C, antithrobin levels, activated protein C resistance assay and factor V Leyden mutation, if necessary, as well as prothrombin G-20210-A mutation, lupus anticoagulant studies, anticardiolipin and β2-glycoprotein 1 antibody, to exclude any known thrombophilia which could have started a coagulation process, leading to consumption of protein S in clot formation.

As one of the shortcomings of this study was that data on hypoglycaemia was not collected, this would need to be included in any further studies expanding on this finding, possibly coupled with continuous glucose monitoring to investigate the relationship of decreased protein S to hypoglycaemic events.

Regarding vitronectin, while our patients with established type 1 diabetes with reduced serum vitronectin levels did not have an increased prevalence of retinopathy, it would be interesting to follow this group for development of retinopathy in the future.

6.3 Serum metabolomics studies

In the snapshot of metabolome, there were not many unexpected findings. Patients with newly-diagnosed type 1 diabetes were found to have less 1,5-anhydroglucitol, consistent with higher glucose levels than controls.

Krebs cycle metabolites malate and succinylcarnitine were less expressed in patients with newly-diagnosed type 1 diabetes, possibly due to relative pyruvate deficiency, or decreased flux of pyruvate into TCA cycle.

Fatty acylcarnitine compounds were present at lower levels in patients with newly-diagnosed type 1 diabetes when compared to controls; this may be related to reduced β-oxidation of fatty acids in our patients.

Gluconeogenic aminoacids arginine and glutamine levels were higher in patients with newly-diagnosed type 1 diabetes, most likely due to increased muscle catabolism in patients with diabetes in fasting state.

Branched chain aminoacids were also less expressed in patients with newly-diagnosed type 1 diabetes.

Peptide and nucleotide metabolism were not significantly different between patients and controls.

Xenometabolites derived from caffeine were more expressed in control subjects, while xenometabolites derived from sodium benzoate were more expressed in patients with type 1 diabetes: medical interns drank more coffee, patients more minerals, one would be led to believe.

Unfortunately, metabolomic analysis of patients with newly diagnosed type 1 diabetes as far as we can observe did not yield any new insights into the patophysiology of the disease. It would be possibly beneficial to perform metabolomic analyses in the acute setting, at the very diagnosis of type 1 diabetes, but, based on experience from this study and low interest in newly diagnosed patients with type 1 diabetes, overwhelmed by the sudden change in their life, I would expect that study to be difficult to recruit for and perform.

List of tables

List of figures

7 References

1. WHO. Diabetes: key facts. 2011.

2. Federation ID. Diabetes Atlas 2011 [30th August 2012]. 5th edition:[Available from: http://www.idf.org/diabetesatlas/5e/the-global-burden.

3. Atkinson MA, Eisenbarth GS. Type 1 diabetes: new perspectives on disease pathogenesis and treatment. Lancet. 2001;358(9277):221-9.

4. Achenbach P, Bonifacio E, Koczwara K, Ziegler A-G. Natural History of Type 1 Diabetes. Diabetes. 2005;54(suppl 2):S25-S31.

5. Van Belle TL, Coppieters KT, Von Herrath MG. Type 1 Diabetes: Etiology, Immunology, and Therapeutic Strategies. Physiological Reviews. 2011;91(1):79-118.

6. Concannon P, Rich SS, Nepom GT. Genetics of Type 1A Diabetes. New England Journal of Medicine. 2009;360(16):1646-54.

7. Erlich H, Valdes AM, Noble J, Carlson JA, Varney M, Concannon P, et al. HLA DR-DQ Haplotypes and Genotypes and Type 1 Diabetes Risk. Diabetes. 2008;57(4):1084-92.

8. Nejentsev S, Howson JM, Walker NM, Szeszko J, Field SF, Stevens HE, et al. Localization of type 1 diabetes susceptibility to the MHC class I genes HLA-B and HLA-A. Nature. 2007;450(7171):887-92.

9. Barrett JC, Clayton DG, Concannon P, Akolkar B, Cooper JD, Erlich HA, et al. Genome-wide association study and meta-analysis find that over 40 loci affect risk of type 1 diabetes. Nature genetics. 2009;41(6):703-7.

10. German M. Pancreatic Hormones And Diabetes Mellitus. Greenspan's Basic & Clinical Endocrinology. 2011(17).

11. Siljander HTA, Simell S, Hekkala A, Lähde J, Simell T, Vähäsalo P, et al. Predictive Characteristics of Diabetes-Associated Autoantibodies Among Children With HLA-Conferred Disease Susceptibility in the General Population. Diabetes. 2009;58(12):2835-42.

12. Verge CF, Gianani R, Kawasaki E, Yu L, Pietropaolo M, Jackson RA, et al. Prediction of type I diabetes in first-degree relatives using a combination of insulin, GAD, and ICA512bdc/IA-2 autoantibodies. Diabetes. 1996;45(7):926-33.

13. Eisenbarth GS. Banting Lecture 2009: An Unfinished Journey: Molecular Pathogenesis to Prevention of Type 1A Diabetes. Diabetes. 2010;59(4):759-74.

14. Riley WJ, Maclaren NK, Krischer J, Spillar RP, Silverstein JH, Schatz DA, et al. A prospective study of the development of diabetes in relatives of patients with insulin-dependent diabetes. The New England journal of medicine. 1990;323(17):1167-72.

15. Lönnrot M, Korpela K, Knip M, Ilonen J, Simell O, Korhonen S, et al. Enterovirus infection as a risk factor for beta-cell autoimmunity in a prospectively observed birth cohort: the Finnish Diabetes Prediction and Prevention Study. Diabetes. 2000;49(8):1314-8.

16. Littorin B, Blom P, Scholin A, Arnqvist HJ, Blohme G, Bolinder J, et al. Lower levels of plasma 25-hydroxyvitamin D among young adults at diagnosis of autoimmune type 1 diabetes compared with control subjects: results from the nationwide Diabetes Incidence Study in Sweden (DISS). Diabetologia. 2006;49(12):2847-52.

17. Israni N, Goswami R, Kumar A, Rani R. Interaction of vitamin D receptor with HLA DRB1 0301 in type 1 diabetes patients from North India. PloS one. 2009;4(12):e8023.

18. Orešič M, Simell S, Sysi-Aho M, Näntö-Salonen K, Seppänen-Laakso T, Parikka V, et al. Dysregulation of lipid and amino acid metabolism precedes islet autoimmunity in children who later progress to type 1 diabetes. The Journal of Experimental Medicine. 2008;205(13):2975-84.

19. Mehta D. Lysophosphatidylcholine: an enigmatic lysolipid. American Journal of Physiology - Lung Cellular and Molecular Physiology. 2005;289(2):L174-L5.

20. Samuel Varman T, Shulman Gerald I. Mechanisms for Insulin Resistance: Common Threads and Missing Links. Cell. 2012;148(5):852-71.

21. PE M. Endocrine pancreas. Endocrine Physiology. 2010(7).

22. Petersen KF, Shulman GI. Etiology of insulin resistance. Am J Med. 119. United States2006. p. S10-6.

23. Wheeler E, Barroso I. Genome-wide association studies and type 2 diabetes. Brief Funct Genomics. 10. England2011. p. 52-60.

24. RH E. The Metabolic Syndrome. *Harrison's Principles of Internal Medicine*. 2012(242).

25. Bosma M, Kersten S, Hesselink MKC, Schrauwen P. Re-evaluating lipotoxic triggers in skeletal muscle: Relating intramyocellular lipid metabolism to insulin sensitivity. Progress in Lipid Research. 2012;51(1):36-49.

26. Harris MI, Klein R, Welborn TA, Knuiman MW. Onset of NIDDM occurs at least 4-7 yr before clinical diagnosis. Diabetes Care. 1992;15(7):815-9.

27. Implications of the United Kingdom Prospective Diabetes Study. Diabetes Care. 2002;25(suppl 1):s28-s32.

28. The effect of intensive treatment of diabetes on the development and progression of long-term complications in insulin-dependent diabetes mellitus. The Diabetes Control and Complications Trial Research Group. N Engl J Med. 1993;329(14):977-86.

29. Hynes RO. Integrins: Bidirectional, Allosteric Signaling Machines. Cell. 2002;110(6):673-87.

30. Greenspan's Basic & Clinical Endocrinology. 8 ed. David G. Gardner Md MS, Dolores Shoback MD, editors: The McGraw-Hill Companies, Inc.; 2007.

31. Geraldes P, King GL. Activation of protein kinase C isoforms and its impact on diabetic complications. Circ Res. 106. United States2010. p. 1319-31.

32. Tesfamariam B. Free radicals in diabetic endothelial cell dysfunction. Free radical biology & medicine. 1994;16(3):383-91.

33. Noh H, King GL. The role of protein kinase C activation in diabetic nephropathy. Kidney Int Suppl. United States2007. p. S49-53.

34. Selvin E, Coresh J, Golden SH, Brancati FL, Folsom AR, Steffes MW. Glycemic Control and Coronary Heart Disease Risk in Persons With and Without Diabetes: The Atherosclerosis Risk in Communities Study. Arch Intern Med. 2005;165(16):1910-6.

35. Association AD. Diagnosis and Classification of Diabetes Mellitus. Diabetes Care. 2011;34(Supplement 1):S62-S9.

36. PJ K, VW. R. Proteins: Myoglobin & Hemoglobin. *Harper's Illustrated Biochemistry*. 2011.

37. American Diabetes A. Diagnosis and Classification of Diabetes Mellitus. Diabetes Care. 2013;36(Supplement 1):S67-S74.

38. Association AD. Standards of medical care in diabetes--2012. Diabetes Care. 2012;35 Suppl 1:S11-63.

39. Inzucchi SE, Bergenstal RM, Buse JB, Diamant M, Ferrannini E, Nauck M, et al. Management of hyperglycemia in type 2 diabetes: a patient-centered approach: position statement of the American Diabetes Association (ADA) and the European Association for the Study of Diabetes (EASD). Diabetes Care. 2012;35(6):1364-79.

40. Nathan DM, Rosenbaum C, Protasowicki VD. Single-void urine samples can be used to estimate quantitative microalbuminuria. Diabetes Care. 1987;10(4):414-8.

41. Group. BDW. Biomarkers and surrogate endpoints: preferred definitions and conceptual framework. Clin Pharmacol Ther. 2001;69(3):89-95.

42. Butler AE, Janson J, Soeller WC, Butler PC. Increased beta-cell apoptosis prevents adaptive increase in beta-cell mass in mouse model of type 2 diabetes: evidence for role of islet amyloid formation rather than direct action of amyloid. Diabetes. 2003;52(9):2304-14.

43. Kloppel G, Lohr M, Habich K, Oberholzer M, Heitz PU. Islet pathology and the pathogenesis of type 1 and type 2 diabetes mellitus revisited. Survey and synthesis of pathology research. 1985;4(2):110-25.

44. Rani S. Investigation of molecular and cellular events associated with beta cell function and elucidation of extracellular RNAs as potential biomarker for diabetes. Dublin: Dublin City University; 2008.

45. Rani S, Clynes M, O'Driscoll L. Detection of amplifiable mRNA extracellular to insulin-producing cells: potential for predicting beta cell mass and function. Clin Chem. 2007;53(11):1936-44.

46. Miyazaki J-I, Araki K, Yamato E, Ikegami H, Asano T, Shibasaki Y, et al. Establishment of a Pancreatic β Cell Line That Retains Glucose-Inducible Insulin Secretion: Special Reference to Expression of Glucose Transporter Isoforms. Endocrinology. 1990;127(1):126-32.

47. Lilla V, Webb G, Rickenbach K, Maturana A, Steiner DF, Halban PA, et al. Differential gene expression in well-regulated and dysregulated pancreatic beta-cell (MIN6) sublines. Endocrinology. 2003;144(4):1368-79.

48. O'Driscoll L, Gammell P, Clynes M. Engineering Vero cells to secrete human insulin. In Vitro Cell Dev Biol Anim. 2002;38(3):146-53.

49. Wieczorek AJ, Sitaramam V, Machleidt W, Rhyner K, Perruchoud AP, Block LH. Diagnostic and Prognostic Value of RNA-Proteolipid in Sera of Patients with Malignant Disorders following Therapy: First Clinical Evaluation of a Novel Tumor Marker. Cancer research. 1987;47(23):6407-12.

50. Hasselmann DO, Rappl G, Tilgen W, Reinhold U. Extracellular tyrosinase mRNA within apoptotic bodies is protected from degradation in human serum. Clin Chem. 2001;47(8):1488-9.

51. Fleischhacker M, Schmidt B. Circulating nucleic acids (CNAs) and cancer--a survey. Biochimica et biophysica acta. 2007;1775(1):181-232.

52. Li Y, St. John MAR, Zhou X, Kim Y, Sinha U, Jordan RCK, et al. Salivary Transcriptome Diagnostics for Oral Cancer Detection. Clinical Cancer Research. 2004;10(24):8442-50.

53. Bryzgunova OE, Skvortsova TE, Kolesnikova EV, Starikov AV, Rykova EY, Vlassov VV, et al. Isolation and comparative study of cell-free nucleic acids from human urine. Ann N Y Acad Sci. 2006;1075:334-40.

54. Kuligina EV, Semenov DV, Shevyrina ON, Richter VA. Ribonucleic acids of human milk. Nucleosides, nucleotides & nucleic acids. 2004;23(6-7):837-42.

55. Schmidt B, Engel E, Carstensen T, Weickmann S, John M, Witt C, et al. Quantification of free RNA in serum and bronchial lavage: a new diagnostic tool in lung cancer detection? Lung Cancer. 2005;48(1):145-7.

56. O'Driscoll L KE, Villarreal M.P.D, Clynes M. Detection of specific mRNAs in culture medium conditioned by human tumour cells: Potential for new class of cancer biomarkers in serum. Cancer genomics & proteomics. 2005;2(1):43-52.

57. Stroun M, Anker P, Beljanski M, Henri J, Lederrey C, Ojha M, et al. Presence of RNA in the nucleoprotein complex spontaneously

released by human lymphocytes and frog auricles in culture. Cancer research. 1978;38(10):3546-54.

58. Kopreski MS, Benko FA, Kwak LW, Gocke CD. Detection of Tumor Messenger RNA in the Serum of Patients with Malignant Melanoma. Clinical Cancer Research. 1999;5(8):1961-5.

59. Rykova EY, Wunsche W, Brizgunova OE, Skvortsova TE, Tamkovich SN, Senin IS, et al. Concentrations of circulating RNA from healthy donors and cancer patients estimated by different methods. Ann N Y Acad Sci. 2006;1075:328-33.

60. Reddi KK, Holland JF. Elevated serum ribonuclease in patients with pancreatic cancer. Proceedings of the National Academy of Sciences. 1976;73(7):2308-10.

61. Valadi H, Ekstrom K, Bossios A, Sjostrand M, Lee JJ, Lotvall JO. Exosome-mediated transfer of mRNAs and microRNAs is a novel mechanism of genetic exchange between cells. Nat Cell Biol. 2007;9(6):654-9.

62. Miranda KC, Bond DT, McKee M, Skog J, Paunescu TG, Da Silva N, et al. Nucleic acids within urinary exosomes/microvesicles are potential biomarkers for renal disease. Kidney international. 78. United States2010. p. 191-9.

63. Sandhu HS, Butt AN, Powrie J, Swaminathan R. Measurement of circulating neuron-specific enolase mRNA in diabetes mellitus. Ann N Y Acad Sci. 2008;1137:258-63.

64. Hamaoui K, Butt A, Powrie J, Swaminathan R. Concentration of circulating rhodopsin mRNA in diabetic retinopathy. Clin Chem. 2004;50(11):2152-5.

65. Butt A, Ahmad MS, Powrie J, Swaminathan R. Assessment of diabetic retinopathy by measuring retina-specific mRNA in blood. Expert opinion on biological therapy. 2012;12 Suppl 1:S79-84.

66. Butt AN, Shalchi Z, Hamaoui K, Samadhan A, Powrie J, Smith S, et al. Circulating nucleic acids and diabetic complications. Ann N Y Acad Sci. 1075. United States2006. p. 258-70.

67. Nishiyama A, Matsui M, Iwata S, Hirota K, Masutani H, Nakamura H, et al. Identification of Thioredoxin-binding Protein-2/Vitamin D3 Up-regulated Protein 1 as a Negative Regulator of Thioredoxin Function and Expression. Journal of Biological Chemistry. 1999;274(31):21645-50.

68. Muoio DM. TXNIP links redox circuitry to glucose control. (1932-7420 (Electronic)).

69. Harel A, Dalah I, Pietrokovski S, Safran M, Lancet D. Omics Data Management and Annotation. In: Mayer B, editor. Bioinformatics for Omics Data. Methods in Molecular Biology. 719: Humana Press; 2011. p. 71-96.

70. Chen K-S, DeLuca HF. Isolation and characterization of a novel cDNA from HL-60 cells treated with 1,25-dihydroxyvitamin D-3. Biochimica et Biophysica Acta (BBA) - Gene Structure and Expression. 1994;1219(1):26-32.

71. Holmgren K, Andersson G, Fagrell B, Johnsson H, Ljungberg B, Nilsson E, et al. One-month versus six-month therapy with oral anticoagulants after symptomatic deep vein thrombosis. Acta medica Scandinavica. 1985;218(3):279-84.

72. Patwari P, Lee RT. An expanded family of arrestins regulate metabolism. Trends in Endocrinology & Metabolism. 2012;23(5):216-22.

73. Luan B, Zhao J, Wu H, Duan B, Shu G, Wang X, et al. Deficiency of a beta-arrestin-2 signal complex contributes to insulin resistance. Nature. 2009;457(7233):1146-9.

74. Chutkow WA, Patwari P, Yoshioka J, Lee RT. Thioredoxin-interacting protein (Txnip) is a critical regulator of hepatic glucose production. Journal of Biological Chemistry. 2008;283(4):2397-406.

75. Schulze PC, Yoshioka J, Takahashi T, He Z, King GL, Lee RT. Hyperglycemia Promotes Oxidative Stress through Inhibition of Thioredoxin Function by Thioredoxin-interacting Protein. Journal of Biological Chemistry. 2004;279(29):30369-74.

76. Dornan S, Sebestyen Z, Gamble J, Nagy P, Bodnar A, Alldridge L, et al. Differential association of CD45 isoforms with CD4 and CD8 regulates the actions of specific pools of p56lck tyrosine kinase in T cell antigen receptor signal transduction. The Journal of biological chemistry. 2002;277(3):1912-8.

77. Hui TY, Sheth SS, Diffley JM, Potter DW, Lusis AJ, Attie AD, et al. Mice lacking thioredoxin-interacting protein provide evidence linking cellular redox state to appropriate response to nutritional signals. The Journal of biological chemistry. 2004;279(23):24387-93.

78. Ørntoft TF, Thykjaer T, Waldman FM, Wolf H, Celis JE. Genome-wide study of gene copy numbers, transcripts, and protein levels in pairs of non-invasive and invasive human transitional cell carcinomas. Mol Cell Proteomics. 2002;1(1):37-45.

79. Parikh H, Carlsson E, Chutkow WA, Johansson LE, Storgaard H, Poulsen P, et al. TXNIP regulates peripheral glucose metabolism in humans. PLoS medicine. 2007;4(5):e158.

80. Minn AH, Hafele C, Shalev A. Thioredoxin-interacting protein is stimulated by glucose through a carbohydrate response element and induces beta-cell apoptosis. Endocrinology. 2005;146(5):2397-405.

81. Brownlee M. Biochemistry and molecular cell biology of diabetic complications. Nature. 2001;414(6865):813-20.

82. Garnett KE, Chapman P, Chambers JA, Waddell ID, Boam DS. Differential gene expression between Zucker Fatty rats and Zucker Diabetic Fatty rats: a potential role for the immediate-early gene Egr-1 in regulation of beta cell proliferation. Journal of molecular endocrinology. 35. England2005. p. 13-25.

83. Aljada A, Ghanim H, Mohanty P, Syed T, Bandyopadhyay A, Dandona P. Glucose intake induces an increase in activator protein 1 and early growth response 1 binding activities, in the expression of tissue factor and matrix metalloproteinase in mononuclear cells, and in plasma tissue factor and matrix metalloproteinase concentrations. The American journal of clinical nutrition. 2004;80(1):51-7.

84. Zierath JR, Kawano Y. The effect of hyperglycaemia on glucose disposal and insulin signal transduction in skeletal muscle. Best practice & research Clinical endocrinology & metabolism. 2003;17(3):385-98.

85. Mootha VK, Lindgren CM, Eriksson KF, Subramanian A, Sihag S, Lehar J, et al. PGC-1alpha-responsive genes involved in oxidative phosphorylation are coordinately downregulated in human diabetes. Nature genetics. 2003;34(3):267-73.

86. Patti ME, Butte AJ, Crunkhorn S, Cusi K, Berria R, Kashyap S, et al. Coordinated reduction of genes of oxidative metabolism in humans with insulin resistance and diabetes: Potential role of PGC1 and NRF1. Proc Natl Acad Sci U S A. 2003;100(14):8466-71.

87. Chen J, Saxena G, Mungrue IN, Lusis AJ, Shalev A. Thioredoxin-interacting protein A critical link between glucose toxicity and β-cell apoptosis. Diabetes. 2008;57(4):938-44.

88. Oslowski Christine M, Hara T, O'Sullivan-Murphy B, Kanekura K, Lu S, Hara M, et al. Thioredoxin-Interacting Protein Mediates ER Stress-Induced ² Cell Death through Initiation of the Inflammasome. Cell metabolism. 2012;16(2):265-73.

89. Chai TF, Hong SY, He H, Zheng L, Hagen T, Luo Y, et al. A potential mechanism of metformin-mediated regulation of glucose homeostasis: Inhibition of Thioredoxin-interacting protein (Txnip) gene expression. Cellular signalling. 2012;24(8):1700-5.

90. Kaimul AM, Nakamura H, Masutani H, Yodoi J. Thioredoxin and thioredoxin-binding protein-2 in cancer and metabolic syndrome. Free Radical Biology and Medicine. 2007;43(6):861-8.

91. Rani S, Mehta JP, Barron N, Doolan P, Jeppesen PB, Clynes M, et al. Decreasing Txnip mRNA and protein levels in pancreatic MIN6 cells reduces reactive oxygen species and restores glucose regulated insulin secretion. Cell Physiol Biochem. 25. Switzerland: 2010 S. Karger AG, Basel.; 2010. p. 667-74.

92. Keeton AB, Bortoff KD, Bennett WL, Franklin JL, Venable DY, Messina JL. Insulin-Regulated Expression of Egr-1 and Krox20: Dependence on ERK1/2 and Interaction with p38 and PI3-Kinase Pathways. Endocrinology. 2003;144(12):5402-10.

93. Committee HGN. [22 Oct 2012]. Available from: http://www.genenames.org/data/hgnc_data.php?hgnc_id=3238.

94. Thiel G, Mayer SI, Müller I, Stefano L, Rössler OG. Egr-1—A Ca2+-regulated transcription factor. Cell Calcium. 2010;47(5):397-403.

95. Josefsen K, Sørensen LR, Buschard K, Birkenbach M. Glucose induces early growth response gene (Egr-1) expression in pancreatic beta cells. Diabetologia. 1999;42(2):195-203.

96. Yao J, Mackman N, Edgington TS, Fan S-T. Lipopolysaccharide Induction of the Tumor Necrosis Factor-a Promoter in Human Monocytic Cells. Journal of Biological Chemistry. 1997;272(28):17795-801.

97. Shen N, Yu X, Pan F-Y, Gao X, Xue B, Li C-J. An Early Response Transcription Factor, Egr-1, Enhances Insulin Resistance in Type 2 Diabetes with Chronic Hyperinsulinism. Journal of Biological Chemistry. 2011;286(16):14508-15.

98. Eto K, Kaur V, Thomas MK. Regulation of Pancreas Duodenum Homeobox-1 Expression by Early Growth Response-1. Journal of Biological Chemistry. 2007;282(9):5973-83.

99. Gygi SP, Corthals GL, Zhang Y, Rochon Y, Aebersold R. Evaluation of two-dimensional gel electrophoresis-based proteome analysis technology. Proc Natl Acad Sci U S A. 2000;97(17):9390-5.

100. Sundsten T, Ortsäter H. Proteomics in diabetes research. Mol Cell Endocrinol. 2009;297(1-2):93-103.

101. Apweiler R, Aslanidis C, Deufel T, Gerstner A, Hansen J, Hochstrasser D, et al. Approaching clinical proteomics: current state and future fields of application in fluid proteomics. Clin Chem Lab Med. 2009;47(6):724-44.

102. Herder C, Karakas M, Koenig W. Biomarkers for the prediction of type 2 diabetes and cardiovascular disease. Clin Pharmacol Ther. 2011;90(1):52-66.

103. Metz TO, Qian WJ, Jacobs JM, Gritsenko MA, Moore RJ, Polpitiya AD, et al. Application of proteomics in the discovery of candidate protein biomarkers in a diabetes autoantibody standardization program sample subset. Journal of proteome research. 2008;7(2):698-707.

104. Zhang R, Barker L, Pinchev D, Marshall J, Rasamoelisolo M, Smith C, et al. Mining biomarkers in human sera using proteomic tools. Proteomics. 2004;4(1):244-56.

105. Hittel DS, Hathout Y, Hoffman EP, Houmard JA. Proteome analysis of skeletal muscle from obese and morbidly obese women. Diabetes. 2005;54(5):1283-8.

106. Hojlund K, Wrzesinski K, Larsen PM, Fey SJ, Roepstorff P, Handberg A, et al. Proteome analysis reveals phosphorylation of ATP synthase beta -subunit in human skeletal muscle and proteins with potential roles in type 2 diabetes. The Journal of biological chemistry. 2003;278(12):10436-42.

107. Giebelstein J, Poschmann G, Hojlund K, Schechinger W, Dietrich JW, Levin K, et al. The proteomic signature of insulin-resistant human skeletal muscle reveals increased glycolytic and decreased mitochondrial enzymes. Diabetologia. 2012;55(4):1114-27.

108. Zhou JY, Dann GP, Liew CW, Smith RD, Kulkarni RN, Qian WJ. Unraveling pancreatic islet biology by quantitative proteomics. Expert review of proteomics. 2011;8(4):495-504.

109. Zhi W, Purohit S, Carey C, Wang M, She JX. Proteomic technologies for the discovery of type 1 diabetes biomarkers. Journal of diabetes science and technology. 2010;4(4):993-1002.

110. Kim HJ, Cho EH, Yoo JH, Kim PK, Shin JS, Kim MR, et al. Proteome analysis of serum from type 2 diabetics with nephropathy. Journal of proteome research. 2007;6(2):735-43.

111. Overgaard AJ, Hansen HG, Lajer M, Pedersen L, Tarnow L, Rossing P, et al. Plasma proteome analysis of patients with type 1 diabetes with diabetic nephropathy. Proteome science. 2010;8:4.

112. Wang H, Feng L, Hu JW, Xie CL, Wang F. Characterisation of the vitreous proteome in proliferative diabetic retinopathy. Proteome science. 10. England2012. p. 15.

113. Ahn BY, Song ES, Cho YJ, Kwon OW, Kim JK, Lee NG. Identification of an anti-aldolase autoantibody as a diagnostic marker for diabetic retinopathy by immunoproteomic analysis. Proteomics. 2006;6(4):1200-9.

114. Schlatzer D, Maahs DM, Chance MR, Dazard JE, Li X, Hazlett F, et al. Novel urinary protein biomarkers predicting the development of microalbuminuria and renal function decline in type 1 diabetes. Diabetes Care. 2012;35(3):549-55.

115. Wishart DS, Knox C, Guo AC, Eisner R, Young N, Gautam B, et al. HMDB: a knowledgebase for the human metabolome. Nucleic acids research. 37. England2009. p. D603-10.

116. Wishart DS, Jewison T, Guo AC, Wilson M, Knox C, Liu Y, et al. HMDB 3.0--The Human Metabolome Database in 2013. Nucleic acids research. 2013;41(Database issue):D801-7.

117. Li X, Xu Z, Lu X, Yang X, Yin P, Kong H, et al. Comprehensive two-dimensional gas chromatography/time-of-flight mass spectrometry for metabonomics: Biomarker discovery for diabetes mellitus. Analytica Chimica Acta. 2009;633(2):257-62.

118. Levy J, Matthews D, Hermans M. Correct homeostasis model assessment (HOMA) evaluation uses the computer program. Diabetes Care. 1998;21(12):2191-2.

119. Unit DT. HOMA calculator The Oxford Centre for Diabetes, Endocrinology and Metabolism [cited 2012 Sep 6, 2012]. Available from: http://www.dtu.ox.ac.uk/homacalculator/index.php.

120. Shaked M, Ketzinel-Gilad M, Cerasi E, Kaiser N, Leibowitz G. AMP-Activated Protein Kinase (AMPK) Mediates Nutrient Regulation of Thioredoxin-Interacting Protein (TXNIP) in Pancreatic Beta-Cells. PloS one. 2011;6(12):e28804.

121. Elgort MG, O'Shea JM, Jiang Y, Ayer DE. Transcriptional and Translational Downregulation of Thioredoxin Interacting Protein Is Required for Metabolic Reprogramming during G1. Genes & Cancer. 2010;1(9):893-907.

122. Patwari P, Chutkow WA, Cummings K, Verstraeten VL, Lammerding J, Schreiter ER, et al. Thioredoxin-independent regulation of metabolism by the alpha-arrestin proteins. The Journal of biological chemistry. 2009;284(37):24996-5003.

123. Seo SK, Yang HI, Lee KE, Kim HY, Cho S, Choi YS, et al. The roles of thioredoxin and thioredoxin-binding protein-2 in endometriosis. Human Reproduction. 2010;25(5):1251-8.

124. Kobayashi T, Uehara S, Ikeda T, Itadani H, Kotani H. Vitamin D3 up-regulated protein-1 regulates collagen expression in mesangial cells. Kidney international. 2003;64(5):1632-42.

125. Shalev A, Pise-Masison CA, Radonovich M, Hoffmann SC, Hirshberg B, Brady JN, et al. Oligonucleotide microarray analysis of intact human pancreatic islets: identification of glucose-responsive genes and a highly regulated TGFbeta signaling pathway. Endocrinology. 2002;143(9):3695-8.

126. Hirota T, Okano T, Kokame K, Shirotani-Ikejima H, Miyata T, Fukada Y. Glucose down-regulates Per1 and Per2 mRNA levels and induces circadian gene expression in cultured Rat-1 fibroblasts. The Journal of biological chemistry. 2002;277(46):44244-51.

127. Schulze PC, Yoshioka J, Takahashi T, He Z, King GL, Lee RT. Hyperglycemia promotes oxidative stress through inhibition of thioredoxin function by thioredoxin-interacting protein. The Journal of biological chemistry. 2004;279(29):30369-74.

128. Hansen L, Gaster M, Oakeley EJ, Brusgaard K, Damsgaard Nielsen EM, Beck-Nielsen H, et al. Expression profiling of insulin action in human myotubes: induction of inflammatory and pro-angiogenic pathways in relationship with glycogen synthesis and type 2 diabetes.

Biochemical and biophysical research communications. 2004;323(2):685-95.

129. Færch K, Borch-Johnsen K, Holst JJ, Vaag A. Pathophysiology and aetiology of impaired fasting glycaemia and impaired glucose tolerance: does it matter for prevention and treatment of type 2 diabetes? Diabetologia. 2009;52(9):1714-23.

130. Bailey CJ. Biguanides and NIDDM. (0149-5992 (Print)).

131. Bailey CJ, Turner RC. Metformin. N Engl J Med. 1996;334(9):574-9.

132. Zhou G, Myers R, Li Y, Chen Y, Shen X, Fenyk-Melody J, et al. Role of AMP-activated protein kinase in mechanism of metformin action. J Clin Invest. 2001;108(8):1167-74.

133. Qu H-Q, Li Q, Rentfro AR, Fisher-Hoch SP, McCormick JB. The Definition of Insulin Resistance Using HOMA-IR for Americans of Mexican Descent Using Machine Learning. PloS one. 2011;6(6):e21041.

134. Ascaso JF, Pardo S, Real JT, Lorente RI, Priego A, Carmena R. Diagnosing Insulin Resistance by Simple Quantitative Methods in Subjects With Normal Glucose Metabolism. Diabetes Care. 2003;26(12):3320-5.

135. Aljada A, Ghanim H, Mohanty P, Kapur N, Dandona P. Insulin inhibits the pro-inflammatory transcription factor early growth response gene-1 (Egr)-1 expression in mononuclear cells (MNC) and reduces plasma tissue factor (TF) and plasminogen activator inhibitor-1 (PAI-1) concentrations. J Clin Endocrinol Metab. 2002;87(3):1419-22.

136. Muller I, Lipp P, Thiel G. Ca2+ signaling and gene transcription in glucose-stimulated insulinoma cells. Cell Calcium. 52. Netherlands: 2012 Elsevier Ltd; 2012. p. 137-51.

137. Chai Tf Fau - Hong SY, Hong Sy Fau - He H, He H Fau - Zheng L, Zheng L Fau - Hagen T, Hagen T Fau - Luo Y, Luo Y Fau - Yu F-X, et al. A potential mechanism of metformin-mediated regulation of glucose homeostasis: inhibition of Thioredoxin-interacting protein (Txnip) gene expression. (1873-3913 (Electronic)).

138. Blaschke F, Bruemmer D, Law RE. Egr-1 is a major vascular pathogenic transcription factor in atherosclerosis and restenosis. Reviews in endocrine & metabolic disorders. 5. United States2004. p. 249-54.

139. McCaffrey TA, Fu C, Du B, Eksinar S, Kent KC, Bush H, Jr., et al. High-level expression of Egr-1 and Egr-1-inducible genes in mouse and human atherosclerosis. J Clin Invest. 2000;105(5):653-62.

140. Gousseva N, Kugathasan K, Chesterman CN, Khachigian LM. Early growth response factor-1 mediates insulin-inducible vascular endothelial cell proliferation and regrowth after injury. Journal of cellular biochemistry. 2001;81(3):523-34.

141. Grundy SM, Brewer HB, Cleeman JI, Smith SC, Lenfant C, for the Conference P. Definition of Metabolic Syndrome. Circulation. 2004;109(3):433-8.

142. Gil N, Goldberg R, Neuman T, Garsen M, Zcharia E, Rubinstein AM, et al. Heparanase Is Essential for the Development of Diabetic Nephropathy in Mice. Diabetes. 2012;61(1):208-16.

143. Ong S-E, Pandey A. An evaluation of the use of two-dimensional gel electrophoresis in proteomics. Biomolecular Engineering. 2001;18(5):195-205.

144. Tuli L, Ressom HW. LC-MS Based Detection of Differential Protein Expression. Journal of proteomics & bioinformatics. 2009;2:416-38.

145. Sandin M, Krogh M, Hansson K, Levander F. Generic workflow for quality assessment of quantitative label-free LC-MS analysis. Proteomics. 2011;11(6):1114-24.

146. Kim G, Kim GH, Oh GS, Yoon J, Kim HW, Kim MS, et al. SREBP-1c regulates glucose-stimulated hepatic clusterin expression. Biochemical and biophysical research communications. 408. United States: 2011 Elsevier Inc; 2011. p. 720-5.

147. Preissner KT, Jenne D. Vitronectin: a new molecular connection in haemostasis. Thrombosis and haemostasis. 1991;66(2):189-94.

148. Preissner KT, Kanse SM, Hammes HP. Integrin chatter and vascular function in diabetic retinopathy. Hormone and metabolic research = Hormon- und Stoffwechselforschung = Hormones et metabolisme. 1997;29(12):643-5.

149. Daimon M, Oizumi T, Karasawa S, Kaino W, Takase K, Tada K, et al. Association of the clusterin gene polymorphisms with type 2 diabetes mellitus. Metabolism. 2011;60(6):815-22.

150. Trougakos IP, Gonos ES. Regulation of clusterin/apolipoprotein J, a functional homologue to the small heat shock proteins, by oxidative stress in ageing and age-related diseases. Free radical research. 2006;40(12):1324-34.

151. Pettersson C, Karlsson H, Stahlman M, Larsson T, Fagerberg B, Lindahl M, et al. LDL-associated apolipoprotein J and lysozyme are associated with atherogenic properties of LDL found in type 2 diabetes and the metabolic syndrome. J Intern Med. 2011;269(3):306-21.

152. Aronis KN, Vamvini MT, Chamberland JP, Mantzoros CS. Circulating clusterin (apolipoprotein J) levels do not have any day/night variability and are positively associated with total and LDL cholesterol levels in young healthy individuals. J Clin Endocrinol Metab. 96. United States2011. p. E1871-5.

153. Hoofnagle AN, Wu M, Gosmanova AK, Becker JO, Wijsman EM, Brunzell JD, et al. Low clusterin levels in high-density lipoprotein associate with insulin resistance, obesity, and dyslipoproteinemia. Arterioscler Thromb Vasc Biol. 30. United States2010. p. 2528-34.

154. Esmon CT. Protein S and protein C Biochemistry, physiology, and clinical manifestation of. Trends in cardiovascular medicine. 1992;2(6):214-9.

155. Maillard C, Berruyer M, Serre CM, Dechavanne M, Delmas PD. Protein-S, a vitamin K-dependent protein, is a bone matrix component synthesized and secreted by osteoblasts. Endocrinology. 1992;130(3):1599-604.

156. Anderson HA, Maylock CA, Williams JA, Paweletz CP, Shu H, Shacter E. Serum-derived protein S binds to phosphatidylserine and stimulates the phagocytosis of apoptotic cells. Nature immunology. 2003;4(1):87-91.

157. Green AR. Postgraduate Haematology. Hoffbrand AV, Catovsky D, Tuddenham EGD, editors: Wiley; 2010.

158. Singh A, Boden G, Homko C, Gunawardana J, Rao AK. Whole-blood tissue factor procoagulant activity is elevated in type 1 diabetes: effects of hyperglycemia and hyperinsulinemia. Diabetes Care. 2012;35(6):1322-7.

159. Targher G, Chonchol M, Zoppini G, Franchini M. Hemostatic disorders in type 1 diabetes mellitus. Seminars in thrombosis and hemostasis. 2011;37(1):58-65.

160. Wieczorek I, Pell AC, McIver B, MacGregor IR, Ludlam CA, Frier BM. Coagulation and fibrinolytic systems in type I diabetes: effects of venous occlusion and insulin-induced hypoglycaemia. Clin Sci (Lond). 1993;84(1):79-86.

161. Schernthaner G, Vukovich T, Knobl P, Hay U, Muller MM. The effect of near-normoglycaemic control on plasma levels of coagulation factor VII and the anticoagulant proteins C and S in insulin-dependent diabetic patients. British journal of haematology. 1989;73(3):356-9.

162. Wullstein C, Woeste G, Zapletal C, Trobisch H, Bechstein WO. Prothrombotic disorders in uremic type-1 diabetics undergoing simultaneous pancreas and kidney transplantation. Transplantation. 2003;76(12):1691-5.

163. Madan R, Gupt B, Saluja S, Kansra UC, Tripathi BK, Guliani BP. Coagulation profile in diabetes and its association with diabetic microvascular complications. The Journal of the Association of Physicians of India. 2010;58:481-4.

164. Bonner-Weir S. Life and death of the pancreatic beta cells. Trends in endocrinology and metabolism: TEM. 2000;11(9):375-8.

165. Metabolon Inc. homepage [28 Oct 2012]. Available from: http://www.metabolon.com/services/mView.aspx.

166. Evans AM, DeHaven CD, Barrett T, Mitchell M, Milgram E. Integrated, nontargeted ultrahigh performance liquid chromatography/electrospray ionization tandem mass spectrometry platform for the identification and relative quantification of the small-molecule complement of biological systems. Analytical chemistry. 2009;81(16):6656-67.

167. Akanuma Y, Morita M, Fukuzawa N, Yamanouchi T, Akanuma H. Urinary excretion of 1,5-anhydro-D-glucitol accompanying glucose excretion in diabetic patients. Diabetologia. 1988;31(11):831-5.

168. Kim W, Park C-Y. 1,5-Anhydroglucitol in diabetes mellitus. Endocrine. 2012:1-8.

169. Dungan KM. 1,5-anhydroglucitol (GlycoMark) as a marker of short-term glycemic control and glycemic excursions. Expert review of molecular diagnostics. 2008;8(1):9-19.

170. Yamanouchi T, Akanuma Y. Serum 1,5-anhydroglucitol (1,5 AG): new clinical marker for glycemic control. Diabetes Res Clin Pract. 1994;24 Suppl:S261-8.

171. Robertson DA, Alberti KG, Dowse GK, Zimmet P, Tuomilehto J, Gareeboo H. Is serum anhydroglucitol an alternative to the oral glucose tolerance test for diabetes screening? The Mauritius Noncommunicable Diseases Study Group. Diabet Med. 1993;10(1):56-60.

172. Watanabe M, Kokubo Y, Higashiyama A, Ono Y, Miyamoto Y, Okamura T. Serum 1,5-anhydro-D-glucitol levels predict first-ever cardiovascular disease: an 11-year population-based cohort study in Japan, the Suita study. Atherosclerosis. 216. Ireland: 2011 Elsevier Ireland Ltd; 2011. p. 477-83.

173. Cline GW, Rothman DL, Magnusson I, Katz LD, Shulman GI. 13C-nuclear magnetic resonance spectroscopy studies of hepatic glucose metabolism. J Clin Invest. 1994;94(6):2369-76.

174. Zhang X, Wang Y, Hao F, Zhou X, Han X, Tang H, et al. Human Serum Metabonomic Analysis Reveals Progression Axes for Glucose Intolerance and Insulin Resistance Statuses. Journal of proteome research. 2009;8(11):5188-95.

175. Carrozzo R, Dionisi-Vici C, Steuerwald U, Lucioli S, Deodato F, Di Giandomenico S, et al. SUCLA2 mutations are associated with mild methylmalonic aciduria, Leigh-like. Brain : a journal of neurology. 2007;130(Pt 3):862-74.

176. Miyamoto Y, Iwao Y, Mera K, Watanabe H, Kadowaki D, Ishima Y, et al. A uremic toxin, 3-carboxy-4-methyl-5-propyl-2-furanpropionate induces cell damage. Biochemical pharmacology. 2012;84(9):1207-14.

177. KM B, PA M. Oxidation of Fatty Acids: Ketogenesis. *Harper's Illustrated Biochemistry*. 2011(22).

178. Evangeliou A, Gourgiotis D, Karagianni C, Markouri M, Anogianaki N, Mamoulakis D, et al. Carnitine status and lactate increase in patients with type I juvenile diabetes. Minerva pediatrica. 2010;62(6):551-7.

179. LW J, ME T. *The Big Picture: Medical Biochemistry*. New York: McGraw-Hill; 2012.

180. Tessari P, Biolo G, Inchiostro S, Sacca L, Nosadini R, Boscarato MT, et al. Effects of insulin on whole body and forearm leucine and KIC metabolism in type 1. The American journal of physiology. 1990;259(1 Pt 1):E96-103.

181. Vannini P, Marchesini G, Forlani G, Angiolini A, Ciavarella A, Zoli M, et al. Branched-chain amino acids and alanine as indices of the metabolic control in. Diabetologia. 1982;22(3):217-9.

182. Gianazza E, Mainini V, Castoldi G, Chinello C, Zerbini G, Bianchi C, et al. Different expression of fibrinopeptide A and related fragments in serum of type 1. Journal of proteomics. 2010;73(3):593-601.

183. Nomura F, Tomonaga T, Sogawa K, Ohashi T, Nezu M, Sunaga M, et al. Identification of novel and downregulated biomarkers for alcoholism by surface. Proteomics. 2004;4(4):1187-94.

184. Matheus AS, Tibirica E, da Silva PB, de Fatima Bevilacqua da Matta M, Gomes MB. Uric acid levels are associated with microvascular endothelial dysfunction in patients with Type 1 diabetes. Diabet Med. 2011;28(10):1188-93.

185. Yu X, Shen N, Zhang ML, Pan FY, Wang C, Jia WP, et al. Egr-1 decreases adipocyte insulin sensitivity by tilting PI3K/Akt and MAPK signal balance in mice. The EMBO journal. 30. England2011. p. 3754-65.

Appendix A

Proteomics label-free LC-MS (raw data)

Patients with newly diagnosed type 1 diabetes vs their healthy controls

List of differentially expressed protein for newly-diagnosed type 1 diabetes and matched controls with DS-169/ T1N8sample used as reference run (raw data)

Accession	Peptides	Score	Anova (p)*	Fold	Description	Average normalised abundances	
						T1DM new	Matched controls
CO4A_HUMAN	43	4138.72	0.02	1.58	Complement C4-A OS=Homo sapiens GN=C4A PE=1 SV=1	1.56E+008	9.88E+007
CO3_HUMAN	35	3123.37	0.05	1.55	Complement C3 OS=Homo sapiens GN=C3 PE=1 SV=2	4.95E+007	3.19E+007
CO5_HUMAN	20	1427.52	0.03	1.65	Complement C5 OS=Homo sapiens GN=C5 PE=1 SV=4	1.88E+006	1.14E+006
APOA1_HUMAN	16	1126.05	0.03	1.53	Apolipoprotein A-I OS=Homo sapiens GN=APOA1 PE=1	7.57E+007	4.94E+007

Accession	Peptides	Score	Anova (p)*	Fold	Description	Average normalised abundances	
						T1DM new	Matched controls
					SV=1		
CLUS_HUMAN	13	988.6	0.04	1.72	Clusterin OS=Homo sapiens GN=CLU PE=1 SV=1	1.78E+007	1.03E+007
CO9_HUMAN	10	950.21	8.86E-003	1.79	Complement component C9 OS=Homo sapiens GN=C9 PE=1 SV=2	4.28E+006	2.39E+006
VTNC_HUMAN	8	689.45	0.05	1.43	Vitronectin OS=Homo sapiens GN=VTN PE=1 SV=1	4.72E+007	3.30E+007
APOA4_HUMAN	9	652.83	0.01	1.58	Apolipoprotein A-IV OS=Homo sapiens GN=APOA4 PE=1 SV=3	9.07E+006	5.74E+006

Accession	Peptides	Score	Anova (p)*	Fold	Description	Average normalised abundances	
						T1DM new	Matched controls
FBLN1_HUMAN	7	640.57	0.03	1.61	Fibulin-1 OS=Homo sapiens GN=FBLN1 PE=1 SV=4	5.67E+006	3.53E+006
ALBU_HUMAN	8	628.35	0.04	1.64	Serum albumin OS=Homo sapiens GN=ALB PE=1 SV=2	9.07E+006	5.54E+006
LG3BP_HUMAN	8	581.72	0.05	1.58	Galectin-3-binding protein OS=Homo sapiens GN=LGALS3BP PE=1 SV=1	1.77E+006	1.12E+006
ITIH4_HUMAN	6	520.69	0.04	7.81	Inter-alpha-trypsin inhibitor heavy chain H4 OS=Homo sapiens GN=ITIH4 PE=1 SV=4	1.23E+006	1.58E+005
A1AT_HUMAN	6	490.95	0.02	1.78	Alpha-1-antitrypsin OS=Homo sapiens GN=SERPINA1 PE=1	8.31E+005	4.66E+005

Accession	Peptides	Score	Anova (p)*	Fold	Description	Average normalised abundances	
						T1DM new	Matched controls
					SV=3		
LBP_HUMAN	4	392.67	0.02	2.29	Lipopolysaccharide-binding protein OS=Homo sapiens GN=LBP PE=1 SV=3	5.66E+005	2.47E+005
TSP1_HUMAN	6	368.73	8.49E-003	1.65	Thrombospondin-1 OS=Homo sapiens GN=THBS1 PE=1 SV=2	3.03E+005	5.00E+005
CRP_HUMAN	6	334.89	0.02	6.09	C-reactive protein OS=Homo sapiens GN=CRP PE=1 SV=1	1.22E+006	2.00E+005
C1QB_HUMAN	3	279.59	0.03	1.59	Complement C1q subcomponent subunit B OS=Homo sapiens GN=C1QB PE=1 SV=2	2.60E+006	1.63E+006

Accession	Peptides	Score	Anova (p)*	Fold	Description	Average normalised abundances	
						T1DM new	Matched controls
CO7_HUMAN	4	272.65	3.75E-003	2.24	Complement component C7 OS=Homo sapiens GN=C7 PE=1 SV=2	4.26E+005	1.90E+005
C4BPA_HUMAN	3	270.68	0.03	1.51	C4b-binding protein alpha chain OS=Homo sapiens GN=C4BPA PE=1 SV=2	3.63E+006	2.40E+006
CERU_HUMAN	4	258.01	0.01	2.41	Ceruloplasmin OS=Homo sapiens GN=CP PE=1 SV=1	2.70E+005	1.12E+005
ACTC_HUMAN	4	232.49	0.02	1.95	Actin, alpha cardiac muscle 1 OS=Homo sapiens GN=ACTC1 PE=1 SV=1	9.88E+004	1.93E+005

Accession	Peptides	Score	Anova (p)*	Fold	Description	Average normalised abundances	
						T1DM new	Matched controls
PROS_HUMAN	4	218.74	0.03	1.51	Vitamin K-dependent protein S OS=Homo sapiens GN=PROS1 PE=1 SV=1	3.45E+005	2.29E+005
TRFL_HUMAN	3	205.82	0.04	1.74	Lactotransferrin OS=Homo sapiens GN=LTF PE=1 SV=6	3.86E+004	6.70E+004
ITIH3_HUMAN	3	180.97	0.01	2.43	Inter-alpha-trypsin inhibitor heavy chain H3 OS=Homo sapiens GN=ITIH3 PE=1 SV=2	9.40E+004	3.88E+004
POTEE_HUMAN	3	178.05	0.02	1.97	POTE ankyrin domain family member E OS=Homo sapiens GN=POTEE PE=1 SV=3	5.39E+004	1.06E+005

Accession	Peptides	Score	Anova (p)*	Fold	Description	Average normalised abundances	
						T1DM new	Matched controls
CO8B_HUMAN	3	171.54	0.05	1.86	Complement component C8 β chain OS=Homo sapiens GN=C8B PE=1 SV=3	5.52E+005	2.97E+005
PROC_HUMAN	2	164.19	0.03	1.81	Vitamin K-dependent protein C OS=Homo sapiens GN=PROC PE=1 SV=1	2.12E+005	1.17E+005
ZPI_HUMAN	2	153.72	0.02	2.69	Protein Z-dependent protease inhibitor OS=Homo sapiens GN=SERPINA10 PE=1 SV=1	1.97E+005	7.33E+004
FBLN3_HUMAN	2	136.33	0.05	1.94	EGF-containing fibulin-like extracellular matrix protein 1 OS=Homo sapiens GN=EFEMP1 PE=1 SV=2	1.78E+005	9.16E+004

Accession	Peptides	Score	Anova (p)*	Fold	Description	Average normalised abundances	
						T1DM new	Matched controls
C1S_HUMAN	3	135.97	0.03	1.5	Complement C1s subcomponent OS=Homo sapiens GN=C1S PE=1 SV=1	4.01E+004	2.67E+004
ACTBL_HUMAN	2	117.48	0.02	1.91	B-actin-like protein 2 OS=Homo sapiens GN=ACTBL2 PE=1 SV=2	5.31E+004	1.02E+005
ACTBM_HUMAN	2	113.28	0.02	1.98	B-actin-like protein 3 OS=Homo sapiens GN=ACTBL3 PE=1 SV=1	4.86E+004	9.63E+004

List of differentially expressed protein for newly-diagnosed type 1 diabetes and matched controls with DS- 175/ U35 sample used as reference run (raw data)

Accession	Peptides	Score	Anova (p)*	Fold	Description	Average normalised abundances	
						T1DM new	Matched controls
CO4B_HUMAN	40	3836.35	5.87E-003	1.65	Complement C4-B OS=Homo sapiens GN=C4B PE=1 SV=1	1.95E+008	1.18E+008
CO3_HUMAN	42	3693.41	0.03	1.56	Complement C3 OS=Homo sapiens GN=C3 PE=1 SV=2	6.88E+007	4.41E+007
CO5_HUMAN	20	1420.08	4.51E-003	1.74	Complement C5 OS=Homo sapiens GN=C5 PE=1 SV=4	2.24E+006	1.28E+006
APOA1_HUMAN	17	1233.71	0.02	1.57	Apolipoprotein A-I OS=Homo sapiens GN=APOA1 PE=1 SV=1	8.52E+007	5.43E+007

Accession	Peptides	Score	Anova (p)*	Fold	Description	Average normalised abundances	
						T1DM new	Matched controls
CLUS_HUMAN	12	1010.99	0.01	1.68	Clusterin OS=Homo sapiens GN=CLU PE=1 SV=1	2.68E+007	1.59E+007
CO9_HUMAN	11	1000.43	3.22E-003	1.86	Complement component C9 OS=Homo sapiens GN=C9 PE=1 SV=2	4.93E+006	2.66E+006
APOA4_HUMAN	14	972.98	5.23E-003	1.64	Apolipoprotein A-IV OS=Homo sapiens GN=APOA4 PE=1 SV=3	1.15E+007	7.06E+006
ALBU_HUMAN	10	777.19	0.03	1.58	Serum albumin OS=Homo sapiens GN=ALB PE=1 SV=2	1.29E+007	8.20E+006
VTNC_HUMAN	7	644.16	0.04	1.46	Vitronectin OS=Homo sapiens GN=VTN PE=1 SV=1	5.38E+007	3.70E+007

Accession	Peptides	Score	Anova (p)*	Fold	Description	Average normalised abundances	
						T1DM new	Matched controls
FBLN1_HUMAN	7	631.79	0.02	1.64	Fibulin-1 OS=Homo sapiens GN=FBLN1 PE=1 SV=4	6.42E+006	3.93E+006
LBP_HUMAN	5	541.79	0.02	2.29	Lipopolysaccharide-binding protein OS=Homo sapiens GN=LBP PE=1 SV=3	1.30E+006	5.68E+005
SAMP_HUMAN	7	530.8	0.04	1.48	Serum amyloid P-component OS=Homo sapiens GN=APCS PE=1 SV=2	7.41E+006	5.02E+006
CFAH_HUMAN	8	521.49	0.02	1.41	Complement factor H OS=Homo sapiens GN=CFH PE=1 SV=4	2.70E+006	1.92E+006

Accession	Peptides	Score	Anova (p)*	Fold	Description	Average normalised abundances	
						T1DM new	Matched controls
ANT3_HUMAN	9	512.66	0.05	1.47	Antithrombin-III OS=Homo sapiens GN=SERPINC1 PE=1 SV=1	2.75E+007	1.87E+007
IGHM_HUMAN	7	500.95	0.05	1.42	Ig mu chain C region OS=Homo sapiens GN=IGHM PE=1 SV=3	1.44E+007	1.02E+007
TSP1_HUMAN	7	425.34	0.01	1.53	Thrombospondin-1 OS=Homo sapiens GN=THBS1 PE=1 SV=2	5.18E+005	7.94E+005
A1AT_HUMAN	5	412.2	4.59E-003	2.19	Alpha-1-antitrypsin OS=Homo sapiens GN=SERPINA1 PE=1 SV=3	9.02E+005	4.11E+005

Accession	Peptides	Score	Anova (p)*	Fold	Description	Average normalised abundances	
						T1DM new	Matched controls
C4BPA_HUMAN	3	346.18	0.01	1.61	C4b-binding protein alpha chain OS=Homo sapiens GN=C4BPA PE=1 SV=2	4.45E+006	2.77E+006
PROS_HUMAN	5	297.77	0.02	1.33	Vitamin K-dependent protein S OS=Homo sapiens GN=PROS1 PE=1 SV=1	1.22E+006	9.16E+005
ITIH3_HUMAN	5	278.62	7.92E-003	2.7	Inter-alpha-trypsin inhibitor heavy chain H3 OS=Homo sapiens GN=ITIH3 PE=1 SV=2	1.53E+005	5.66E+004
CO7_HUMAN	3	267.47	1.61E-003	2.35	Complement component C7 OS=Homo sapiens GN=C7 PE=1 SV=2	5.43E+005	2.31E+005

Accession	Peptides	Score	Anova (p)*	Fold	Description	Average normalised abundances	
						T1DM new	Matched controls
ACTS_HUMAN	5	246.04	0.01	2.19	Actin, alpha skeletal muscle OS=Homo sapiens GN=ACTA1 PE=1 SV=1	1.11E+005	2.43E+005
C1QA_HUMAN	2	241.96	0.02	1.47	Complement C1q subcomponent subunit A OS=Homo sapiens GN=C1QA PE=1 SV=2	2.71E+006	1.84E+006
CRP_HUMAN	4	236.68	0.01	6.22	C-reactive protein OS=Homo sapiens GN=CRP PE=1 SV=1	1.24E+006	1.99E+005
ZPI_HUMAN	3	228.52	0.03	2.51	Protein Z-dependent protease inhibitor OS=Homo sapiens GN=SERPINA10 PE=1 SV=1	3.81E+005	1.52E+005

Accession	Peptides	Score	Anova (p)*	Fold	Description	Average normalised abundances	
						T1DM new	Matched controls
TRFL_HUMAN	3	218.44	0.02	2.26	Lactotransferrin OS=Homo sapiens GN=LTF PE=1 SV=6	4.63E+004	1.05E+005
IGKC_HUMAN	2	210.45	0.05	1.5	Ig kappa chain C region OS=Homo sapiens GN=IGKC PE=1 SV=1	1.23E+007	8.18E+006
FA5_HUMAN	3	200.05	0.04	1.63	Coagulation factor V OS=Homo sapiens GN=F5 PE=1 SV=3	2.57E+005	1.57E+005
C1QB_HUMAN	2	195.39	0.02	1.55	Complement C1q subcomponent subunit B OS=Homo sapiens GN=C1QB PE=1 SV=2	1.68E+006	1.09E+006
CO6_HUMAN	3	185.01	0.04	1.58	Complement component C6 OS=Homo sapiens GN=C6 PE=1	4.21E+005	2.66E+005

Accession	Peptides	Score	Anova (p)*	Fold	Description	Average normalised abundances	
						T1DM new	Matched controls
					SV=3		
C1S_HUMAN	2	124.24	0.03	1.7	Complement C1s subcomponent OS=Homo sapiens GN=C1S PE=1 SV=1	2.47E+005	1.46E+005
ACTBM_HUMAN	2	113.96	0.03	1.92	B-actin-like protein 3 OS=Homo sapiens GN=ACTBL3 PE=1 SV=1	6.34E+004	1.22E+005
POTEE_HUMAN	2	113.96	0.03	1.92	POTE ankyrin domain family member E OS=Homo sapiens GN=POTEE PE=1 SV=3	6.34E+004	1.22E+005
POTEF_HUMAN	2	113.96	0.03	1.92	POTE ankyrin domain family member F OS=Homo sapiens	6.34E+004	1.22E+005

Accession	Peptides	Score	Anova (p)*	Fold	Description	Average normalised abundances	
						T1DM new	Matched controls
					GN=POTEF PE=1 SV=2		
HRG_HUMAN	2	95.38	0.05	2.61	Histidine-rich glycoprotein OS=Homo sapiens GN=HRG PE=1 SV=1	1.13E+004	2.94E+004

List of differentially expressed protein for patients with newly-diagnosed type 1 diabetes and matched controls with DS-178/ U36 sample used as a reference run (raw data)

Accession	Peptides	Score	Anova (p)*	Fold	Description	Average normalised abundances	
						T1DM new	Matched controls
CO4B_HUMAN	26	2000.08	0.05	3.01	Complement C4-B OS=Homo sapiens GN=C4B PE=1 SV=1	4.46e+007	1.48e+007
CO5_HUMAN	9	586.25	0.04	1.63	Complement C5 OS=Homo sapiens GN=C5 PE=1 SV=4	4.70e+005	2.88e+005
THRB_HUMAN	7	555.88	0.04	35.59	Prothrombin OS=Homo sapiens GN=F2 PE=1 SV=2	1.05e+007	2.96e+005
ACTB_HUMAN	8	446.32	0.04	1.66	Actin, cytoplasmic 1 OS=Homo sapiens GN=ACTB PE=1 SV=1	3.25e+005	5.40e+005

Accession	Peptides	Score	Anova (p)*	Fold	Description	Average normalised abundances	
						T1DM new	Matched controls
ACTC_HUMAN	7	357.51	9.94e-003	2.30	Actin, alpha cardiac muscle 1 OS=Homo sapiens GN=ACTC1 PE=1 SV=1	1.24e+005	2.84e+005
ACTH_HUMAN	6	314.33	9.62e-003	2.23	Actin, gamma-enteric smooth muscle OS=Homo sapiens GN=ACTG2 PE=1 SV=1	1.16e+005	2.60e+005
CLUS_HUMAN	4	246.38	0.02	1.57	Clusterin OS=Homo sapiens GN=CLU PE=1 SV=1	8.49e+005	5.41e+005
CRP_HUMAN	4	196.23	0.02	8.05	C-reactive protein OS=Homo sapiens GN=CRP PE=1 SV=1	4.21e+005	5.23e+004
POTEF_HUMAN	3	178.73	0.03	2.02	POTE ankyrin domain family member F OS=Homo sapiens	6.91e+004	1.40e+005

Accession	Peptides	Score	Anova (p)*	Fold	Description	Average normalised abundances	
						T1DM new	Matched controls
					GN=POTEF PE=1 SV=2		
POTEE_HUMAN	3	178.73	0.03	2.02	POTE ankyrin domain family member E OS=Homo sapiens GN=POTEE PE=1 SV=3	6.91e+004	1.40e+005
IPSP_HUMAN	3	167.73	0.02	2.08	Plasma serine protease inhibitor OS=Homo sapiens GN=SERPINA5 PE=1 SV=2	2.81e+004	5.83e+004
LG3BP_HUMAN	2	121.06	0.04	1.54	Galectin-3-binding protein OS=Homo sapiens GN=LGALS3BP PE=1 SV=1	4.31e+005	2.79e+005
ITIH3_HUMAN	2	117.79	0.02	2.50	Inter-alpha-trypsin inhibitor heavy chain H3 OS=Homo sapiens	8.37e+004	3.34e+004

Accession	Peptides	Score	Anova (p)*	Fold	Description	Average normalised abundances	
						T1DM new	Matched controls
					GN=ITIH3 PE=1 SV=2		
ACTBL_HUMAN	2	117.48	0.03	1.87	B-actin-like protein 2 OS=Homo sapiens GN=ACTBL2 PE=1 SV=2	6.40e+004	1.20e+005
ACTBM_HUMAN	2	113.96	0.03	2.03	B-actin-like protein 3 OS=Homo sapiens GN=ACTBL3 PE=1 SV=1	6.31e+004	1.28e+005
A2AP_HUMAN	2	111.80	0.03	1.58	Alpha-2-antiplasmin OS=Homo sapiens GN=SERPINF2 PE=1 SV=3	7.70e+004	1.22e+005

Patients with established type 1 diabetes vs their healthy controls

List of all proteins expressed in samples from patients with established type 1 diabetes (raw data) vs. their matched controls with DS-84/T1O10 as a reference run (raw data)

Accession	Peptides	Score	Anova (p)*	Fold	Description	Average normalised abundances	
						T1DM old	Matched controls
APOB_HUMAN	56	4308.27	0.05	2.5	Apolipoprotein B-100 OS=Homo sapiens GN=APOB PE=1 SV=1	7.65E+006	1.91E+007
ANT3_HUMAN	18	1712.09	0.05	2.55	Antithrombin-III OS=Homo sapiens GN=SERPINC1 PE=1 SV=1	6.43E+007	1.64E+008
APOE_HUMAN	12	1248.2	0.02	2.19	Apolipoprotein E OS=Homo sapiens GN=APOE PE=1 SV=1	1.46E+007	3.20E+007
PROS_HUMAN	7	545.67	0.05	2.47	Vitamin K-dependent protein S OS=Homo sapiens GN=PROS1	1.52E+006	3.75E+006

Accession	Peptides	Score	Anova (p)*	Fold	Description	Average normalised abundances	
						T1DM old	Matched controls
					PE=1 SV=1		
VTNC_HUMAN	5	491.62	0.03	1.72	Vitronectin OS=Homo sapiens GN=VTN PE=1 SV=1	2.55E+007	4.39E+007
APOC2_HUMAN	4	456.03	0.01	2.41	Apolipoprotein C-II OS=Homo sapiens GN=APOC2 PE=1 SV=1	4.06E+006	9.79E+006
APOA1_HUMAN	5	429.1	0.05	1.9	Apolipoprotein A-I OS=Homo sapiens GN=APOA1 PE=1 SV=1	2.66E+007	5.06E+007
CERU_HUMAN	6	412.71	0.03	1.7	Ceruloplasmin OS=Homo sapiens GN=CP PE=1 SV=1	5.53E+005	3.25E+005
FCN2_HUMAN	5	406.23	0.02	3	Ficolin-2 OS=Homo sapiens GN=FCN2 PE=1 SV=2	5.81E+005	1.75E+006

Accession	Peptides	Score	Anova (p)*	Fold	Description	Average normalised abundances	
						T1DM old	Matched controls
TTHY_HUMAN	4	377.31	0.04	2.69	Transthyretin OS=Homo sapiens GN=TTR PE=1 SV=1	2.14E+006	5.74E+006
SAA4_HUMAN	2	245.71	0.02	2.34	Serum amyloid A-4 protein OS=Homo sapiens GN=SAA4 PE=1 SV=1	8.40E+005	1.97E+006
MASP1_HUMAN	4	243.86	5.95E-003	1.97	Mannan-binding lectin serine protease 1 OS=Homo sapiens GN=MASP1 PE=1 SV=3	4.04E+005	7.95E+005
C4BPA_HUMAN	3	243.28	0.04	2.62	C4b-binding protein alpha chain OS=Homo sapiens GN=C4BPA PE=1 SV=2	5.67E+006	1.49E+007

Accession	Peptides	Score	Anova (p)*	Fold	Description	Average normalised abundances	
						T1DM old	Matched controls
FHR1_HUMAN	3	227.79	6.65E-003	1.88	Complement factor H-related protein 1 OS=Homo sapiens GN=CFHR1 PE=1 SV=2	2.30E+006	4.34E+006
HV315_HUMAN	1	211.45	4.00E-002	2.78	Ig heavy chain V-III region WAS OS=Homo sapiens PE=1 SV=1	4.24E+005	1.18E+006
HV313_HUMAN	1	211.45	4.00E-002	2.78	Ig heavy chain V-III region POM OS=Homo sapiens PE=1 SV=1	4.24E+005	1.18E+006
PLF4_HUMAN	2	211.02	0.05	2.1	Platelet factor 4 OS=Homo sapiens GN=PF4 PE=1 SV=2	7.12E+005	1.49E+006
ACTG_HUMAN	4	201.04	0.03	3.42	Actin, cytoplasmic 2 OS=Homo sapiens GN=ACTG1 PE=1 SV=1	1.28E+005	4.38E+005

Accession	Peptides	Score	Anova (p)*	Fold	Description	Average normalised abundances	
						T1DM old	Matched controls
HEP2_HUMAN	3	189.86	0.04	1.98	Heparin cofactor 2 OS=Homo sapiens GN=SERPIND1 PE=1 SV=3	2.49E+004	4.94E+004
APOL1_HUMAN	2	189.67	3.71E-003	4.07	Apolipoprotein L1 OS=Homo sapiens GN=APOL1 PE=1 SV=5	7.27E+004	2.96E+005
FHR2_HUMAN	2	168.18	0.02	1.88	Complement factor H-related protein 2 OS=Homo sapiens GN=CFHR2 PE=1 SV=1	7.12E+005	1.34E+006
CO8B_HUMAN	3	158.26	0.01	1.46	Complement component C8 β chain OS=Homo sapiens GN=C8B PE=1 SV=3	8.24E+004	5.64E+004
ACTBM_HUMAN	3	154.69	0.01	3.99	B-actin-like protein 3 OS=Homo sapiens GN=ACTBL3 PE=1 SV=1	6.77E+004	2.70E+005

Accession	Peptides	Score	Anova (p)*	Fold	Description	Average normalised abundances	
						T1DM old	Matched controls
POTEE_HUMAN	3	154.69	0.01	3.99	POTE ankyrin domain family member E OS=Homo sapiens GN=POTEE PE=1 SV=3	6.77E+004	2.70E+005
APOC4_HUMAN	2	135.66	0.02	2.9	Apolipoprotein C-IV OS=Homo sapiens GN=APOC4 PE=1 SV=1	5.04E+004	1.46E+005
VWF_HUMAN	2	117.51	0.02	4.42	von Willebrand factor OS=Homo sapiens GN=VWF PE=1 SV=3	1.76E+004	7.80E+004
CO8A_HUMAN	2	98.35	0.03	1.73	Complement component C8 alpha chain OS=Homo sapiens GN=C8A PE=1 SV=2	5.12E+004	2.96E+004
A2MG_HUMAN	2	96.72	0.02	2.27	Alpha-2-macroglobulin OS=Homo sapiens GN=A2M PE=1 SV=2	8.06E+004	3.55E+004

List of proteins expressed in samples from patients with established type 1 diabetes vs. their matched controls with DS-162/M16 as a reference run (raw data).

Accession	Peptides	Score	Anova (p)*	Fold	Description	Average normalised abundances	
						T1DM old	Matched controls
ANT3_HUMAN	17	1510.35	0.03	2.31	Antithrombin-III OS=Homo sapiens GN=SERPINC1 PE=1 SV=1	3.15E+007	7.27E+007
APOE_HUMAN	15	1226.65	0.02	2.05	Apolipoprotein E OS=Homo sapiens GN=APOE PE=1 SV=1	1.07E+007	2.19E+007
FCN2_HUMAN	7	544.62	0.02	2.81	Ficolin-2 OS=Homo sapiens GN=FCN2 PE=1 SV=2	4.37E+005	1.23E+006
APOC2_HUMAN	5	518.44	0.01	2.25	Apolipoprotein C-II OS=Homo sapiens GN=APOC2 PE=1 SV=1	3.13E+006	7.05E+006
VTNC_HUMAN	5	446.27	0.03	1.62	Vitronectin OS=Homo sapiens GN=VTN PE=1 SV=1	1.71E+007	2.77E+007

Accession	Peptides	Score	Anova (p)*	Fold	Description	Average normalised abundances	
						T1DM old	Matched controls
CERU_HUMAN	8	445.18	0.04	1.44	Ceruloplasmin OS=Homo sapiens GN=CP PE=1 SV=1	4.51E+005	3.13E+005
APOA1_HUMAN	4	347.03	0.04	1.76	Apolipoprotein A-I OS=Homo sapiens GN=APOA1 PE=1 SV=1	1.99E+007	3.50E+007
PROS_HUMAN	4	337.83	6.32E-003	2.13	Vitamin K-dependent protein S OS=Homo sapiens GN=PROS1 PE=1 SV=1	4.03E+005	8.59E+005
TTHY_HUMAN	3	335.64	0.03	2.39	Transthyretin OS=Homo sapiens GN=TTR PE=1 SV=1	1.63E+006	3.91E+006
ITIH1_HUMAN	4	298.01	0.01	2.14	Inter-alpha-trypsin inhibitor heavy chain H1 OS=Homo sapiens GN=ITIH1 PE=1 SV=3	2.66E+005	5.69E+005

Accession	Peptides	Score	Anova (p)*	Fold	Description	Average normalised abundances	
						T1DM old	Matched controls
MASP1_HUMAN	4	243.86	2.11E-003	1.95	Mannan-binding lectin serine protease 1 OS=Homo sapiens GN=MASP1 PE=1 SV=3	2.82E+005	5.49E+005
C4BPA_HUMAN	3	243.28	0.03	2.39	C4b-binding protein alpha chain OS=Homo sapiens GN=C4BPA PE=1 SV=2	4.23E+006	1.01E+007
HV304_HUMAN	1	211.45	0.05	2.5	Ig heavy chain V-III region TIL OS=Homo sapiens PE=1 SV=1	3.20E+005	8.00E+005
PLF4_HUMAN	2	211.02	0.05	1.98	Platelet factor 4 OS=Homo sapiens GN=PF4 PE=1 SV=2	5.30E+005	1.05E+006
SAA4_HUMAN	2	202.91	0.02	2.25	Serum amyloid A-4 protein OS=Homo sapiens GN=SAA4 PE=1	5.16E+005	1.16E+006

Accession	Peptides	Score	Anova (p)*	Fold	Description	Average normalised abundances	
						T1DM old	Matched controls
					SV=1		
ACTG_HUMAN	4	201.04	0.02	3.14	Actin, cytoplasmic 2 OS=Homo sapiens GN=ACTG1 PE=1 SV=1	1.45E+005	4.56E+005
APOL1_HUMAN	3	186.21	0.03	2.44	Apolipoprotein L1 OS=Homo sapiens GN=APOL1 PE=1 SV=5	7.75E+004	1.89E+005
IPSP_HUMAN	2	184.05	0.05	2.01	Plasma serine protease inhibitor OS=Homo sapiens GN=SERPINA5 PE=1 SV=2	5.14E+004	1.03E+005
FHR1_HUMAN	3	160.96	0.02	1.74	Complement factor H-related protein 1 OS=Homo sapiens GN=CFHR1 PE=1 SV=2	1.42E+006	2.47E+006

Accession	Peptides	Score	Anova (p)*	Fold	Description	Average normalised abundances	
						T1DM old	Matched controls
A2AP_HUMAN	3	159.38	0.03	3.54	Alpha-2-antiplasmin OS=Homo sapiens GN=SERPINF2 PE=1 SV=3	2.47E+004	8.74E+004
POTEE_HUMAN	3	154.69	9.51E-003	3.72	POTE ankyrin domain family member E OS=Homo sapiens GN=POTEE PE=1 SV=3	4.79E+004	1.78E+005
POTEF_HUMAN	3	154.69	9.51E-003	3.72	POTE ankyrin domain family member F OS=Homo sapiens GN=POTEF PE=1 SV=2	4.79E+004	1.78E+005
ACTBM_HUMAN	3	154.69	9.51E-003	3.72	B-actin-like protein 3 OS=Homo sapiens GN=ACTBL3 PE=1 SV=1	4.79E+004	1.78E+005
CO8A_HUMAN	3	139.62	0.02	1.67	Complement component C8 alpha chain OS=Homo sapiens	4.30E+004	2.58E+004

Accession	Peptides	Score	Anova (p)*	Fold	Description	Average normalised abundances	
						T1DM old	Matched controls
					GN=C8A PE=1 SV=2		
APOC4_HUMAN	2	135.66	3.89E-03	3.53	Apolipoprotein C-IV OS=Homo sapiens GN=APOC4 PE=1 SV=1	2.86E+004	1.01E+005
A2MG_HUMAN	2	133.61	0.03	2.08	Alpha-2-macroglobulin OS=Homo sapiens GN=A2M PE=1 SV=2	8.89E+004	4.28E+004
APOC1_HUMAN	2	117.67	0.02	2.32	Apolipoprotein C-I OS=Homo sapiens GN=APOC1 PE=1 SV=1	1.37E+006	3.18E+006
VWF_HUMAN	2	117.51	0.01	3.51	von Willebrand factor OS=Homo sapiens GN=VWF PE=1 SV=3	1.67E+004	5.87E+004
ACTC_HUMAN	2	108.97	0.01	3.64	Actin, alpha cardiac muscle 1 OS=Homo sapiens GN=ACTC1 PE=1 SV=1	4.64E+004	1.69E+005

Accession	Peptides	Score	Anova (p)*	Fold	Description	Average normalised abundances	
						T1DM old	Matched controls
ACTS_HUMAN	2	108.97	0.01	3.64	Actin, alpha skeletal muscle OS=Homo sapiens GN=ACTA1 PE=1 SV=1	4.64E+004	1.69E+005
VTDB_HUMAN	2	106.33	0.05	3.04	Vitamin D-binding protein OS=Homo sapiens GN=GC PE=1 SV=1	2.71E+004	8.23E+004
FHR2_HUMAN	2	101.35	0.02	1.71	Complement factor H-related protein 2 OS=Homo sapiens GN=CFHR2 PE=1 SV=1	2.27E+005	3.89E+005
CO8B_HUMAN	2	92.06	1.57E-003	1.86	Complement component C8 β chain OS=Homo sapiens GN=C8B PE=1 SV=3	6.35E+004	3.41E+004

List of proteins expressed in samples from patients with established type 1 diabetes vs. their matched controls with DS-39/U14 as a reference run (raw data).

Accession	Peptides	Score	Anova (p)*	Fold	Description	Average normalised abundances	
						T1DM old	Matched controls
ANT3_HUMAN	16	1381.27	0.03	2.37	Antithrombin-III OS=Homo sapiens GN=SERPINC1 PE=1 SV=1	2.79E+007	6.63E+007
APOE_HUMAN	15	1269.56	0.02	2.05	Apolipoprotein E OS=Homo sapiens GN=APOE PE=1 SV=1	1.05E+007	2.16E+007
APOC2_HUMAN	5	518.44	7.13E-003	2.5	Apolipoprotein C-II OS=Homo sapiens GN=APOC2 PE=1 SV=1	2.76E+006	6.88E+006
VTNC_HUMAN	6	501.23	0.03	1.57	Vitronectin OS=Homo sapiens GN=VTN PE=1 SV=1	1.76E+007	2.77E+007

Accession	Peptides	Score	Anova (p)*	Fold	Description	Average normalised abundances	
						T1DM old	Matched controls
FCN2_HUMAN	6	494.26	0.02	2.88	Ficolin-2 OS=Homo sapiens GN=FCN2 PE=1 SV=2	4.10E+005	1.18E+006
CERU_HUMAN	7	477.04	0.03	1.6	Ceruloplasmin OS=Homo sapiens GN=CP PE=1 SV=1	5.17E+005	3.23E+005
PROS_HUMAN	6	446.97	5.34E-003	2.24	Vitamin K-dependent protein S OS=Homo sapiens GN=PROS1 PE=1 SV=1	4.03E+005	9.04E+005
APOA1_HUMAN	5	429.1	0.05	1.75	Apolipoprotein A-I OS=Homo sapiens GN=APOA1 PE=1 SV=1	1.96E+007	3.44E+007
TTHY_HUMAN	3	335.64	0.04	2.46	Transthyretin OS=Homo sapiens GN=TTR PE=1 SV=1	1.51E+006	3.71E+006

Accession	Peptides	Score	Anova (p)*	Fold	Description	Average normalised abundances	
						T1DM old	Matched controls
C4BPA_HUMAN	4	316.54	0.03	2.4	C4b-binding protein alpha chain OS=Homo sapiens GN=C4BPA PE=1 SV=2	4.16E+006	9.97E+006
SAA4_HUMAN	3	287.7	0.01	2.37	Serum amyloid A-4 protein OS=Homo sapiens GN=SAA4 PE=1 SV=1	5.00E+005	1.19E+006
IPSP_HUMAN	3	245.51	0.05	2.13	Plasma serine protease inhibitor OS=Homo sapiens GN=SERPINA5 PE=1 SV=2	5.80E+004	1.24E+005
MASP1_HUMAN	4	243.86	2.59E-003	1.91	Mannan-binding lectin serine protease 1 OS=Homo sapiens GN=MASP1 PE=1 SV=3	2.79E+005	5.35E+005

Accession	Peptides	Score	Anova (p)*	Fold	Description	Average normalised abundances	
						T1DM old	Matched controls
APOL1_HUMAN	3	233.39	0.02	2	Apolipoprotein L1 OS=Homo sapiens GN=APOL1 PE=1 SV=5	1.25E+005	2.49E+005
ITIH1_HUMAN	3	224.52	7.72E-003	2.26	Inter-alpha-trypsin inhibitor heavy chain H1 OS=Homo sapiens GN=ITIH1 PE=1 SV=3	2.13E+005	4.81E+005
HV313_HUMAN	1	211.45	5.00E-002	2.51	Ig heavy chain V-III region POM OS=Homo sapiens PE=1 SV=1	3.13E+005	7.87E+005
HV315_HUMAN	1	211.45	5.00E-002	2.51	Ig heavy chain V-III region WAS OS=Homo sapiens PE=1 SV=1	3.13E+005	7.87E+005
PLF4_HUMAN	2	211.02	0.05	1.97	Platelet factor 4 OS=Homo sapiens GN=PF4 PE=1 SV=2	5.22E+005	1.03E+006

Accession	Peptides	Score	Anova (p)*	Fold	Description	Average normalised abundances	
						T1DM old	Matched controls
ACTG_HUMAN	4	201.04	0.03	3.09	Actin, cytoplasmic 2 OS=Homo sapiens GN=ACTG1 PE=1 SV=1	1.52E+005	4.71E+005
POTEF_HUMAN	3	154.69	0.02	3.63	POTE ankyrin domain family member F OS=Homo sapiens GN=POTEF PE=1 SV=2	5.17E+004	1.88E+005
ACTBM_HUMAN	3	154.69	0.02	3.63	B-actin-like protein 3 OS=Homo sapiens GN=ACTBL3 PE=1 SV=1	5.17E+004	1.88E+005
POTEE_HUMAN	3	154.69	0.02	3.63	POTE ankyrin domain family member E OS=Homo sapiens GN=POTEE PE=1 SV=3	5.17E+004	1.88E+005

Accession	Peptides	Score	Anova (p)*	Fold	Description	Average normalised abundances	
						T1DM old	Matched controls
APOC4_HUMAN	2	135.66	4.00E-003	3.03	Apolipoprotein C-IV OS=Homo sapiens GN=APOC4 PE=1 SV=1	3.58E+004	1.08E+005
HEP2_HUMAN	2	125.29	0.02	2.81	Heparin cofactor 2 OS=Homo sapiens GN=SERPIND1 PE=1 SV=3	1.05E+004	2.95E+004
VWF_HUMAN	2	117.51	0.01	3.9	von Willebrand factor OS=Homo sapiens GN=VWF PE=1 SV=3	1.41E+004	5.50E+004
ZPI_HUMAN	2	112.45	0.02	1.98	Protein Z-dependent protease inhibitor OS=Homo sapiens GN=SERPINA10 PE=1 SV=1	3.47E+004	1.75E+004
FA10_HUMAN	2	111.84	0.04	2.96	Coagulation factor X OS=Homo sapiens GN=F10 PE=1 SV=2	3.78E+004	1.12E+005

Accession	Peptides	Score	Anova (p)*	Fold	Description	Average normalised abundances	
						T1DM old	Matched controls
ACTC_HUMAN	2	108.97	0.02	3.59	Actin, alpha cardiac muscle 1 OS=Homo sapiens GN=ACTC1 PE=1 SV=1	4.97E+004	1.79E+005
FHR1_HUMAN	2	106.76	0.03	1.74	Complement factor H-related protein 1 OS=Homo sapiens GN=CFHR1 PE=1 SV=2	1.34E+006	2.33E+006
VTDB_HUMAN	2	106.33	0.05	3.2	Vitamin D-binding protein OS=Homo sapiens GN=GC PE=1 SV=1	2.52E+004	8.07E+004
CO8B_HUMAN	2	92.06	5.89E-004	1.91	Complement component C8 β chain OS=Homo sapiens GN=C8B PE=1 SV=3	6.34E+004	3.31E+004

Patients with newly diagnosed type 1 diabetes vs. patients with established type 1 diabetes

List of differentially expressed proteins in samples from type 1 newly diagnosed diabetes (T1DM new) and established type 1 diabetes (T1DM old) with DS-169/T1N8 control sample used as reference run (raw data)

Accession	Peptides	Score	Anova (p)*	Fold	Description	Av. normalised abundances	
						T1DM new	T1DM old
CO4B_HUMAN	47	4330.13	0.02	1.35	Complement C4-B OS=Homo sapiens GN=C4B PE=1 SV=1	1.11E+08	8.23E+07
THRB_HUMAN	19	1580.52	0.05	1.39	Prothrombin OS=Homo sapiens GN=F2 PE=1 SV=2	3.08E+07	2.22E+07
CERU_HUMAN	12	841.03	0.03	1.55	Ceruloplasmin OS=Homo sapiens GN=CP PE=1 SV=1	8.18E+05	1.27E+06

Accession	Peptides	Score	Anova (p)*	Fold	Description	Av. normalised abundances	
						T1DM new	T1DM old
CLUS_HUMAN	7	766.66	5.00E-03	1.43	Clusterin OS=Homo sapiens GN=CLU PE=1 SV=1	2.10E+07	1.47E+07
IGHM_HUMAN	4	763.61	0.04	1.57	Ig mu chain C region OS=Homo sapiens GN=IGHM PE=1 SV=3	6.61E+06	4.21E+06
CO5_HUMAN	13	749.38	0.03	1.59	Complement C5 OS=Homo sapiens GN=C5 PE=1 SV=4	6.09E+05	3.83E+05
ANT3_HUMAN	10	724.15	6.47E-03	1.44	Antithrombin-III OS=Homo sapiens GN=SERPINC1 PE=1 SV=1	2.35E+07	1.63E+07
ITIH2_HUMAN	9	697.1	0.02	1.47	Inter-alpha-trypsin inhibitor heavy chain H2 OS=Homo sapiens	2.58E+06	1.76E+06

Accession	Peptides	Score	Anova (p)*	Fold	Description	Av. normalised abundances	
						T1DM new	T1DM old
					GN=ITIH2 PE=1 SV=2		
A1AT_HUMAN	8	586.08	0.05	1.49	Alpha-1-antitrypsin OS=Homo sapiens GN=SERPINA1 PE=1 SV=3	5.32E+05	3.57E+05
IGKC_HUMAN	4	483.7	0.03	1.54	Ig kappa chain C region OS=Homo sapiens GN=IGKC PE=1 SV=1	6.15E+06	4.00E+06
VTNC_HUMAN	4	375.94	0.03	1.45	Vitronectin OS=Homo sapiens GN=VTN PE=1 SV=1	1.72E+07	1.18E+07
PROS_HUMAN	4	316.49	7.49E-03	1.71	Vitamin K-dependent protein S OS=Homo sapiens GN=PROS1 PE=1 SV=1	6.27E+05	3.67E+05
ALBU_HUMAN	4	255.52	7.77E-	1.69	Serum albumin OS=Homo sapiens GN=ALB PE=1 SV=2	4.50E+05	2.66E+05

Accession	Peptides	Score	Anova (p)*	Fold	Description	Av. normalised abundances	
						T1DM new	T1DM old
			03				
PLMN_HUMAN	3	255.02	0.05	1.29	Plasminogen OS=Homo sapiens GN=PLG PE=1 SV=2	3.79E+05	4.91E+05
APOC1_HUMAN	4	213.76	4.51E-03	1.55	Apolipoprotein C-I OS=Homo sapiens GN=APOC1 PE=1 SV=1	2.59E+06	1.67E+06
ITIH3_HUMAN	4	213.07	0.05	1.81	Inter-alpha-trypsin inhibitor heavy chain H3 OS=Homo sapiens GN=ITIH3 PE=1SV=2	1.03E+05	5.70E+04
LCAT_HUMAN	3	183.51	0.05	1.24	Phosphatidylcholine-sterol acyltransferase OS=Homo sapiens GN=LCAT PE=1 SV=1	5.96E+05	4.80E+05

Accession	Peptides	Score	Anova (p)*	Fold	Description	Av. normalised abundances	
						T1DM new	T1DM old
TSP1_HUMAN	3	171.19	0.05	1.48	Thrombospondin-1 OS=Homo sapiens GN=THBS1 PE=1 SV=2	1.52E+05	2.24E+05
FHR1_HUMAN	2	153.94	0.02	1.77	Complement factor H-related protein 1 OS=Homo sapiens GN=CFHR1 PE=1 SV=2	6.05E+04	3.42E+04
KV204_HUMAN	2	121.2	0.05	1.48	Ig kappa chain V-II region TEW OS=Homo sapiens PE=1 SV=1	2.07E+05	1.40E+05
K2C1_HUMAN	2	96.61	0.04	4.01	Keratin, type II cytoskeletal 1 OS=Homo sapiens GN=KRT1 PE=1 SV=6	1.49E+04	3.72E+03

List of differentially expressed proteins for type 1 newly diagnosed diabetes (T1DM new) and established type 1 diabetes (T1DM old) with DS-74/T1O7 used as reference run (raw data)

Accession	Peptides	Score	Anova (p)*	Fold	Description	Average normalised abundances	
						T1DM new	T1DM old
CO4B_HUMAN	46	4003.47	0.01	1.45	Complement C4-B OS=Homo sapiens GN=C4B PE=1 SV=1	1.56E+08	1.08E+08
THRB_HUMAN	15	1402.27	0.05	1.4	Prothrombin OS=Homo sapiens GN=F2 PE=1 SV=2	4.57E+07	3.27E+07
IGHM_HUMAN	5	1006.7	0.04	1.57	Ig mu chain C region OS=Homo sapiens GN=IGHM PE=1 SV=3	1.26E+07	8.04E+06

Accession	Peptides	Score	Anova (p)*	Fold	Description	Average normalised abundances	
						T1DM new	T1DM old
		3					
CLUS_HUMAN	9	889.94	3.88E-03	1.42	Clusterin OS=Homo sapiens GN=CLU PE=1 SV=1	3.31E+07	2.34E+07
ANT3_HUMAN	13	886.97	0.01	1.43	Antithrombin-III OS=Homo sapiens GN=SERPINC1 PE=1 SV=1	3.12E+07	2.18E+07
ITIH1_HUMAN	9	781.46	0.04	1.46	Inter-alpha-trypsin inhibitor heavy chain H1 OS=Homo sapiens GN=ITIH1 PE=1 SV=3	2.25E+06	1.55E+06
IGKC_HUMAN	5	524.66	0.02	1.55	Ig kappa chain C region OS=Homo sapiens GN=IGKC PE=1 SV=1	9.42E+06	6.07E+06

Accession	Peptides	Score	Anova (p)*	Fold	Description	Average normalised abundances	
						T1DM new	T1DM old
VTNC_HUMAN	5	437.98	0.03	1.46	Vitronectin OS=Homo sapiens GN=VTN PE=1 SV=1	2.57E+07	1.76E+07
CO9_HUMAN	5	355.88	0.05	1.53	Complement component C9 OS=Homo sapiens GN=C9 PE=1 SV=2	2.39E+06	1.56E+06
CFAH_HUMAN	4	287.58	0.04	1.57	Complement factor H OS=Homo sapiens GN=CFH PE=1 SV=4	7.80E+05	4.96E+05
PROS_HUMAN	5	259.26	9.13E-04	1.49	Vitamin K-dependent protein S OS=Homo sapiens GN=PROS1 PE=1 SV=1	6.24E+05	4.18E+05
APOC1_HUMAN	2	123.48	2.43E-03	1.56	Apolipoprotein C-I OS=Homo sapiens GN=APOC1 PE=1 SV=1	3.78E+06	2.42E+06

List of differentially expressed proteins for type 1 newly diagnosed diabetes (T1DM new) and established type 1 diabetes (T1DM old) with DS-90/T1O12 sample used as reference run (raw data).

Accession	Peptides	Score	Anova (p)*	Fold	Description	Average normalised abundances	
						T1DM new	T1DM old
CO4B_HUMAN	44	3766.11	1.00E-02	1.48	Complement C4-B OS=Homo sapiens GN=C4B PE=1 SV=1	1.62E+08	1.09E+08
THRB_HUMAN	17	1532.49	0.03	1.42	Prothrombin OS=Homo sapiens GN=F2 PE=1 SV=2	4.69E+07	3.31E+07
IGHM_HUMAN	6	963.76	3.00E-02	1.55	Ig mu chain C region OS=Homo sapiens GN=IGHM PE=1 SV=3	1.43E+07	9.25E+06
CLUS_HUMAN	10	962.19	0.00308	1.45	Clusterin OS=Homo sapiens GN=CLU PE=1 SV=1	3.35E+07	2.31E+07

Accession	Peptides	Score	Anova (p)*	Fold	Description	Average normalised abundances	
						T1DM new	T1DM old
ITIH1_HUMAN	10	959.99	0.04	1.48	Inter-alpha-trypsin inhibitor heavy chain H1 OS=Homo sapiens GN=ITIH1 PE=1 SV=3	2.56E+06	1.73E+06
ANT3_HUMAN	13	912.25	7.92E-03	1.46	Antithrombin-III OS=Homo sapiens GN=SERPINC1 PE=1 SV=1	4.18E+07	2.87E+07
ITIH2_HUMAN	10	766.5	9.83E-03	1.46	Inter-alpha-trypsin inhibitor heavy chain H2 OS=Homo sapiens GN=ITIH2 PE=1 SV=2	4.43E+06	3.04E+06
VTNC_HUMAN	4	447.26	0.03	1.42	Vitronectin OS=Homo sapiens GN=VTN PE=1 SV=1	3.39E+07	2.38E+07

Accession	Peptides	Score	Anova (p)*	Fold	Description	Average normalised abundances	
						T1DM new	T1DM old
IGKC_HUMAN	4	418.25	0.02	1.58	Ig kappa chain C region OS=Homo sapiens GN=IGKC PE=1 SV=1	9.56E+06	6.06E+06
PROS_HUMAN	2	190.82	0.00338	2.2	Vitamin K-dependent protein S OS=Homo sapiens GN=PROS1 PE=1 SV=1	6.16E+05	2.80E+05
LCAT_HUMAN	3	183.5	0.03	1.26	Phosphatidylcholine-sterol acyltransferase OS=Homo sapiens GN=LCAT PE=1 SV=1	8.95E+05	7.09E+05
APOC1_HUMAN	3	171.86	0.00283	1.59	Apolipoprotein C-I OS=Homo sapiens GN=APOC1 PE=1 SV=1	3.88E+06	2.45E+06

Accession	Peptides	Score	Anova (p)*	Fold	Description	Average normalised abundances	
						T1DM new	T1DM old
APOL1_HUMAN	3	147.63	0.02	1.88	Apolipoprotein L1 OS=Homo sapiens GN=APOL1 PE=1 SV=5	1.43E+05	7.61E+04

Healthy controls to patients with newly diagnosed type 1 diabetes vs. healthy controls to patients with established type 1 diabetes

List of differentially expressed proteins for 'new' and 'old' controls. DS-162 'old' control sample was used as reference run (raw data)

Accession	Peptides	Score	Anova (p)*	Fold	Description	Average Normalised Abundances	
						control new	control old
APOE_HUMAN	9	844.42	0.02	2.35	Apolipoprotein E OS=Homo sapiens GN=APOE PE=1 SV=1	8.81E+06	2.07E+07
LG3BP_HUMAN	8	786.36	0.02	2.55	Galectin-3-binding protein OS=Homo sapiens GN=LGALS3BP PE=1 SV=1	1.65E+06	4.22E+06
IGHM_HUMAN	8	557.04	0.04	1.6	Ig mu chain C region OS=Homo sapiens GN=IGHM PE=1 SV=3	5.71E+06	3.57E+06

Accession	Peptides	Score	Anova (p)*	Fold	Description	Average Normalised Abundances	
						control new	control old
CLUS_HUMAN	6	516.52	0.05	2.33	Clusterin OS=Homo sapiens GN=CLU PE=1 SV=1	7.93E+06	1.85E+07
PROS_HUMAN	6	429.17	0.05	2.69	Vitamin K-dependent protein S OS=Homo sapiens GN=PROS1 PE=1 SV=1	8.16E+05	2.19E+06
APOC2_HUMAN	3	422.95	4.73E-03	2.61	Apolipoprotein C-II OS=Homo sapiens GN=APOC2 PE=1 SV=1	2.76E+06	7.18E+06
CRP_HUMAN	5	353.29	0.01	10.84	C-reactive protein OS=Homo sapiens GN=CRP PE=1 SV=1	2.18E+05	2.36E+06
C4BPA_HUMAN	3	251.9	0.03	2.61	C4b-binding protein alpha chain OS=Homo sapiens GN=C4BPA PE=1 SV=2	4.22E+06	1.10E+07

Accession	Peptides	Score	Anova (p)*	Fold	Description	Average Normalised Abundances	
						control new	control old
FBLN3_HUMAN	2	212.06	0.04	2.35	EGF-containing fibulin-like extracellular matrix protein 1 OS=Homo sapiens GN=EFEMP1 PE=1 SV=2	1.62E+05	3.82E+05
LBP_HUMAN	2	210.94	0.04	2.01	Lipopolysaccharide-binding protein OS=Homo sapiens GN=LBP PE=1 SV=3	2.92E+05	5.88E+05
MASP1_HUMAN	3	191.72	0.02	1.77	Mannan-binding lectin serine protease 1 OS=Homo sapiens GN=MASP1 PE=1 SV=3	2.71E+05	4.79E+05
ITIH3_HUMAN	3	178.07	0.01	2.21	Inter-alpha-trypsin inhibitor heavy chain H3 OS=Homo sapiens GN=ITIH3 PE=1 SV=2	4.41E+04	9.75E+04
CFAH_HUMAN	2	176.85	3.73E-03	1.52	Complement factor H OS=Homo sapiens GN=CFH PE=1	1.12E+06	7.35E+05

Accession	Peptides	Score	Anova (p)*	Fold	Description	Average Normalised Abundances	
						control new	control old
					SV=4		
SAA4_HUMAN	2	173.1	0.03	2.34	Serum amyloid A-4 protein OS=Homo sapiens GN=SAA4 PE=1 SV=1	5.48E+05	1.28E+06

List of differentially expressed proteins for 'new' and 'old' controls. DS-178 'new' control sample was used as reference run (raw data).

Accession	Peptides	Score	Anova (p)*	Fold	Description	Av. normalised abundances	
						Control new	Control old
THRB_HUMAN	12	1100.82	0.05	2.31	Prothrombin OS=Homo sapiens GN=F2 PE=1 SV=2	2.30E+07	5.31E+07
APOE_HUMAN	9	844.42	0.02	2.33	Apolipoprotein E OS=Homo sapiens GN=APOE PE=1 SV=1	8.78E+06	2.05E+07
LG3BP_HUMAN	6	676.81	5.44E-03	2.94	Galectin-3-binding protein OS=Homo sapiens GN=LGALS3BP PE=1 SV=1	1.40E+06	4.10E+06
IGHM_HUMAN	9	612.42	0.04	1.57	Ig mu chain C region OS=Homo sapiens GN=IGHM PE=1 SV=3	7.37E+06	4.68E+06

Accession	Peptides	Score	Anova (p)*	Fold	Description	Av. normalised abundances	
						Control new	Control old
CLUS_HUMAN	6	516.52	0.05	2.25	Clusterin OS=Homo sapiens GN=CLU PE=1 SV=1	8.14E+06	1.83E+07
ITIH2_HUMAN	7	512.82	0.04	1.39	Inter-alpha-trypsin inhibitor heavy chain H2 OS=Homo sapiens GN=ITIH2 PE=1 SV=2	8.33E+05	5.98E+05
FIBA_HUMAN	6	507.25	0.01	2.34	Fibrinogen alpha chain OS=Homo sapiens GN=FGA PE=1 SV=2	4.72E+05	1.10E+06
APOC2_HUMAN	3	422.95	8.61E-03	2.83	Apolipoprotein C-II OS=Homo sapiens GN=APOC2 PE=1 SV=1	2.52E+06	7.13E+06
CFAH_HUMAN	6	357.17	5.49E-	1.5	Complement factor H OS=Homo sapiens GN=CFH PE=1 SV=4	1.54E+06	1.02E+06

Accession	Peptides	Score	Anova (p)*	Fold	Description	Av. normalised abundances	
						Control new	Control old
			03				
CRP_HUMAN	5	353.28	0.01	10.73	C-reactive protein OS=Homo sapiens GN=CRP PE=1 SV=1	2.20E+05	2.37E+06
FA5_HUMAN	3	263.39	0.02	2.58	Coagulation factor V OS=Homo sapiens GN=F5 PE=1 SV=3	1.80E+05	4.64E+05
SAA4_HUMAN	3	260.7	0.01	2.21	Serum amyloid A-4 protein OS=Homo sapiens GN=SAA4 PE=1 SV=1	6.65E+05	1.47E+06
ITIH3_HUMAN	4	259.04	0.01	2.32	Inter-alpha-trypsin inhibitor heavy chain H3 OS=Homo sapiens GN=ITIH3 PE=1 SV=2	4.72E+04	1.09E+05

Accession	Peptides	Score	Anova (p)*	Fold	Description	Av. normalised abundances	
						Control new	Control old
C4BPA_HUMAN	3	251.9	0.03	2.51	C4b-binding protein alpha chain OS=Homo sapiens GN=C4BPA PE=1 SV=2	4.33E+06	1.09E+07
PROC_HUMAN	3	240.46	0.05	2.24	Vitamin K-dependent protein C OS=Homo sapiens GN=PROC PE=1 SV=1	1.66E+05	3.72E+05
MASP1_HUMAN	3	191.72	0.02	1.72	Mannan-binding lectin serine protease 1 OS=Homo sapiens GN=MASP1 PE=1 SV=3	2.80E+05	4.81E+05
FETUA_HUMAN	2	112.69	0.03	1.4	Alpha-2-HS-glycoprotein OS=Homo sapiens GN=AHSG PE=1 SV=1	3.06E+05	2.19E+05

Accession	Peptides	Score	Anova (p)*	Fold	Description	Av. normalised abundances	
						Control new	Control old
IGKC_HUMAN	2	106.69	0.03	1.79	Ig kappa chain C region OS=Homo sapiens GN=IGKC PE=1 SV=1	4.31E+05	2.40E+05
TSP1_HUMAN	2	105.63	0.05	1.72	Thrombospondin-1 OS=Homo sapiens GN=THBS1 PE=1 SV=2	7.02E+04	4.07E+04
TRFL_HUMAN	2	100.03	0.02	3.19	Lactotransferrin OS=Homo sapiens GN=LTF PE=1 SV=6	1.88E+04	5.89E+03

List of differentially expressed proteins for 'new' and 'old' controls. DS-39 'old' control sample was used as reference run. DS-7 was excluded from this analysis as protein expression pattern for this sample differed from other samples in the same group (raw data).

Accession	Peptides	Score	Anova (p)*	Fold	Description	Average normalised abundances	
						Control new	Control old
CO4B_HUMAN	53	4906.74	0.05	1.53	Complement C4-B OS=Homo sapiens GN=C4B PE=1 SV=1	1.21E+08	1.85E+08
APOE_HUMAN	15	1315.95	0.02	1.71	Apolipoprotein E OS=Homo sapiens GN=APOE PE=1 SV=1	1.13E+07	1.92E+07
THRB_HUMAN	16	1221.3	0.05	1.34	Prothrombin OS=Homo sapiens GN=F2 PE=1 SV=2	2.48E+07	3.33E+07

Accession	Peptides	Score	Anova (p)*	Fold	Description	Average normalised abundances	
						Control new	Control old
		7					
LG3BP_HUMAN	12	964.88	0.02	1.73	Galectin-3-binding protein OS=Homo sapiens GN=LGALS3BP PE=1 SV=1	1.78E+06	3.08E+06
CLUS_HUMAN	12	927.6	0.01	1.64	Clusterin OS=Homo sapiens GN=CLU PE=1 SV=1	1.47E+07	2.41E+07
PROS_HUMAN	8	566.62	0.05	1.55	Vitamin K-dependent protein S OS=Homo sapiens GN=PROS1 PE=1 SV=1	9.76E+05	1.52E+06
C4BPA_HUMAN	7	503.36	5.92E-03	1.55	C4b-binding protein alpha chain OS=Homo sapiens GN=C4BPA PE=1 SV=2	5.05E+06	7.83E+06

Accession	Peptides	Score	Anova (p)*	Fold	Description	Average normalised abundances	
						Control new	Control old
APOC2_HUMAN	4	469.21	3.74E-03	1.99	Apolipoprotein C-II OS=Homo sapiens GN=APOC2 PE=1 SV=1	2.91E+06	5.80E+06
CFAH_HUMAN	5	446.31	1.17E-03	1.6	Complement factor H OS=Homo sapiens GN=CFH PE=1 SV=4	1.90E+06	1.19E+06
CERU_HUMAN	5	441.73	0.05	1.5	Ceruloplasmin OS=Homo sapiens GN=CP PE=1 SV=1	1.99E+05	3.00E+05
CRP_HUMAN	5	353.29	0.03	10.3	C-reactive protein OS=Homo sapiens GN=CRP PE=1 SV=1	2.19E+05	2.25E+06
FIBA_HUMAN	4	308.39	0.03	2.24	Fibrinogen alpha chain OS=Homo sapiens GN=FGA PE=1 SV=2	1.26E+05	2.81E+05
SAA4_HUMAN	4	295.89	8.06E-03	1.66	Serum amyloid A-4 protein OS=Homo sapiens GN=SAA4 PE=1 SV=1	7.99E+05	1.32E+06

Accession	Peptides	Score	Anova (p)*	Fold	Description	Average normalised abundances	
						Control new	Control old
KV302_HUMAN	3	226.98	0.04	1.5	Ig kappa chain V-III region SIE OS=Homo sapiens PE=1 SV=1	6.89E+05	4.60E+05
MASP1_HUMAN	3	191.72	0.03	1.38	Mannan-binding lectin serine protease 1 OS=Homo sapiens GN=MASP1 PE=1 SV=3	2.80E+05	3.85E+05
ITIH3_HUMAN	3	178.07	0.03	1.93	Inter-alpha-trypsin inhibitor heavy chain H3 OS=Homo sapiens GN=ITIH3 PE=1 SV=2	4.42E+04	8.54E+04
PROC_HUMAN	2	169.94	0.05	1.58	Vitamin K-dependent protein C OS=Homo sapiens GN=PROC PE=1 SV=1	1.36E+05	2.15E+05

Accession	Peptides	Score	Anova (p)*	Fold	Description	Average normalised abundances	
						Control new	Control old
APOC3_HUMAN	2	168.49	8.73E-03	1.58	Apolipoprotein C-III OS=Homo sapiens GN=APOC3 PE=1 SV=1	4.03E+06	6.38E+06
LCAT_HUMAN	3	161.32	0.04	1.41	Phosphatidylcholine-sterol acyltransferase OS=Homo sapiens GN=LCAT PE=1 SV=1	1.72E+05	2.43E+05
APOC4_HUMAN	2	120.95	7.18E-06	3.07	Apolipoprotein C-IV OS=Homo sapiens GN=APOC4 PE=1 SV=1	2.65E+04	8.13E+04
ANGI_HUMAN	2	118.53	0.01	1.69	Angiogenin OS=Homo sapiens GN=ANG PE=1 SV=1	6.20E+04	1.05E+05

Patients with various autoimmune diseases vs. healthy controls to all patients with type 1 diabetes

List of differentially expressed proteins in 'autoimmune' versus 'control-all' samples. Control sample DS-175 was used as reference run.

Accession	Peptides	Score	Anova (p)*	Fold	Description	Average normalised abundances	
						Autoimmune	All controls
P02751	32	2998	0.02	1.52	Fibronectin	3.23E+07	4.91E+07
P02768	24	2101	0.009	1.86	Serum albumin	2.72E+07	1.46E+07
P20742	17	1420	0.01	5.03	Pregnancy zone protein	2.40E+06	4.78E+05

Accession	Peptides	Score	Anova (p)*	Fold	Description	Average normalised abundances	
						Autoimmune	All controls
P06727	10	990	0.02	1.53	Apolipoprotein A-IV	2.12E+07	1.39E+07
P02748	10	968	0.02	1.6	Complement component C9	5.83E+06	3.64E+06
P00450	6	736	0.05	1.42	Ceruloplasmin	1.20E+06	8.48E+05
P01009	10	626	0.02	1.53	Alpha-1-antitrypsin	1.07E+06	7.00E+05
P04264	5	546	0.05	2.95	Keratin, type II cytoskeletal 1	3.49E+05	1.18E+05
P13645	7	509	0.04	3.27	Keratin, type I cytoskeletal 10	2.57E+05	7.84E+04

Accession	Peptides	Score	Anova (p)*	Fold	Description	Average normalised abundances	
						Autoimmune	All controls
P18428	6	457	0.05	1.77	Lipopolysaccharide-binding protein	1.60E+06	9.04E+05
P00734	5	404	0.03	1.79	Prothrombin	2.71E+06	1.51E+06
P10643	5	396	0.02	2	Complement component C7	1.07E+06	5.38E+05
P01008	5	396	0.05	1.94	Antithrombin-III	3.50E+06	1.80E+06
P51884	6	395	0.03	1.9	Lumican	4.56E+05	2.40E+05
Q06033	6	364	0.01	1.77	Inter-alpha-trypsin inhibitor heavy chain H3	2.21E+05	1.25E+05

Accession	Peptides	Score	Anova (p)*	Fold	Description	Average normalised abundances	
						Autoimmune	All controls
P35527	2	177	0.04	2.37	Keratin, type I cytoskeletal 9	4.22E+04	1.78E+04
Q15848	2	174	0.02	1.83	Adiponectin	1.98E+06	1.08E+06
P07357	3	170	0.003	1.44	Complement component C8 alpha chain	9.45E+04	6.56E+04
P00488	2	146	0.03	2.47	Coagulation factor XIII A chain	1.45E+04	3.58E+04
P55056	2	121	0.04	2.12	Apolipoprotein C-IV	3.88E+04	8.23E+04
P07360	2	108	0.05	1.47	Complement component C8 gamma chain	7.82E+04	5.31E+04

Accession	Peptides	Score	Anova (p)*	Fold	Description	Average normalised abundances	
						Autoimmune	All controls
P02746	2	96	0.02	1.48	Complement C1q subcomponent subunit B	8.02E+04	5.43E+04

List of differentially expressed proteins in 'autoimmune' versus 'control-all' samples. Control sample DS-178 was used as reference run.

Accession	Peptides	Score	Anova (p)*	Fold	Description	Average normalised abundances	
						Autoimmune	All controls
P02751	36	2983.27	0.005	1.53	Fibronectin	2.59E+07	3.97E+07
P04114	36	2388.22	0.03	1.52	Apolipoprotein B-100	1.72E+06	2.60E+06
P02768	24	1979.44	0.01	1.93	Serum albumin	2.41E+07	1.25E+07
P20742	18	1452.68	0.009	5.19	Pregnancy zone protein	2.43E+06	4.69E+05
P06727	12	1049.54	0.02	1.53	Apolipoprotein A-IV	1.87E+07	1.22E+07

Accession	Peptides	Score	Anova (p)*	Fold	Description	Average normalised abundances	
						Autoimmune	All controls
P02748	12	973.92	0.02	1.65	Complement component C9	4.92E+06	2.97E+06
P00450	7	787.88	0.05	1.44	Ceruloplasmin	1.16E+06	8.06E+05
P13645	9	661.8	0.04	3.78	Keratin, type I cytoskeletal 10	2.87E+05	7.58E+04
P01009	10	625.66	0.03	1.55	Alpha-1-antitrypsin	9.69E+05	6.24E+05
P10643	4	347.48	0.01	2.5	Complement component C7	6.79E+05	2.71E+05
P18428	5	312.49	0.03	1.7	Lipopolysaccharide-binding protein	9.40E+05	5.53E+05
P51884	5	307.51	0.04	1.88	Lumican	4.02E+05	2.14E+05

Accession	Peptides	Score	Anova (p)*	Fold	Description	Average normalised abundances	
						Autoimmune	All controls
Q06033	5	305.6	0.02	1.65	Inter-alpha-trypsin inhibitor heavy chain H3	1.94E+05	1.17E+05
P13671	4	286.31	0.03	1.53	Complement component C6	4.13E+05	2.69E+05
Q15848	3	251.12	0.02	1.86	Adiponectin	2.00E+06	1.08E+06
P00734	3	219.48	0.03	1.78	Prothrombin	2.39E+06	1.34E+06
O14791	3	185.39	0.03	1.35	Apolipoprotein L1	1.13E+05	1.53E+05
P07360	3	162.9	0.05	1.44	Complement component C8 gamma chain	9.52E+04	6.63E+04
P07357	2	121.76	0.03	1.38	Complement component C8 alpha chain	5.57E+04	4.03E+04

Accession	Peptides	Score	Anova (p)*	Fold	Description	Average normalised abundances	
						Autoimmune	All controls
P01700	2	113.45	0.02	1.6	Ig lambda chain V-I region HA	7.18E+04	4.47E+04

List of differentially expressed proteins in autoimmune versus control samples. Control sample DS-39 was used as reference run.

Accession	Peptides	Score	Anova (p)*	Fold	Description	Average normalised abundances	
						Autoimmune	All Controls
P02751	35	3096.62	0.03	1.53	Fibronectin	3.14E+07	4.80E+07
P0C0L4	27	2157.02	0.05	1.39	Complement C4-A	5.43E+07	3.92E+07
P02768	25	2054.78	0.02	1.86	Serum albumin	2.53E+07	1.36E+07
P20742	22	1472.88	0.009	4.39	Pregnancy zone protein	3.21E+06	7.32E+05
P06727	13	1084.59	0.02	1.52	Apolipoprotein A-IV	1.98E+07	1.31E+07

Accession	Peptides	Score	Anova (p)*	Fold	Description	Average normalised abundances	
						Autoimmune	All Controls
P02748	13	997.78	0.03	1.59	Complement component C9	5.33E+06	3.35E+06
P04264	10	906.06	0.05	2.67	Keratin, type II cytoskeletal 1	4.86E+05	1.82E+05
P13645	10	685.93	0.04	3.24	Keratin, type I cytoskeletal 10	3.06E+05	9.45E+04
P35908	5	606.39	0.03	4.21	Keratin, type II cytoskeletal 2 epidermal	7.93E+04	1.88E+04
P01009	8	479.04	0.04	1.48	Alpha-1-antitrypsin	9.45E+05	6.40E+05
Q06033	7	407.35	0.01	1.75	Inter-alpha-trypsin inhibitor heavy chain H3	2.23E+05	1.27E+05
P51884	5	335.57	0.01	2.06	Lumican	2.87E+05	1.39E+05

Accession	Peptides	Score	Anova (p)*	Fold	Description	Average normalised abundances	
						Autoimmune	All Controls
P10643	4	283.97	0.02	2.26	Complement component C7	8.63E+05	3.81E+05
Q15848	3	265.93	0.02	1.81	Adiponectin	2.57E+06	1.42E+06
P07357	3	170.49	0.006	1.39	Complement component C8 alpha chain	9.01E+04	6.50E+04
P02671	2	165.21	0.03	1.63	Fibrinogen alpha chain	9.25E+04	1.51E+05
P04220	2	134.48	0.02	16.64	Ig mu heavy chain disease protein	2.01E+03	3.35E+04